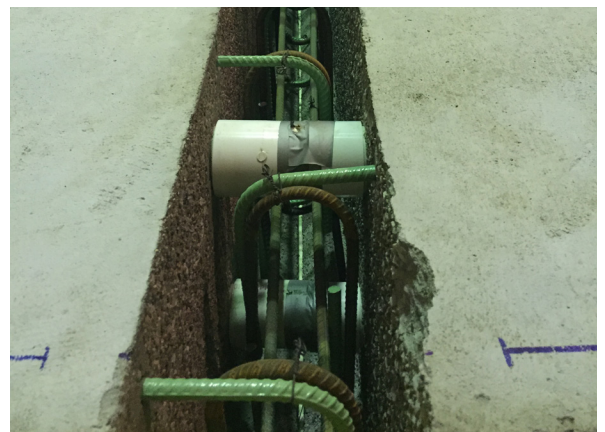
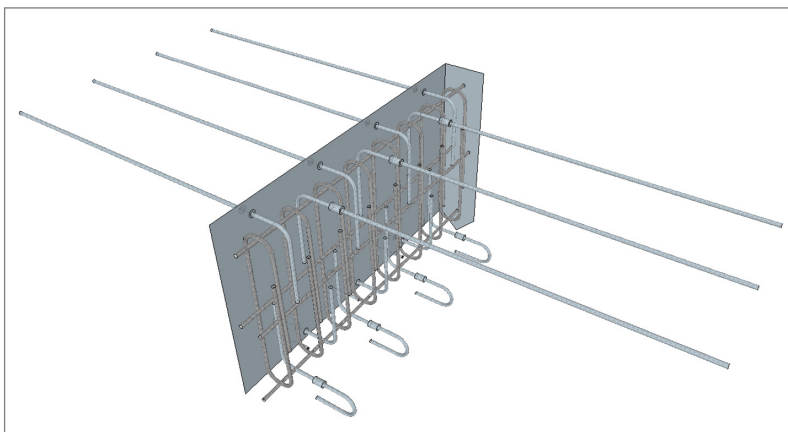


# Context Sensitive Designs: Testing of Multi-Performance Level Box Beam Standards

Final Report  
June 2017



IOWA STATE UNIVERSITY  
**Institute for Transportation**

**Sponsored by**

Iowa Highway Research Board  
(IHRB Project TR-681)  
Iowa Department of Transportation  
(InTrans Project 14-513)  
Federal Highway Administration

## **About the Bridge Engineering Center**

The mission of the Bridge Engineering Center (BEC) is to conduct research on bridge technologies to help bridge designers/owners design, build, and maintain long-lasting bridges.

## **About the Institute for Transportation**

The mission of the Institute for Transportation (InTrans) at Iowa State University is to develop and implement innovative methods, materials, and technologies for improving transportation efficiency, safety, reliability, and sustainability while improving the learning environment of students, faculty, and staff in transportation-related fields.

## **Disclaimer Notice**

The contents of this report reflect the views of the authors, who are responsible for the facts and the accuracy of the information presented herein. The opinions, findings and conclusions expressed in this publication are those of the authors and not necessarily those of the sponsors.

The sponsors assume no liability for the contents or use of the information contained in this document. This report does not constitute a standard, specification, or regulation.

The sponsors do not endorse products or manufacturers. Trademarks or manufacturers' names appear in this report only because they are considered essential to the objective of the document.

## **Iowa State University Non-Discrimination Statement**

Iowa State University does not discriminate on the basis of race, color, age, ethnicity, religion, national origin, pregnancy, sexual orientation, gender identity, genetic information, sex, marital status, disability, or status as a U.S. veteran. Inquiries regarding non-discrimination policies may be directed to Office of Equal Opportunity, 3410 Beardshear Hall, 515 Morrill Road, Ames, Iowa 50011, Tel. 515-294-7612, Hotline: 515-294-1222, email [eooffice@iastate.edu](mailto:eooffice@iastate.edu).

## **Iowa Department of Transportation Statements**

Federal and state laws prohibit employment and/or public accommodation discrimination on the basis of age, color, creed, disability, gender identity, national origin, pregnancy, race, religion, sex, sexual orientation or veteran's status. If you believe you have been discriminated against, please contact the Iowa Civil Rights Commission at 800-457-4416 or Iowa Department of Transportation's affirmative action officer. If you need accommodations because of a disability to access the Iowa Department of Transportation's services, contact the agency's affirmative action officer at 800-262-0003.

The preparation of this report was financed in part through funds provided by the Iowa Department of Transportation through its "Second Revised Agreement for the Management of Research Conducted by Iowa State University for the Iowa Department of Transportation" and its amendments.

The opinions, findings, and conclusions expressed in this publication are those of the authors and not necessarily those of the Iowa Department of Transportation or the U.S. Department of Transportation Federal Highway Administration.

**Technical Report Documentation Page**

<b>1. Report No.</b> IHRB Project TR-681		<b>2. Government Accession No.</b>		<b>3. Recipient's Catalog No.</b>	
<b>4. Title</b> Context Sensitive Designs: Testing of Multi-Performance Level Box Beam Standards				<b>5. Report Date</b> June 2017	
				<b>6. Performing Organization Code</b>	
<b>7. Author(s)</b> Brent Phares (orcid.org/0000-0001-5894-4774), Lowell Greimann (orcid.org/0000-0003-2488-6865), Zhengyu Liu (orcid.org/0000-0002-7407-0912), and Katelyn Freeseaman (orcid.org/0000-0003-0546-3760)				<b>8. Performing Organization Report No.</b> InTrans Project 14-513	
<b>9. Performing Organization Name and Address</b> Bridge Engineering Center Iowa State University 2711 South Loop Drive, Suite 4700 Ames, IA 50010-8664				<b>10. Work Unit No. (TRAIS)</b>	
				<b>11. Contract or Grant No.</b>	
<b>12. Sponsoring Organization Name and Address</b> Iowa Highway Research Board and Iowa Department of Transportation 800 Lincoln Way Ames, IA 50010				<b>13. Type of Report and Period Covered</b> Final Report	
				<b>14. Sponsoring Agency Code</b> IHRB SPR TR-681	
<b>15. Supplementary Notes</b> Visit <a href="http://www.intrans.iastate.edu">www.intrans.iastate.edu</a> for color pdfs of this and other research reports.					
<b>16. Abstract</b> <p>For this project, an innovative wide joint was designed with a roughened interface surface, shrinkage-compensating concrete, and reinforcement steel. The researchers built and tested a specimen that consisted of two box beams and one innovative intermediate joint under early-age thermal loading and cyclic live loading in the laboratory. During these tests, no cracking was found in the joint and no trend of increasing differential displacement was found between the two beams over the course of millions of live load and thermal cycles.</p> <p>Based on the results of the literature review and laboratory tests, this wide joint between the roughened interface surface, filled with shrinkage-compensating concrete and reinforced by reinforcement steel, can create a crack-free joint without the utilization of a shear key or transverse post-tensioning.</p> <p>This joint is as functional as the traditional cement grout-filled narrow joint with respect to the transfer of the moment and shear between the girders, while also performing better than the traditional joint in resisting joint cracks in both early-age loading and the long-term service life of the bridge. At the same time, the test results for the new innovative joint detail appear to compare very well with the ultra-high performance concrete (UHPC) based joint detail developed and tested previously by the Federal Highway Administration (FHWA). However, the UHPC joint may have greater durability due to the very low material permeability</p> <p>To further investigate the performance of this joint detail, the researchers recommend that a field trial be completed. During this field trial, the bridge should be monitored and evaluated during early-age concrete curing as well as for a period of at least two years following construction.</p>					
<b>17. Key Words</b> box beam joints—bridge joint cracks—cyclic load tests—early-age thermal loading—post-tensioning—reinforced joints—shrinkage-compensating cement—Type K cement				<b>18. Distribution Statement</b> No restrictions.	
<b>19. Security Classification (of this report)</b> Unclassified.		<b>20. Security Classification (of this page)</b> Unclassified.		<b>21. No. of Pages</b> 97	<b>22. Price</b> NA



# **CONTEXT SENSITIVE DESIGNS: TESTING OF MULTI-PERFORMANCE LEVEL BOX BEAM STANDARDS**

**Final Report  
June 2017**

**Principal Investigator**  
Brent Phares, Director  
Bridge Engineering Center

**Bridge Engineer**  
Lowell Greimann, Bridge Engineer  
Bridge Engineering Center

**Research Assistants**  
Zhengyu Liu and Weizhuo Shi

**Authors**  
Brent Phares, Lowell Greimann, Zhengyu Liu, and Katelyn Freeseaman

Sponsored by  
Iowa Highway Research Board  
(IHRB Project TR-681),  
Iowa Department of Transportation, and  
Federal Highway Administration

Preparation of this report was financed in part  
through funds provided by the Iowa Department of Transportation  
through its Research Management Agreement  
with the Institute for Transportation  
(InTrans Project 14-513)

A report from  
**Bridge Engineering Center**  
**Iowa State University**  
2711 South Loop Drive, Suite 4700  
Ames, IA 50010-8664  
Phone: 515-294-8103 / Fax: 515-294-0467  
[www.instrans.iastate.edu](http://www.instrans.iastate.edu)



## TABLE OF CONTENTS

ACKNOWLEDGMENTS .....	xi
EXECUTIVE SUMMARY .....	xiii
CHAPTER 1. INTRODUCTION .....	1
1.1 Background .....	1
1.2 Objective and Research Plan .....	2
CHAPTER 2. LITERATURE REVIEW .....	3
2.1 NCHRP Synthesis 393 .....	3
2.2 Publication before 2008 .....	9
2.3 Publication after 2008 .....	17
2.4 FHWA-UHPC Joint Test .....	24
2.5 HDR Box Girder Design .....	25
2.6 Literature Search Synthesis and Summary .....	25
CHAPTER 3. FIELD BRIDGE INSPECTION .....	32
3.1 Inspection Results from Bridge-A: Madison County, Iowa .....	32
3.2 Inspection Results from Bridge-B: Buena Vista County, Iowa .....	33
CHAPTER 4. SPECIMEN DESIGN AND CONSTRUCTION .....	35
4.1 Wide Joint .....	35
4.2 Type K Cement Jointed Concrete .....	36
4.3 Form Retarder .....	37
4.4 Joint Reinforcement .....	37
4.5 Box Girder Construction .....	38
4.6 Joint Construction .....	41
CHAPTER 5. EARLY-AGE AND CYCLIC LOAD TESTING .....	43
5.1 Early-Age Loading Test .....	43
5.2 Joint Pouring .....	45
5.3 Cyclic Loading Test .....	47
5.4 Instrumentation .....	50
Strain Data .....	50
Temperature Strain Data .....	51
Displacement Data .....	52
5.5 Material Test Results .....	54
CHAPTER 6. TEST RESULTS .....	56
6.1 Results of Early-Age Thermal Test .....	56
Temperature .....	56
Strain .....	62
Displacement .....	68
Cracks .....	69
6.2 Results of Cyclic Load Test .....	69
Displacement .....	69

Strain .....	72
Cracks .....	75
6.3 Results of Horizontal Load .....	76
CHAPTER 7. SUMMARY AND CONCLUSIONS .....	78
7.1 Summary .....	78
7.2 Conclusions and Recommendations .....	79
REFERENCES .....	81

## LIST OF FIGURES

Figure 1. Basic keyway geometries .....	9
Figure 2. Basic shear key shapes .....	15
Figure 3. Keyway geometries for PCI- and TxDOT-style box girder bridges .....	16
Figure 4. Typical Michigan keyway geometry and post-tensioning.....	17
Figure 5. Common shear key locations.....	18
Figure 6. Common bearing pad details .....	20
Figure 7. Connection details proposed by Hanna et al. 2011 .....	21
Figure 8. Connection details proposed by Hansen et al. 2012.....	23
Figure 9. UHPC joints.....	24
Figure 10. Design of box girder jointed by UHPC .....	25
Figure 11. Madison County, Iowa bridge .....	32
Figure 12. Buena Vista County, Iowa bridge .....	33
Figure 13. Water leakage stains under the Buena Vista County, Iowa bridge .....	34
Figure 14. Innovative joint design .....	35
Figure 15. Shrinkage of Type K cement.....	36
Figure 16. 3D view of joint reinforcement design.....	37
Figure 17. Design details for the reinforcing steel across the interface.....	38
Figure 18. Coupler embedded in the box girder concrete (left) and hook bar installed (right) .....	38
Figure 19. Elevation and plan view of the box girder.....	39
Figure 20. Cross-section view of the box girder.....	39
Figure 21. Box girder construction .....	40
Figure 22. Water blasting on the side of box girder painted with form retarder .....	41
Figure 23. Side of the box girder with hook bars installed.....	41
Figure 24. Placement of joint reinforcement .....	42
Figure 25. Specimen before pouring of the joint material.....	42
Figure 26. Temporary temperature isolation room.....	43
Figure 27. Heating devices in the temperature isolation room .....	44
Figure 28. Locations of heating devices and fans.....	44
Figure 29. Average temperature on the top and bottom surface of specimen .....	45
Figure 30. Pouring joint concrete.....	46
Figure 31. Curing joint.....	46
Figure 32. Simply supported detail for cyclic live loading.....	47
Figure 33. Cross-section view of load application.....	48
Figure 34. Cyclic loading under the simply supported condition.....	48
Figure 35. Cyclic live loading detail for one beam restrained.....	49
Figure 36. Restraints under one beam.....	49
Figure 37. Vibrating wire strain gauge (VWSG) instrumentation map on top surface (similar for bottom surface) .....	51
Figure 38. Locations of thermal couples in Sections 3 and 5 in the joint.....	52
Figure 39. Thermal couples on the exterior side of the specimen .....	52
Figure 40. Thermal couples on the exterior end of the specimen.....	52
Figure 41. Displacement transducers in Sections 1 and 5 .....	53
Figure 42. Displacement transducers in Section 2.....	53

Figure 43. Displacement transducers in Section 3.....	53
Figure 44 Displacement Transducers in Section 4 .....	54
Figure 45. Compressive strength of joint concrete .....	54
Figure 46. Flexural tensile strength of joint concrete .....	55
Figure 47. Temperatures from Section 1 at the bottom surface.....	56
Figure 48. Temperatures from Section 2 at the bottom surface.....	56
Figure 49. Temperatures from Section 3 at the bottom surface-1 .....	57
Figure 50. Temperatures from Section 3 at the bottom surface-2 .....	57
Figure 51. Temperatures from Section 4 at the bottom surface.....	57
Figure 52. Temperatures from Section 5 at the bottom surface.....	58
Figure 53. Temperatures from Section 1 at the top surface .....	58
Figure 54. Temperatures from Section 2 at the top surface .....	58
Figure 55. Temperatures from Section 3 at the top surface-1.....	59
Figure 56. Temperatures from Section 3 at the top surface-2.....	59
Figure 57. Temperatures from Section 4 at the top surface .....	59
Figure 58. Temperatures from Section 5 at the top surface .....	60
Figure 59. Average temperatures on top and bottom surfaces.....	60
Figure 60. Temperatures in the joint at Section 3.....	61
Figure 61. Temperatures in the joint at Section 5.....	61
Figure 62. Temperatures at the side of specimen .....	62
Figure 63. Temperatures at the end of the specimen .....	62
Figure 64. Strains from Section 1 at the bottom surface.....	63
Figure 65. Strains from Section 2 at the bottom surface.....	63
Figure 66. Strains from Section 3 at the bottom surface-1 .....	63
Figure 67. Strains from Section 3 at the bottom surface-2 .....	64
Figure 68. Strains from Section 4 at the bottom surface.....	64
Figure 69. Strains from Section 5 at the bottom surface.....	64
Figure 70. Strains from Section 1 at the top surface-1 .....	65
Figure 71. Strains from Section 1 at the top surface-2 .....	65
Figure 72. Strains from Section 2 at the top surface.....	65
Figure 73. Strains from Section 3 at the top surface-1 .....	66
Figure 74. Strains from Section 3 at the top surface-2 .....	66
Figure 75. Strains from Section 3 at the top surface-3 .....	66
Figure 76. Strains from Section 4 at the top surface.....	67
Figure 77. Strains from Section 5 at the top surface-1 .....	67
Figure 78. Strains from Section 5 at the top surface-2 .....	67
Figure 79 Vertical displacement at the middle span at early-age .....	68
Figure 80. Displacement from 18 kips static tests .....	69
Figure 81. Displacement from 36 kips static tests .....	70
Figure 82. Displacement from 42 kips static tests .....	70
Figure 83. Distribution factor change during the first three million cycles.....	71
Figure 84. Displacement from 42 kips static tests with one beam restrained.....	71
Figure 85. Bottom longitudinal strains from 18 kips static tests .....	72
Figure 86. Bottom longitudinal strains from 36 kips static tests .....	73
Figure 87. Bottom longitudinal strains from 42 kips static tests .....	73
Figure 88. Bottom longitudinal strains from 42 kips static tests (one beam restrained) .....	73

Figure 89. Top transverse strains from 18 kips static tests .....	74
Figure 90. Top transverse strains from 36 kips static tests .....	74
Figure 91. Top transverse strains from 42 kips static tests .....	75
Figure 92. Top transverse strains from 42 kips static tests (one beam restrained) .....	75
Figure 93. Transverse cracks on bottom of box girder after first cycle loading of 18 kips .....	76
Figure 94. Crushed box girder due to horizontal load .....	77

## LIST OF TABLES

Table 1. Structural design and details .....	4
Table 2. Specifications and construction practices .....	6
Table 3. Recommended practices .....	8
Table 4. Design and construction attributes.....	27
Table 5. Summary of FE analysis .....	29
Table 6. Summary of laboratory testing .....	30
Table 7. Summary of field testing.....	31
Table 8. Summary of cyclic loading test .....	50
Table 9. Joint performance comparison to FHWA's (Yuan and Graybeal 2016) .....	77



## **ACKNOWLEDGMENTS**

This research was sponsored by the Iowa Highway Research Board and Iowa Department of Transportation using Federal Highway Administration state planning and research funding.



## EXECUTIVE SUMMARY

Adjacent concrete box beam bridges constitute more than 15% of the bridges built or replaced each year. This type of bridge is generally constructed by placing box beams next to one another, grouting adjoining shear keys, applying a transverse post-tensioning force, and then placing either a thin (~3-in.) wearing surface or a thick (~6-in.) structural deck. Historically, these and other similar adjacent precast elements have suffered from differential displacements, which cause cracking in adjoining joint material (or, in some cases, in cast-in-place topping material).

For this project, a comprehensive literature review was conducted to locate the potential source of the joint cracking. Based on the findings of the literature review, joint cracks are suspected to be caused by low bond strength between the joint material and the box girder, large shrinkage of the joint material, stress concentrations near the shear key, and temperature changes. Some potential solutions noted by previous research include the use of low- or zero-shrinkage joint material, increased bond strength and shear strength, and additional reinforcement in the joint.

Based on the results of the literature review, an innovative wide joint was designed with a roughened interface surface, shrinkage-compensating concrete, and reinforcement steel. The researchers built and tested a specimen that consisted of two box beams and one innovative intermediate joint under early-age thermal loading and cyclic live loading in the laboratory. During these tests, no crack was found in the joint and no trend of increasing differential displacement was found between the two beams. The specimen was eventually cracked by the direct horizontal load.

The results indicate that the innovative joint is as functional as the traditional cement grout-filled narrow joint with respect to the transfer of the moment and shear between the girders, while also performing better than the traditional joint in resisting joint cracks in both early-age loading and the long-term service life of the bridge. At the same time, the test results for the new innovative joint detail appear to compare very well with the ultra-high performance concrete (UHPC) based joint detail developed and tested previously by the Federal Highway Administration (FHWA). However, it should be pointed out that the permeability/durability of UHPC is likely better than that of the shrinkage-compensating concrete used here.

To further investigate the performance of this joint detail, the researchers recommend that a field trial be completed. During this field trial, the bridge should be monitored and evaluated during early-age concrete curing as well as for a period of at least two years following construction.



## CHAPTER 1. INTRODUCTION

### 1.1 Background

Adjacent concrete box beam bridges constitute more than 15% of bridges built or replaced each year. This type of bridge is generally constructed by placing box beams next to one another, grouting a shear key, applying a transverse post-tensioning force, and then placing either a thin (~3-in.) wearing surface or a thick (~6-in.) structural deck. In some cases, the top of the box beams are left bare to serve as the riding surface. These bridges are attractive because of their relatively shallow superstructure depth, ease of construction, and simple aesthetic attributes.

Adjacent precast, prestressed box beam bridges have been used by multiple departments of transportation (DOTs) with varying levels of success. Historically, these, and other similar adjacent precast elements, have suffered from differential displacements, which cause cracking in the material used to connect the boxes (or, in some cases, in cast-in-place topping material). Sources of differential deflection can come from a variety of conditions including live loads, temperature effects, and others.

Generally, these reflective cracks in-and-of themselves do not pose a safety hazard. However, these cracks provide a direct path for water (plus chlorides) to enter the structural system causing corrosion of the mild and prestressing steel. Ultimately, this situation can lead to significant maintenance costs and/or safety concerns. Because of this, some early users of adjacent box beams now only allow them on low-volume roads where salt application does not occur.

Even with the known issues associated with adjacent box beams, they can still result in an economical short- to medium-span bridge that is generally quick and easy to construct. For example, the Missouri DOT (MoDOT) recently completed their Safe and Sound bridge replacement program in which 554 bridges were replaced over three construction seasons. The design/build team made extensive use of adjacent box beams, constructing more than 170 bridges using this system, for spans up to 90 ft in length.

The Iowa DOT, in principal cooperation with HDR, Inc., has been working to develop a new set of bridge standards particularly targeted toward use by counties. As is widely known, counties have a large number of bridges in their systems that must be constructed and maintained. As such, they are increasingly in need of low-cost bridge concepts. For many counties, the ideal construction strategy is one that could be executed using county forces. Due to these constraints, the utilization of prestressed and heavy-weight members are not plausible scenarios.

During a meeting on May 2, 2014, interested parties (from the Iowa DOT, the Federal Highway Administration/FHWA, designers, counties, and academia) discussed possible concepts for the desired bridge standard. Because the decision had previously been made (based on preliminary work completed by HDR) to use a box beam shape, the discussion principally centered on needs associated with this concept. Of particular importance was information presented by Ben

Graybeal of the FHWA, who has been conducting testing on adjacent box beams at the Turner-Fairbank Highway Research Center.

The results of this work have resulted in a connection detail that appears to perform well. The main drawback associated with this connection detail (from a county perspective) is the fact that ultra-high performance concrete (UHPC) is needed. This material tends to be very expensive and requires a high level of expertise for proper mixing, placement, etc. Thus, it was discussed that perhaps work could be done to develop alternatives that would have sufficient performance when placed in the right location. This is frequently termed context-sensitive design and is the main focus of the research presented in this report.

## **1.2 Objective and Research Plan**

The goal of the project was to develop a new joint design for use between adjacent box beams with a particular interest in county road usage. This design will provide a cost-effective bridge solution that counties could, if desired, construct themselves.

To achieve the final goal, the original plan was to develop standards with three performance “levels.” Level I performance—the highest—would basically constitute the connection system tested by the FHWA. Level II performance—the middle—would use a connection detail similar to the Level I system, but the UHPC would be replaced with a more widely available material. Level III performance—the lowest—would be a concept where the adjacent box beams are not connected at all.

The original scope of work planned to conduct testing and other work to evaluate details deemed important to the Level II and Level III concepts. However, after discussions with the project technical advisory committee, the research plan was modified with the most significant changes being a singular focus on developing and testing connection details targeting Level II performance or better.

To achieve the project goal, the scope was modified to include the following:

- Conduct on-site inspections of two box beam bridges previously constructed on the Iowa county road system
- Conduct a comprehensive literature search to determine the cause of joint cracking
- Design an innovative crack-free joint based on the results of the literature review
- Construct and test a full-length joint based on this innovative design and perform laboratory testing, following the procedures established by the FHWA, to determine/verify joint performance

## **CHAPTER 2. LITERATURE REVIEW**

A comprehensive literature search was conducted to collect information relevant to the project. The material was gathered, categorized, and summarized to help guide subsequent tasks. A complete understanding of the current state-of-the-art and state-of-practice was extremely important and invaluable when finalizing the plans for the analytical and experimental investigations of this project. One notable source of pertinent information for this project proved to be the NCHRP Synthesis 393 by Russell (2009), which described current concrete box beam practices from multiple DOTs at multiple levels and also provides extensive literature search results from before 2008.

The literature search for this project is summarized as follows. First, NCHRP Synthesis 393 is summarized, including the conclusions and recommendations. Second, literature published before 2008 is reviewed to take note of the important information beneficial to this project. Finally, literature published after 2008 is reviewed with emphasis on the literature with a connection to the results of the NCHRP Synthesis 393. This literature is then summarized, synthesized, and categorized as it relates to design and construction attributes for adjacent box girder bridges, finite element (FE) analysis, laboratory testing, and field testing. Note that to provide a brief summary of each piece of literature, take-away points for each source (with the exception of NCHRP Synthesis 393) are provided after each general summary.

### **2.1 NCHRP Synthesis 393**

The NCHRP Synthesis (Russell 2009) summarized the observed types of distress associated with the joints used in adjacent box girder bridge systems. These distresses included longitudinal cracking along the joint material and box beam interface, water and salt leakage through the joint, cracking within the grout, spalling of the grout, spalling of the girder corners, differential vertical movement, corrosion of transverse ties and longitudinal prestressing strands, and freeze-thaw damage to the grout and concrete near the joint. Note that the most common types of distress are longitudinal cracking along the grout and box beam interface, water and salt leakage through the joint, and reflective cracks that are commonly observed in the road surface.

Based on the survey of state DOTs and the literature search, Russell also began the process of identifying factors impacting the long-term performance of adjacent box beam bridge systems. In the synthesis, practices for structural design and detailing for adjacent box girder bridges from state DOTs and the literature are summarized as listed in Table 1. Specifications and construction practices for adjacent box girder bridges from state DOTs and the literature are summarized as listed in Table 2. Finally, the recommended and not-recommended design and construction practices are summarized as listed in Table 3.

**Table 1. Structural design and details**

<b>Practices</b>	<b>Survey summary</b>	<b>Literature cited by Russell 2009</b>
<b>Girder cross sections</b>	About 50% of states use AASHTO/PCI-shaped box beams	
<b>Span lengths</b>	Below 20 ft to above 80 ft	40 to 140 ft (PCI 1997/2004)
<b>Bridge skew</b>	0°-60°, Most common: 30°	
<b>Composite deck</b>	<ul style="list-style-type: none"> <li>• Most states use simple spans with composite deck (3-9 in. depth)</li> <li>• Bridges with multi-span and composite deck are usually designed continuous for live load</li> </ul>	The use of a deck does not eliminate differential rotation of girders and is not an economically and structurally efficient solution (El-Remaily et al. 1996)
<b>Keyway geometries</b>	Most states use partial-depth keyways; some use full-depth keyways	<ul style="list-style-type: none"> <li>• Longitudinal cracks were found in 54% of bridges with 12 in. partial-depth keyway and 6 in. depth concrete deck and in 23% of the bridges with full-depth keyways, concrete deck and more transverse ties (Lall et al. 1997, 1998)</li> <li>• No longitudinal cracks were found in Japanese bridges with 6 in. wide full-depth keyway, cast-in-place concrete grout, and 2-3 in. concrete or asphalt wearing surface (El-Remaily et al. 1996)</li> <li>• The full-depth keyway hinders the joint from opening (Miller et al. 1999)</li> <li>• Wider full-depth keyways improve the interaction between adjacent girders and the contact between grout and girders, but forms are needed to contain the fresh grout during placement (Nottingham 1995)</li> </ul>

Practices	Survey summary	Literature cited by Russell 2009
<b>Transverse ties</b>	<ul style="list-style-type: none"> <li>• Most states use unbonded post-tensioned strands or bars; some states use bonded post-tensioned strands or bars; other states use non-prestressed reinforcements</li> <li>• Number of tie locations: 1-5 per span</li> <li>• Most states placed ties at mid-depth of girders (one tie per location)</li> <li>• Ties are typically placed at the third points when two ties are used at a single location</li> </ul>	<ul style="list-style-type: none"> <li>• Illinois DOT equation for the number ties per span (Anderson 2007):  <math display="block">N = \frac{\text{span}}{25} - 1 \geq 1</math> </li> <li>• Less longitudinal cracking: Three transverse tie locations for the span less than 50 ft, five for the span more than 50 ft (Lall et al. 1997, 1998)</li> <li>• Durable system in Japan: 4-7 evenly spaced transverse diaphragms with post-tensioning ties and post-tensioning is determined by flexural design (Yamane et al. 1994)</li> <li>• Partial-depth keyway: Due to eccentricity of post-tensioning, cracks may be induced by post-tensioning ties at the girder mid-depth</li> <li>• Full-depth keyway: Good with post-tensioning ties at the girder mid-depth</li> </ul>
<b>Post-tensioning force</b>	<ul style="list-style-type: none"> <li>• Most states specify the required post-tensioning force without extensive calculations</li> <li>• For 11 states: 0.5-12.5 kip/ft</li> </ul>	<ul style="list-style-type: none"> <li>• 4-14 kip/ft (El-Remaily et al. 1996)</li> <li>• 7-14 kip/ft (Hanna et al. 2007)</li> <li>• 27 kip/ft for 15 in. beam depth (Badwan and Liang 2007a)</li> <li>• 21 kip/ft per AASHTO LRFD specification (2007, 2008)</li> <li>• 4-11 kip/ft per PCI Bridge Design Manual (1997/2004)</li> <li>• Average of 11 kip/ft is Japanese practice (Yamane et al. 1994)</li> </ul>
<b>Exterior girders</b>	<ul style="list-style-type: none"> <li>• Most states have the same design for exterior and interior girders</li> </ul>	<ul style="list-style-type: none"> <li>• No concrete barriers were used by Illinois DOT for box girder system because the increased stiffness of exterior girders might cause increased differential deflections (Macioce et al. 2007)</li> <li>• The barrier load could be counteracted by the increased exterior girder section property (Harries et al. 2006)</li> </ul>

**Table 2. Specifications and construction practices**

<b>Practices</b>	<b>Survey summary</b>	<b>Literature cited by Russell 2009</b>
<b>Standard specifications (AASHTO 2002)</b>		No guidelines are provided for the design and construction of the connection details of adjacent box girders
<b>LRFD specifications (AASHTO 2007, 2008)</b>		<ul style="list-style-type: none"> <li>• A compression depth (<math>\geq 7</math> in.) should be provided with a transverse post-tensioning <math>\geq 0.25</math> ksi</li> <li>• Post-tensioning ties are required to be placed at the centerline of the keyway</li> </ul>
<b>Bearing types</b>	<ul style="list-style-type: none"> <li>• Plain elastomeric bearing: three-quarters of respondents</li> <li>• Laminated elastomeric bearing: one-quarter of respondents</li> <li>• Full-width support or full-point support on ends: 42% of states for each; Two-point support and one-point support: the other states</li> <li>• Uneven seating: half the respondents (especially for a full-width support)</li> </ul>	
<b>Construction sequence</b>	<ul style="list-style-type: none"> <li>• One-stage construction: erect all beams and connect them at one time</li> <li>• Two-stage construction: variety of sequences</li> <li>• Grout before or after post-tensioning: 50% of states for each</li> <li>• Grout after post-tensioning: higher cracking resistance</li> <li>• Construction sequence is affected by the skew of the bridge and intermediate diaphragm locations</li> </ul>	Greuel et al. (2000) reported that spalling of beam bottom flanges occurred near the shear key for the two half bridges when the shear key was not grouted prior to post-tensioning

Practices	Survey summary	Literature cited by Russell 2009
<b>Differential camber</b>	<ul style="list-style-type: none"> <li>• Restrictions for differential camber: one-third of respondents</li> <li>• Maximum differential camber: 0.5 in. (half of respondents)</li> <li>• Others: 0.25 in. in 10 ft; 0.75 in. maximum; 1 in. relative deflection for high and low beams in one span</li> <li>• Improving methods: load high beam before grouting and post-tensioning; adjust bearing seat elevations; concrete or asphalt topping; preassemble girders before shipment</li> </ul>	
<b>Keyway preparation</b>	<ul style="list-style-type: none"> <li>• Sandblast keyway: 45% of states</li> <li>• Sandblast and power wash keyway: one-third of respondents</li> </ul>	<ul style="list-style-type: none"> <li>• Poor adherence of keyway mortar (Attanayake and Aktan 2008)</li> </ul>
<b>Grout materials and practices</b>	<ul style="list-style-type: none"> <li>• Nonshrink grout: 40% of respondents; mortar: 25% of respondents; epoxy grout, epoxy resin, or concrete topping: other respondents</li> <li>• No curing: 40% of respondents; curing compounds: 5%; wet curing: about 45% of states</li> <li>• Most states manually place the grout</li> </ul>	<ul style="list-style-type: none"> <li>• High-quality joint: prepackage mix with predetermined amount of water (e.g., prepackaged magnesium-ammonium-phosphate grout with pea gravel) (Nottingham 1995)</li> <li>• Improvements by West Virginia DOT (El-Remaily et al 1996): a pourable epoxy replacing a nonshrink grout; sandblasting surfaces; post-tensioning ties</li> <li>• Andover Dam Bridge in Maine: wider shear key rapidly grouted with shrinkage-restrained self-consolidating concrete (Russell 2009)</li> <li>• Illinois DOT (2008): use a mechanical mixer for mixing nonshrink grout; place with a pencil vibrator; smooth surface; cover with cotton mats for more than 7 days</li> </ul>

**Table 3. Recommended practices**

<b>Practices</b>	<b>Recommended</b>	<b>Not recommended</b>
<b>Design practices</b>	<ul style="list-style-type: none"> <li>• Full-depth keyway: grouted easily</li> <li>• Post-tensioning transverse ties: eliminating tensile stresses in the shear key</li> <li>• Cast-in-place reinforced concrete deck (compressive strength of more than 4 ksi and thickness of more than 5 in.): restrains longitudinal deck cracking</li> </ul>	<ul style="list-style-type: none"> <li>• Non-tensioned transverse ties: no crack resistant ability</li> </ul>
<b>Construction practices</b>	<ul style="list-style-type: none"> <li>• Form the void using stay-in-place expanded polystyrene</li> <li>• Sandblast the keyway surface before shipment: ensuring a better bonding surface for the grout</li> <li>• Power wash the keyway surfaces (compressed air or water) before erection of girders: ensuring a better surface for the grout</li> <li>• Grout keyways before post-tensioning: the grout under compression</li> <li>• Grout with high bond strength: limit cracking</li> <li>• Provide suitable curing for the grout: developing desired strength and minimize shrinkage effects</li> <li>• Provide suitable wet curing for the concrete deck (more than 7 days): ensuring durable surface and minimize shrinkage cracks</li> </ul>	<ul style="list-style-type: none"> <li>• Use asphalt wearing surface with non-water proofing membrane: water gathers under the asphalt</li> <li>• Use non-prepackaged products for the keyway grout</li> </ul>

Compiled from Russell 2009/NCHRP Synthesis 393

Russell (2009) indicated that keyway configurations consist of partial-depth and full-depth keyways. In the US, there are three typically used generic partial-depth keyway geometries (Types I, II, and III), and one generic full-depth keyway geometry (Type IV), all of which are shown in Figure 1. Conversely, the typical Japanese keyway is the full-depth keyway (Type V, also shown in Figure 1).

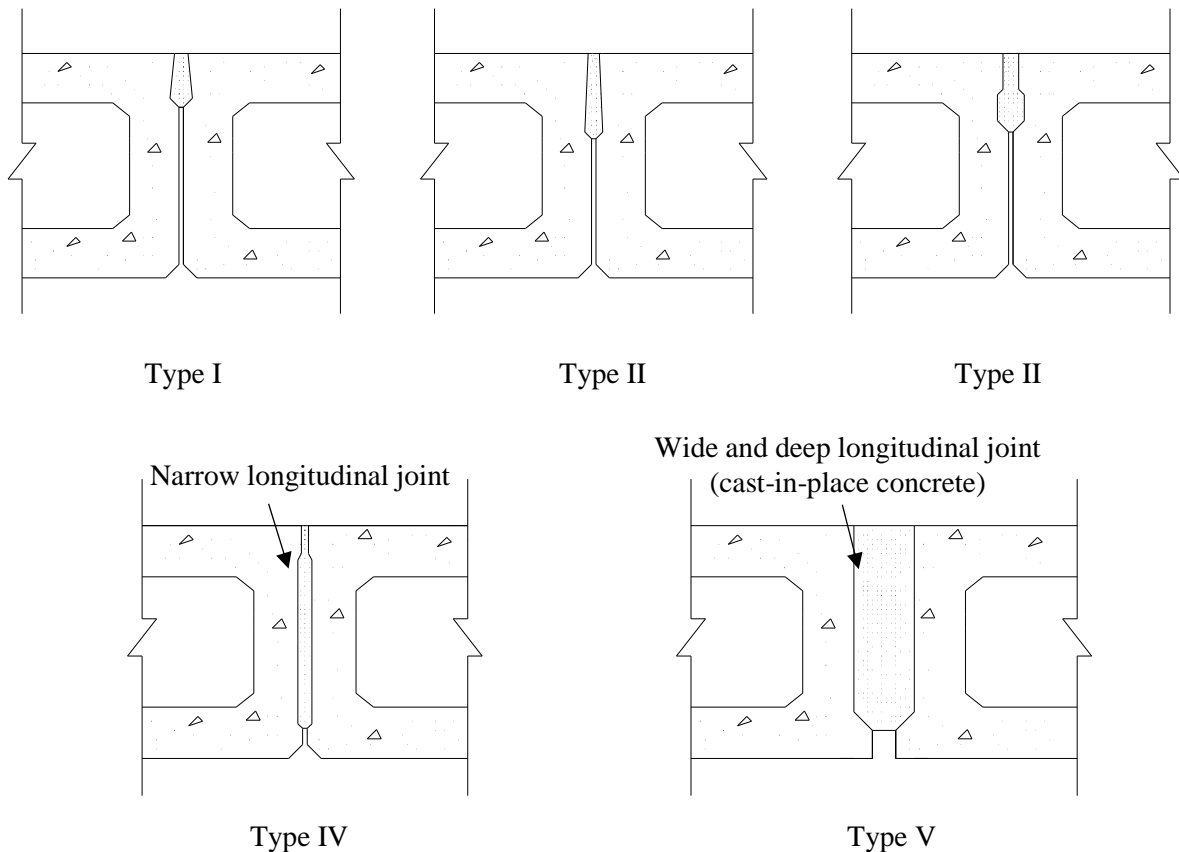


**Figure 1. Basic keyway geometries**

Note that in Figure 1, the box beams are shown to be in direct contact. This may or may not always be the case; however, sweep is typically removed with the application of post-tensioning. It is also worth noting that El-Remaily et al. (1996) reported that longitudinal cracking was seldom found in adjacent box beam bridges with Type V full-depth keyways.

## 2.2 Publication before 2008

Huckelbridge et al. (1995) revealed that precast prestressed adjacent box beams have been mostly used for the construction of bridges with short and medium spans ranging from 30 to 100 ft. The authors conducted field testing of several adjacent box girder bridges and the test results from two of these bridges were summarized in the 1995 paper: one for a simply supported bridge and one for a four-span continuous bridge. A dump truck with a front axle weight of 12 kips and tandem axles weighing 38 kips was used to conduct on-site, controlled tests. During those tests, deflection transducers were installed on the bottom of adjacent beams near the keyway to record the relative deflections between those box beams; flexural strains were also collected on the girder bottom.

The maximum relative deflection was found to be 0.2 and 0.15 in. for the two bridges, respectively. According to results from the FE analysis (details of the FE analysis were not

given) and field tests, the authors pointed out that intact shear keys should not permit relative deflection of more than 0.001 in. between adjacent girders. As they expected, reflective cracks were found around the shear keys on both bridges. Partially fractured shear keys were generally found close to the wheel positions and in driving lanes with heavy truck traffic. However, they did note that the partially fractured shear keys still displayed adequate lateral live load distribution characteristics.

The addition of lateral tie bars was found to have insignificant influence on shear key performance. The transverse tie bars used in the tested bridges were made of 1 in. diameter mild steel spaced at no more than 25 ft and not post-tensioned.

#### Take-Away Points

- Intact shear keys (i.e., crack free) should not permit relative deflection between adjacent box beams.
- Partially fractured shear keys still have adequate strength to distribute live loads laterally.
- Mild steel lateral tie-bars have insignificant influence on shear key performance.

In the experimental work by Gulyas et al. (1995), the performance of grouted keyways using non-shrink grouts and magnesium ammonium phosphate mortars was studied and compared. Three types of tests were conducted including a direct vertical shear test considering truckloads on the bridge, a direct transverse tension test considering transverse creep and shrinkage effects, and a direct longitudinal shear test considering longitudinal creep and shrinkage effects. All 16 of the tested specimens had small dimensions and grout strengths ranging from 5.9 to 7.3 ksi.

The researchers found that the composite keyway specimens using mortar containing magnesium ammonium phosphate showed higher direct tensile bond strengths, vertical shear, and longitudinal shear than those of the non-shrink grout keyway specimens. They also found that magnesium ammonium phosphate mortar showed significantly lower chloride absorption ability, which is of benefit for roadways exposed to salts or sea sprays. Finally, the authors recommended not using non-shrink grouts for the keyway unless the tensile and shear strengths satisfy the requirements in their study.

#### Take-Away Point

- Mortars containing ammonium phosphate for use in shear keys displayed high bond and shear strengths and also had low chloride absorption.

El-Remaily et al. (1996) compared the American and Japanese approaches to designing adjacent concrete box beam bridges primarily because longitudinal cracking was very rarely associated with Japanese box beam bridges. The authors found that the primary differences between American and Japanese designs were the size and shape of longitudinal joints and the amount of transverse post-tensioning.

After further review, the authors proposed a new precast prestressed box girder bridge design along with a design methodology suitable for US practice. The proposed design methodology takes the transverse diaphragms as the only components that sustain the post-tensioning forces from the post-tensioning ties. The transverse diaphragms are connected at the joints and laterally distribute live loads among those box girders.

The authors performed grillage analysis using beam elements with common nodes for the diaphragms and beams and considering dead and live loads (including barriers). They used working stress methodologies to compute the transverse stresses in the top and bottom of the diaphragms after the bending moments in the diaphragms were derived from the grillage model. The post-tensioning was determined to counteract the calculated stresses in the diaphragms such that no lateral tensile stress is induced in the diaphragms.

The authors' parametric studies indicated that the needed transverse post-tensioning remains constant per unit span length and varies significantly with the bridge width. This method was adopted in the Precast/Prestressed Concrete Institute (PCI) Bridge Design Manual (2003). The authors described a design example but provided no information on either experimental validation or analytical evaluations using a rigorous finite element approach.

#### Take-Away Points

- The primary differences between American and Japanese designs are the size and shape of longitudinal joints and the amount of transverse post-tensioning.
- The amount of post-tensioning remains constant on a per foot basis (for constant width of bridge); the amount of post-tensioning needed varies with bridge width.

A study conducted in Ohio examined the performance of the state's standard box beam shear key design, investigated the cause of shear key failure, and developed new types of keyway connection details (Huckelbridge and El-Esnawi 1997). Initially, a three-dimensional (3D) FE model of a three-box beam bridge with a length of 40 ft and a width of 12 ft was established. A concentrated load, simulating that of a truck wheel load, was applied on the center of the interior beam.

The analytical results indicated that transverse tensile stresses in the bridge top flange are the main factor causing many shear key failures. To deal with the issue, a new type of shear key was proposed by placing the shear key at the neutral axis of the beam cross section. FE results showed that the proposed shear key sustained much smaller tensile stresses, which would not cause shear key cracking nor failure.

To complete the examination, small-scale testing of a multi-beam bridge cross section was conducted. The small-scale specimens are slices of the three-beam assembly with a length of 12 in., a width of 144 in., and a depth of 33 in. Static and cyclic loads were applied at the center of these specimens.

The experimental results showed that the mid-depth shear key design (only the shear key was grouted instead of the whole keyway) had significantly improved the static load carrying capacity and provided a longer fatigue life than the previous shear key design.

In the end, the authors also proposed a water-proofing shear key design with a mid-depth shear key, which uses a water-proofing membrane, asphalt topping, and foam filler above the shear key. The test results indicated that this shear key design maintained water tightness after fatigue testing in the laboratory environment. However, further evaluations at real bridge sites were noted to be needed.

#### Take-Away Point

- A shear key placed at mid-depth of the beam can resist cracking due to decreased tensile stresses.

Research conducted by Lall et al. (1998) compared the long-term performance of a partial-depth shear key system and a modified, full-depth shear key/transverse tie system based on a survey of bridges in New York. The modified full-depth shear key/transverse tie system was developed based on the results of bridge inspections in the state and information from other states, and Michigan in particular. The new system possesses two post-tensioning ties located at the third points of the girder depth instead of one tie at the girder mid-depth.

Survey results indicated that the new full-depth shear key/transverse tendon system showed superior cracking prevention ability and reduced the frequency of reflective cracking in the deck. As a result of the work, the authors recommended using the new full-depth shear key for future adjacent box beam bridges. Additionally, the authors recommended the use of full-width bearing pads, more reinforcement in the concrete topping, higher transverse post-tensioning forces, and two ties at each post-tensioning location.

#### Take-Away Points

- Two ties at each post-tensioning location are preferred to single ties.
- Full-depth shear keys show improved performance.
- Additional reinforcement in a cast-in-place topping also resulted in improved performance.
- Higher transverse post-tensioning also led to improved performance.

Miller et al. (1999) evaluated the performance of box girder shear keys with different shear key locations and different grouting materials. Three types of specimens, made of four box beams, were fabricated with a top shear key plus non-shrink grout, a mid-depth shear key plus non-shrink grout, and a top shear key plus epoxy grout. The specimens were fabricated and tested outside under real environmental conditions and thus experienced continuous temperature gradients. For each specimen, a total of 1,000,000 cycles of load (20 kips) were applied on one interior beam and then moved to the other interior beam. The cracks that developed in the shear keys were inspected using ultrasonic pulse velocity. A static load (20 kips) was also applied on

the interior beams separately and simultaneously to check the live load distribution characteristics before and after the development of cracks caused by cyclic loads.

The test results indicated that temperature induced stresses, when a shear key was located near the top of the beam, were consistently high enough to cause significant cracking of the shear key material. These cracks propagated significantly from the two ends near the supports to the bridge mid-span after cyclic loads. Conversely, when the shear key was placed at member mid-depth, the shear key did not experience significant cracking under thermal or live loads. The researchers also found that live loads did not cause new cracking but instead appeared to propagate existing thermal cracks. In addition, static load test results showed that the cracking in the shear key had no significant effect on the live load distributions among box beams, but did cause leakage in the joints.

In the end, the authors recommended the use of a grout material with high bond strength for the joints of the adjacent box girders, even though this results in some concerns such as: thermal compatibility due to the high thermal expansion coefficient of the epoxy, undesired failure in the concrete rather than the epoxy, inconvenience, and the use of poisonous methylethyketone (MEK) for the epoxy.

#### Take-Away Points

- Shear keys located near the top of the beam can experience stresses high enough to induce cracking from temperature changes.
- Cracking tends to start near the ends of the beams.
- Shear keys located near the beam mid-depth did not experience cracking of the joint material.

Follow-up work by Greuel et al. (2000) studied the field performance of a bridge constructed with a mid-depth shear key. Only the shear key was grouted and the gap above the shear key was filled with compacted sand, with a sealant encapsulating the exposed longitudinal joint. Non-prestressed tie rods were used to connect the box beam together before grouting. Field testing was conducted using four Ohio DOT dump trucks—with a total weight ranging from 27 to 32 kips—at various transverse positions. In addition to the static load test, the bridge responses were continuously collected when trucks traveled cross the bridge at a speed of about 50 miles per hour.

The results indicated no significant differential displacement between girders. The authors further concluded that the shear key and transverse rod system adequately resisted the applied live loads.

#### Take-Away Point

- A bridge with only the shear key grouted and non-tensioned transverse rods can result in a bridge that shows no differential displacement under live loads.

Issa et al. (2003) conducted small-scale tests of keyway specimens to investigate the performance of four grout materials using direct shear, direct tension, and flexural tests. The chloride permeability and shrinkage of the four grouts were also measured.

The test results indicated that the polymer concrete showed the highest shear, tensile, and flexural strengths. The polymer concrete also had superior chloride resistance and less shrinkage compared to the other grouts, while the grout had significant shrinkage due to its high water content. In addition, FE analysis of tension test specimens showed that the polymer concrete specimens sustained the highest load with a minimum of cracking and crushing compared to others.

#### Take-Away Point

- Polymer concrete has good strength and chloride resistance characteristics.

Badwan and Liang (2007a) performed a grillage analysis to determine the needed transverse post-tensioning for a precast adjacent, solid, multi-beam deck. The grillage model was established using beam elements for the beams while also considering the stiffness at the keyway locations. Parametric studies were performed to investigate the importance of factors such as skew, deck width, thickness, and span length on the design of such a system.

The results indicated that the required post-tensioning stress decreases with an increase in the deck width, deck thickness, and skew angles (especially for skew angles greater than 30 degrees). The authors note that the influence of skew is due to the fact that transverse bending in the skew direction decreases with skew angle. The span length affects the needed post-tensioning stress when the bridge skew is very large.

In the end, the authors concluded it is adequate to design the needed post-tensioning for such a system (especially with high skew) based on current American Association of State Highway and Transportation Officials (AASHTO) specifications.

#### Take-Away Points

- The amount of post-tensioning decreases with an increased deck width, thickness, and skew.
- Span length affects the needed post-tensioning when the skew is very large.

A literature search conducted by Badwan and Liang (2007b) revealed that little research has been conducted to study the performance of full-depth keyways even though testing has been conducted to investigate the behavior of partial-depth keyways. Thus, the authors implemented field testing and associated FE analysis of a post-tensioned adjacent solid box girder bridge with full-depth keyways, mid-depth shear keys, and transverse post-tensioning.

The 3D FE model was established using solid elements for the concrete and grout and link elements were used for the post-tensioning tendons. During testing, longitudinal strains in the girders were recorded. The adequacy of the FE model was validated using the strain data.

Based on the testing and analytical results, the authors concluded that the lateral load distribution was not affected as long as no cracks were induced in the shear keys. Serviceability issues caused by shear key cracking were not addressed by the authors.

#### Take-Away Point

- Lateral load distribution is not impacted by keyway geometry as long as no cracks are induced in the shear keys.

Dong et al. (2007) established 3D finite element models to investigate and compare the behavior of the three types of joints shown in Figure 2.

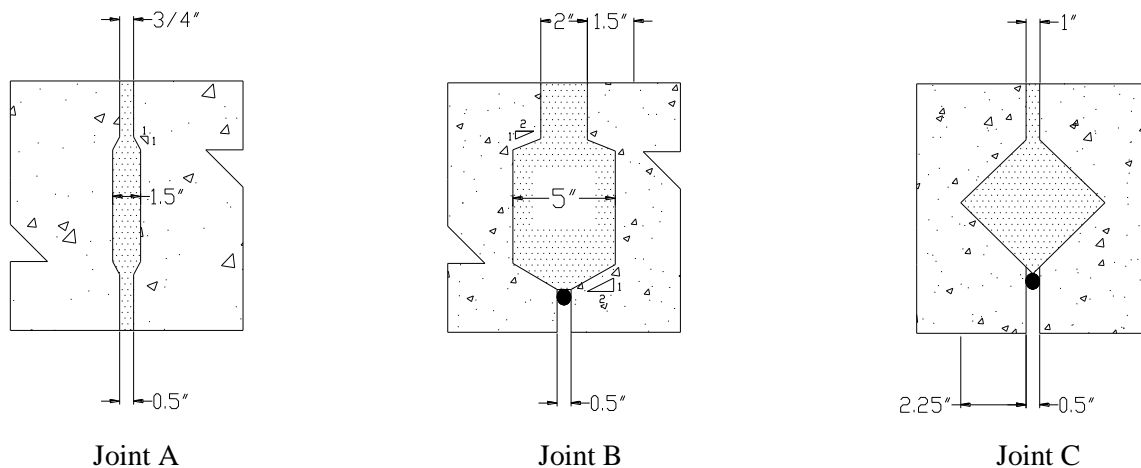


**Figure 2. Basic shear key shapes**

FE models were established using solid elements for both the concrete and grout. Parametric studies were then conducted considering the three types of joints and three strengths of grouts.

The results showed that no cracking was found in the FE model of Joint A, but significant stress concentrations and cracking occurred in joint types B and C. The authors concluded that cracks that developed in Joints B and C were due to the significant change of the keyway shape. In addition, they also found that higher strength grout material does not reduce cracking.

#### Take-Away Point

- Radical changes in shear key geometry (i.e., very sharp corners) may result in higher stress levels.

Sharpe (2007) conducted extensive FE analysis of PCI- and Texas DOT-(TxDOT-)style box girder bridges to investigate the performances of the shear keys. FE models were established using solid elements for the beams, diaphragms, and keyways, and elastomeric bearing pads were modeled using spring elements whose vertical and lateral stiffness were determined based on the material properties of the bearing pad and basic mechanics of materials. The AASHTO HS-25 truck load, strains due to shrinkage, and a temperature gradient were applied to those bridge models. Sharpe considered two types of failure in the shear keys: debonding and cracking (with different failure stresses).

The FE analysis results indicated that reflective cracking was due to high tensile stresses in the shear keys caused by temperature gradients and shrinkage strains instead of live loads. The author also found that these cracks usually developed near the supports instead of at the bridge mid-span. Analytical results showed that composite slabs are most effective at alleviating high tensile stresses in the shear keys although post-tensioning and full-depth keyways also reduce the tensile stresses. Note that the full-depth keyways shown in Figure 3(a) and (b) and examined by Sharpe extend the partial-depth keyways shown in Figure 3(c) and (d) to the beam bottom.

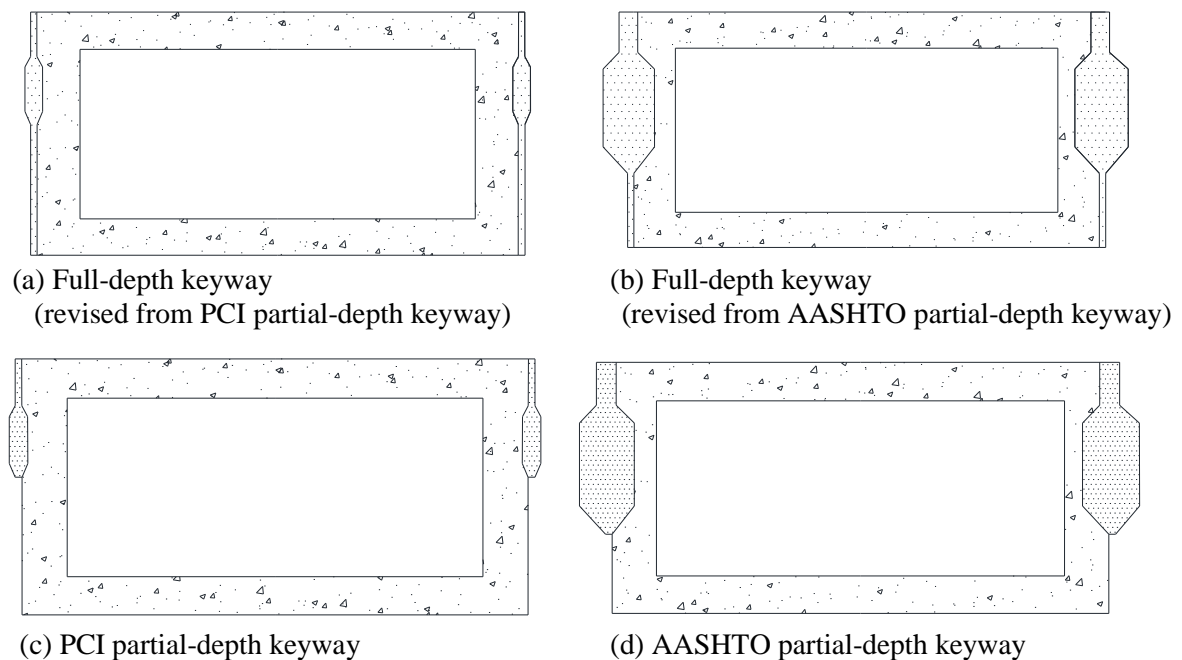


**Figure 3. Keyway geometries for PCI- and TxDOT-style box girder bridges**

#### Take-Away Points

- Cracking is due to shrinkage strains and temperature and not live loads.
- Cracks usually develop near the end of the bridge first.
- Composite slabs are the most effective means of alleviating high tensile stresses.

### 2.3 Publication after 2008

The work done by Attanayake and Aktan (2008) summarized the evolution of the Michigan design procedures for adjacent box beam bridges and their performance since the 1950s. The Michigan Bridge Design Guide had adopted many recommended practices provided in NCHRP Synthesis 393, such as higher transverse post-tensioning forces, full-depth keyways, top shear keys, and using a 6 in. thick cast-in-place concrete deck, as shown in Figure 4.

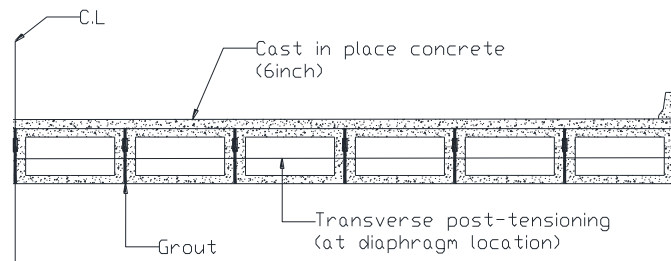


**Figure 4. Typical Michigan keyway geometry and post-tensioning**

The researchers found that reflective cracks were still found in the Michigan adjacent box beam bridges. To identify the main source of the formation of longitudinal reflective cracks, they monitored an adjacent box beam bridge (with narrow, full-depth keyways and top shear keys) starting from construction.

Inspection results revealed that cracks were found at the interfaces between beams and keyways before and after the post-tensioning was applied. They also found reflective cracks in the concrete deck (mostly near supports) 15 days after placement, even before constructing the barrier or applying live loads. The researchers concluded that reflective cracks are due to effects such as hydration heat and drying shrinkage.

#### Take-Away Points

- Cracking forms at the interface between the joint material and the box beam concrete.
- Reflective cracks are principally due to shrinkage.

Kim et al. (2008) presented recent applications of precast adjacent box beam bridges with full-depth keyways with mid-depth shear keys grouted with cast-in-place concrete and transverse post-tensioning in South Korea. The authors performed two-dimensional (2D) FE analysis of three box beam sections without transverse post-tensioning to investigate the performance of four placement conditions for the shear key (i.e., no shear key, top shear key, mid-depth shear key, and bottom shear key) as shown in Figure 5(a), Figure 5 (b), Figure 5 (c), and Figure 5 (d).

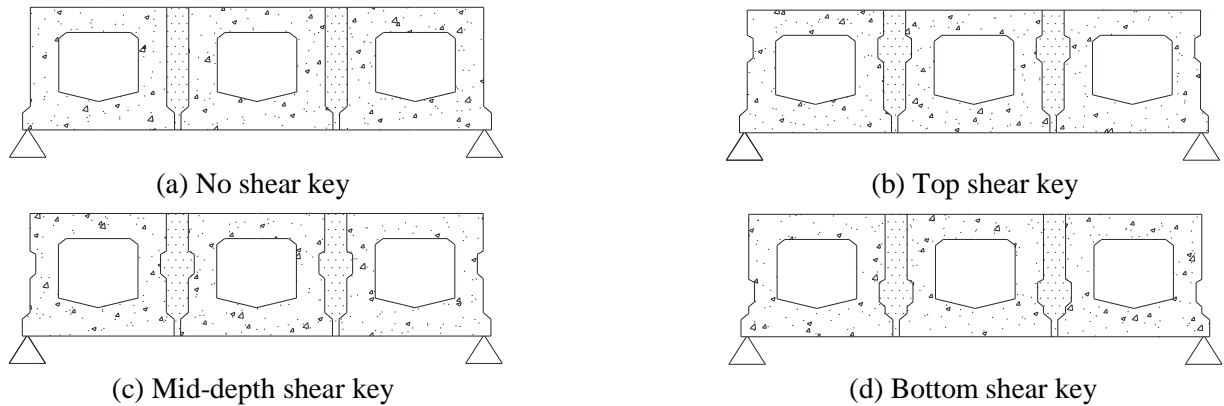


**Figure 5. Common shear key locations**

Various loading and boundary conditions were applied. The beam differential deflection results indicated that the top, mid-depth, and bottom shear keys all showed superior performance compared to no shear key, with the mid-depth shear key performing the best of the four configurations. Sang (2010) confirmed the results and concluded that the location of the shear key does not significantly affect the performance of full-depth keyways.

To verify the feasibility of the proposed full-depth keyway (with the mid-depth shear key grouted with cast-in-place concrete and high transverse post-tensioning), Kim et al. (2008) conducted flexural testing and 3D FE modeling of a three-box beam specimen. The failure and cracking loads both exceeded the ultimate load and service load based on the Korea design code, which is similar to the AASHTO bridge design specifications. No longitudinal cracks were found in the joints when the specimen sustained service and ultimate loads. The relative displacements indicated that effective load transfer by the shear key connections was occurring.

Kim et al. (2008) also conducted fatigue testing (2 million cycles) of the three-box beam specimen. The test results indicated that no cracks were found in the longitudinal joints and the specimen exhibited excellent fatigue resistance with the residual deflection being recovered 24 hours after fatigue testing.

Finally, Kim et al. (2008) applied the proposed full-depth keyway to an actual bridge. Field tests were conducted using static and moving dump trucks on the bridge. The authors concluded that the box beam bridge performed well structurally under static and moving dump truck loads. Further, no longitudinal cracking in the keyway joints was reported by the authors.

It should be pointed out that long-term behavior of the three-box beam specimens and the constructed bridge were not evaluated.

#### Take-Away Point

- Mid-depth shear key placement results in the best joint performance—particularly when used with high post-tensioning and cast-in-place concrete.

Attanayake and Aktan (2009) developed a simple analytical model consisting of plate elements based on the macro-mechanics concept. In this model, the plate element represents a combination of two half-box beam sections, one shear key, and the concrete deck. The cross-section of the plate element had the identical section properties as those of the combination cross-section. The stiffness of the box beam sections, shear keys, and concrete deck were calculated and then incorporated into the plate elements. The transverse moments along the longitudinal joints between the adjacent beams were determined from the macro-mechanical model based on the AAHSTO LRFD Bridge Design Specifications. These calculated moments were then used to determine the needed transverse post-tensioning. Further, the authors demonstrated a design example in their paper.

#### Take-Away Point

- Macro-mechanical modeling fails to simulate the interaction between the keyway and the beam.

Follow-up work by Ulku et al. (2010) proposed a rational design procedure utilizing the macro-mechanical model developed by Attanayake and Aktan (2009) to calculate the transverse moments along the transverse joints, and thus determine the required transverse post-tensioning. The concept is based on the use of multi-stage post-tensioning to minimize the longitudinal cracking in the keyway and reflective cracking in the concrete deck.

A 3D FE model was established using solid elements for the beams, keyways, diaphragms, and deck. Multi-stage post-tensioning after grouting the keyway and after the deck placement was simulated.

The authors concluded that the two stage post-tensioning process is effective at reducing cracking issues for the bridge subjected to dead and live loads and temperature effects. However, in their designs, the tensile stresses in the deck near the fascia beams due to live loads are significant and may not be easily offset by two-stage post-tensioning.

The authors also found that the temperature gradient is the main factor causing the cracks, which developed at the interface of the top shear keys. Another cause of cracks is that the post-tensioning is not uniformly distributed at the keyway because of shear lag.

#### Take-Away Points

- Two stage post-tensioning may minimize longitudinal cracking.
- The temperature gradient is the main factor causing cracks to develop at the joint interface.

Sang (2010) performed grillage analysis of adjacent box girder bridges subjected to live loads to determine shear forces and moments that must be sustained by the shear keys. Subsequently, the performance of the keyway joint was investigated using a 2D FE model, which sustained loads equivalent to the shear forces and moments derived from the grillage model. The FE model was

established using plane strain elements for the concrete and the grout, which share common nodes at the interfaces. Shear tests were conducted to examine the failure modes of the keyway joints grouted with cementitious grout and epoxy. The test results were also used to validate the adequacy of the FE model. Finally, parametric studies were performed using the validated FE models to investigate the influences of keyway geometry, grouting materials, post-tensioning, and bearing locations on the performance of the shear key.

Fiber-reinforced cementitious material was recommended by the author to grout the shear key due to its high tensile strength and was also used in the FE shear key models, although no previous research was found in the literature using fiber-reinforced concrete for grouting the shear key. Based on the FE analysis results, the author concluded that cracks developed in both the full-depth and partial-depth keyways using cementitious grout, while cracks were found in only the partial-depth keyways but not in the full-depth shear key using the epoxy grout and fiber-reinforced cementitious grout.

The author also found that the vertical locations of the shear key did not affect its behavior. The author recommended using a higher transverse post-tensioning force upon finding that the post-tensioning specified by the Pennsylvania DOT (PennDOT) was not enough to provide crack resistance.

The FE results indicated that the shared bearing pad (bearing under the shear key as shown in Figure 6(a)) reduces the cracks in the shear key relative to isolated bearing pads (bearing under the beam flanges as shown in Figure 6(b)).



**Figure 6. Common bearing pad details**

#### Take-Away Points

- Epoxy grout and fiber-reinforced cementitious materials perform well when used in a full-depth shear key.
- High post-tensioning may be needed to completely eliminate cracking.

Fu et al. (2011) proposed an approach to designing the required post-tensioning for a solid, multi-beam bridge system based on the shear friction concept and FE modeling techniques. The FE models were established using solid elements, link elements, and contact elements for the beams, post-tensioning ties, and interfaces between the shear key and the beam. The adequacy of the FE models were validated against the strain data collected during field tests using an on-site controlled dump truck.

Based on the FE results, the authors recommended different levels of post-tensioning for bridges with different span lengths. The authors found that the boundary conditions had great influence on the predicted bridge response. They found that the post-tensioning does not affect the live load distribution until cracks develop in the keyway and/or concrete topping. Finally, the authors gave recommendations for improving the use of shear keys in Maryland (e.g., using a two-staged construction sequence, such as 16.7% and 100% of the designed post-tensioning of design level before and after grouting the keyways, and using full-depth shear keys).

### Take-Away Points

- Bridges of different span lengths may require different amounts of post-tensioning.
- Two-stage post-tensioning may help reduce the development of cracks.

With the goal of achieving simple and economic fabrication and construction of precast adjacent box girder systems, Hanna et al. (2011) developed and evaluated two types of non-post-tensioned transverse connection details that don't use diaphragms or a concrete deck (i.e., the wide joint system and the narrow joint system shown in Figure 7.

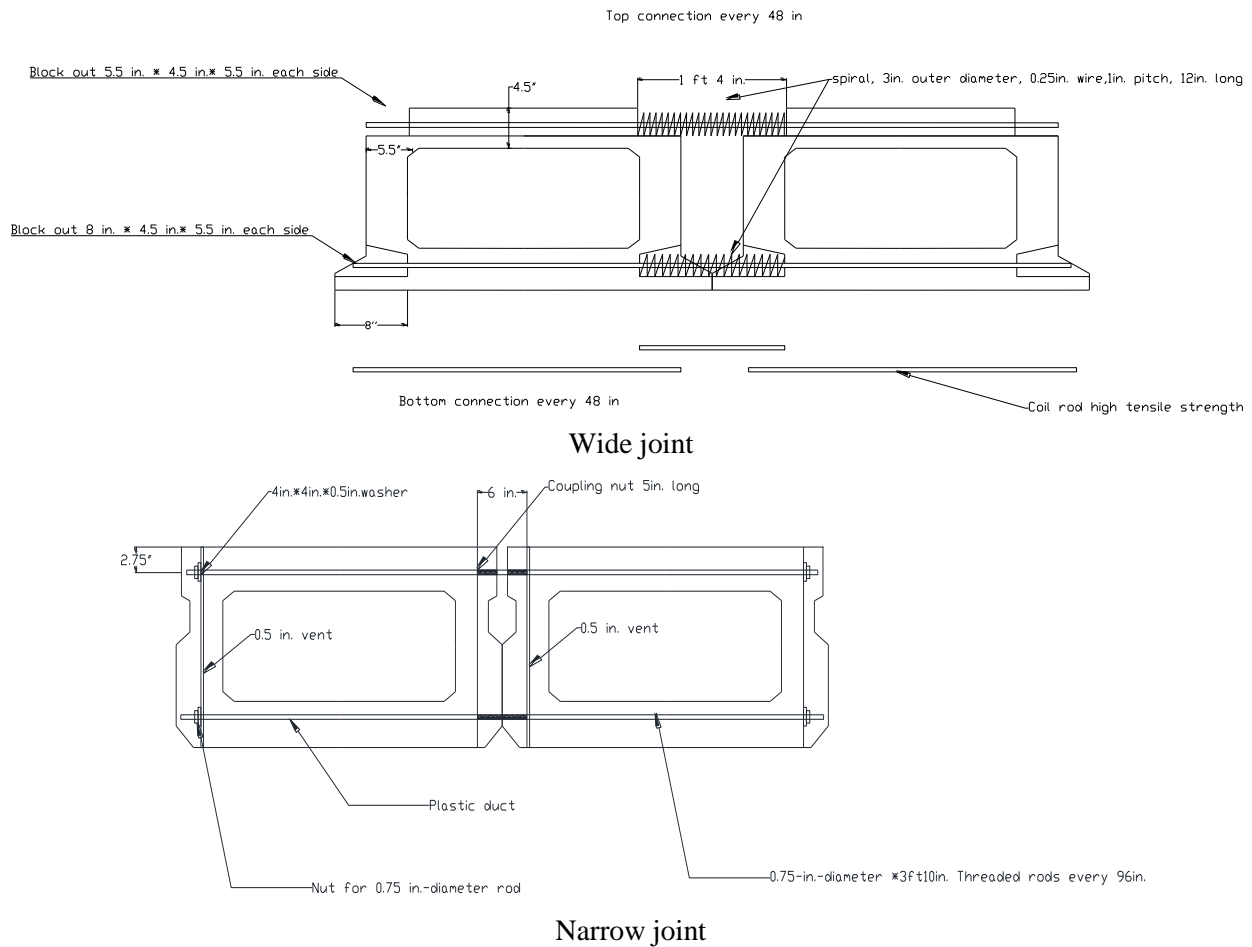


**Figure 7. Connection details proposed by Hanna et al. 2011**

The two systems were developed based on the AASHTO/PCI and the Illinois DOT (IDOT) box beam connection details, respectively. The wide joint system incorporates a wide full-depth keyway joint filled with cast-in-place concrete and utilizes top and bottom reinforcement placed in the top and bottom flanges of the box beams to resist transverse tensile stresses. The narrow joint system incorporates a narrow joint with a partial-depth keyway, top shear key, and non-shrink grout, and utilizes top and bottom threaded rods placed in the top and bottom flanges of the box beams to resist the transverse tensile stresses.

3D FE models were established using shell elements for the beam flanges and webs and frame elements for the reinforcement and threaded rods. Design charts were developed for determining the needed tension force at the connection (i.e., the required amount of reinforcement or number of threaded rods).

Two-beam specimens using the two systems were fabricated and tested under cyclic loads. Water dams were constructed on the top surface of the specimens to monitor for crack development and water leakage.

Test results indicated that, for the two system specimens, neither cracks nor water leakage were found in the keyway after 2 million cycles, and the differential deflections were found to be below 0.07 in. after 3 million cycles. However, in their study, no apparent consideration was given to performance under thermal loads.

#### Take-Away Point

- It may be possible to design a bridge without transverse post-tensioning that performs adequately.

Follow-up work by Hansen et al. (2012) developed another joint system based on the narrow joint system proposed by Hanna et al. (2011). This system was developed without using diaphragms or concrete topping and utilizes post-tensioning to reduce the possibility of cracking or leakage. As shown in Figure 8, the sleeves, located below the beam top flange and above the bottom flange, were used to accommodate the duct, the post-tensioning rods, and couplers.

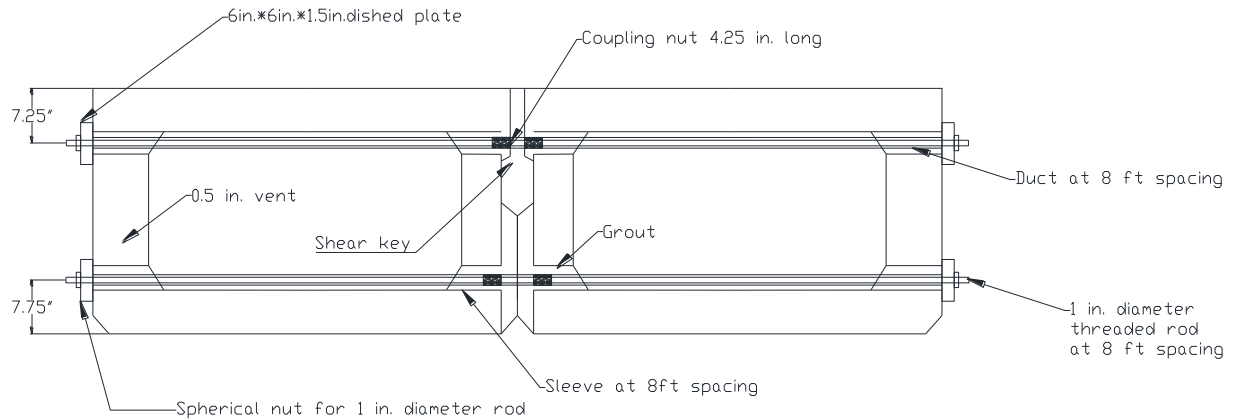


**Figure 8. Connection details proposed by Hansen et al. 2012**

The required post-tensioning was determined based on the design chart for the required tension force in the connection developed by Hanna et al. (2009). Experimental testing was conducted for four-box beam specimens placed in a cantilever and mid-span loading setups, successively.

In the cantilever setup, the specimen was supported at the transverse center and edge and a load with 5 million cycles was applied on the joint. In the mid-span loading setup, the specimen was supported at the two transverse edges and the load was applied on the specimen center.

Results indicated that no significant strain change, cracking, or leakage near the shear key region occurred. The authors recommend this system for actual bridge construction. However, temperature gradient and shrinkage effects were not considered in their study.

#### Take-Away Point

- A cast-in-place topping may further improve the performance of a non-post-tensioned box beam bridge.

Grace et al. (2012) inspected a bridge in Michigan that was constructed based on recent Michigan design procedures. The bridge had two simply supported spans of 122.5 ft, seven diaphragms with post-tensioning bars that were highly post-tensioned before grouting, and full-depth keyways with a top shear key and a concrete deck.

The inspection results found that significant longitudinal cracks were formed in the shear key and deck even though the traffic on the bridge was light and was judged to not likely have induced the cracks. In addition, inspection on some other adjacent box girder bridges in Michigan revealed that reflective cracks had formed in their decks.

To investigate the source of the cracks, the researchers conducted an experimental test of a bridge specimen in the laboratory. A four-point concentrated load up to the service load of 80

kips was applied on the specimen, and no reflective cracks in the deck were found even when the transverse post-tensioning decreased to zero.

The authors concluded that the traffic loads were not the main cause of the reflective cracking in the bridge decks. Thus, the authors considered temperature effects in subsequent FE analyses.

The FE model was established using solid elements for the beams, diaphragms, and deck, and link elements for the post-tensioning ties. After the FE model was validated against the results from the experimental tests, FE analyses of actual bridges were performed considering dead and live loads and temperature gradients according to the AASHTO bridge design specifications.

Based on the FE results, the required amount of transverse post-tensioning required to mitigate reflective cracking for the actual bridges was then established. For practical applications, the required number of diaphragms and the required amount of post-tensioning per diaphragm were given for the adjacent box beam bridges in Michigan.

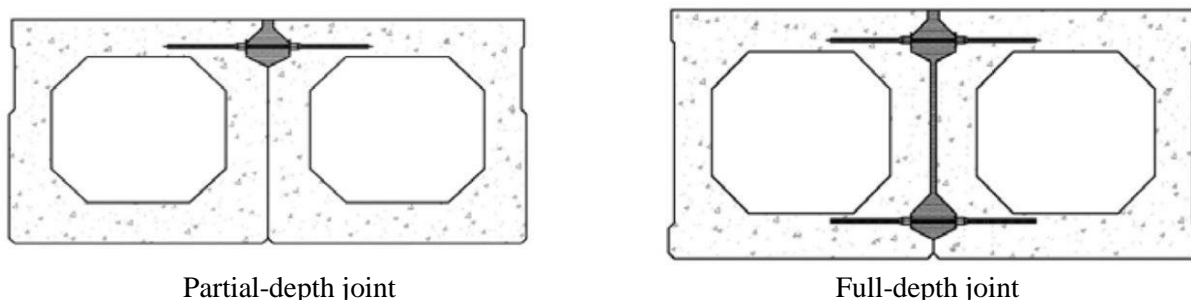
The authors found that the post-tensioning effects were mainly localized at the diaphragm regions due to shear lag effects and the required number of diaphragms for eliminating reflective cracks increases with an increase in span length, while the required post-tensioning increases with increased bridge width.

#### Take-Away Points

- Traffic loads are not the primary factor in the development of cracks.
- Temperature-induced effects may be the primary source of crack development.

#### 2.4 FHWA-UHPC Joint Test

Yuan et al. (2014) developed and two joints filled with UHPC. Figure 9 shows the two joint configurations: partial-depth and full-depth.



Yuan et al. 2014

**Figure 9. UHPC joints**

The joint was reinforced at the interface between the joint material and the box girder by the reinforcement extending out from the box girder (Yuan and Graybeal 2016).

Both joints were subjected in the laboratory to simulated daily temperature change and cyclic traffic loading. The temperature loading was applied by pumping steam through a copper tube embedded in the beams. The traffic load was simulated by four-point cyclic bending. The maximum loading applied on the beam was about 80 kips, which is approximately the distributed load on a single beam from a design truck based on the AASHTO LRFD Bridge Design Specifications (2013).

During the thermal and cyclic loading test, no cracking initiated and the connection detail was deemed a “structural success.” In many ways, the details developed and tested by the FHWA have become the standard by which other connections might be evaluated.

## 2.5 HDR Box Girder Design

Given that part of this research involves the performance comparison between UHPC joints and innovative non-UHPC joints, the box girder used in this project was designed based on the UHPC jointed box girder design. Figure 10 shows the details of the box girder jointed using UHPC developed by HDR, Inc.

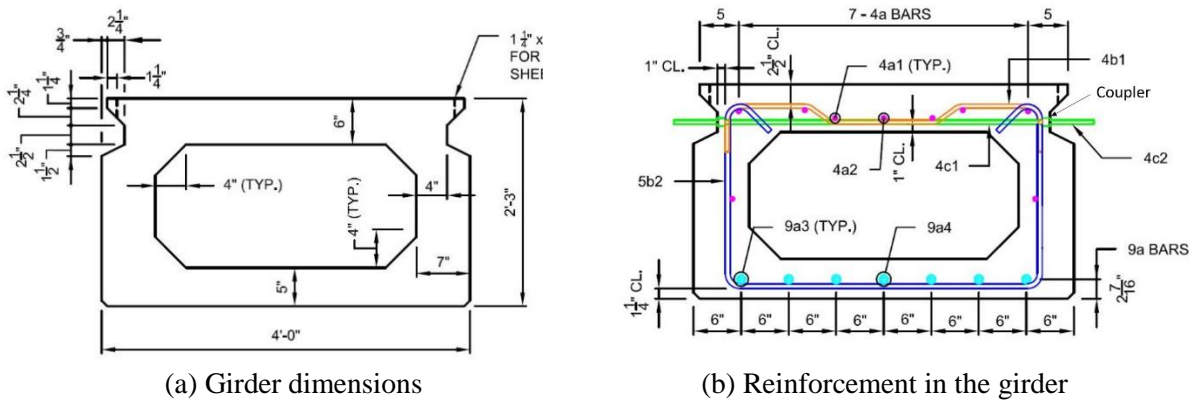


**Figure 10. Design of box girder jointed by UHPC**

As shown in Figure 10(b), the green bar (4c2) extends from the box girder into the UHPC-filled joint. The outside portion, which will be in the joint, was connected to the transverse reinforcing steel bar in the box girder by a coupler.

## 2.6 Literature Search Synthesis and Summary

A significant amount of information related to adjacent box beams was presented and summarized in this chapter. Although there are many important points to take away from these sources, the following synthesis and summary was formulated to provide a brief synopsis of the

information that had the greatest impact on the design of the innovative joint and the testing plan for this research.

Cracking of the shear key between adjacent box beams appears to principally be a service-related problem, as multiple sources indicate that even with a cracked joint, a bridge can continue to effectively distribute loads throughout the primary load carrying members. With regards to cracking, it appears that cracking tends to be most prominent at the interface between the joint material and the box beam due to the low bond strength. Use of a shear key may induce stress concentration in the joint. Further, cracking seems to first initiate near the ends of beams.

Consistent throughout the literature is the conclusion that joints that use full-depth keyways have the best performance. The use of transverse post-tensioning seems to be the most effective when two ties are used at each location (e.g., one near the top and one near the bottom) with high amounts of force. However, there have been some reported instances where no post-tensioning also performed well.

Cracking does not seem to be first initiated by the application of live loads. There are, however, differing opinions on the relative contribution to cracking from shrinkage and temperature. Nevertheless, once cracking is initiated by either shrinkage and/or temperature, cracks can continue to grow with subsequent live load application.

To summarize information useful for the design of the innovative joint and the development of testing plans, design/construction aspects, FE analyses, and testing on adjacent box beam bridges were grouped into four tables. These four tables were found to be very helpful in developing the plan for the analytical and experimental evaluations:

- Design and construction attributes for the adjacent box girder bridges in studies reported above are summarized in Table 4.
- FE analysis details are summarized in Table 5.
- Laboratory tests of small-scale, medium-scale, and full-scale specimens are summarized in Table 6.
- Field testing of adjacent box girder bridges are summarized in Table 7.

**Table 4. Design and construction attributes**

References	Keyway Geometries	Transverse Tie Details	Diaphragms	Grout	Keyway Preparation	Bearing Details	Construction Sequence	Concrete Deck	FE Analysis	Laboratory Testing	Field Testing
Huckelbridge 1995	Partial-depth keyway	Girder mid-height; Non-post-tension mild steel (1 in. diameter)	Yes	NG	NG	NG	NG	None	Yes	No	Yes
Gulyas et al. 1995	Full-depth keyway and top shear key; Narrow joint	No	No	Non-shrink grout; MAP mortars	Sandblast/wash off	NA	NA	NA	No	Yes	No
El-Remaily et al. 1996	Partial-depth keyway and top shear key (pocket near diaphragms)	Post-tensioning (determined by design calculations)	5	NG	NG	NG	Post-tensioning after grouting	No	Yes	No	No
Huckelbridge and El-Esnawi 1997	Partial-depth keyway and top and mid-depth shear keys	No	No	Non-shrink grout; MAP mortars; epoxy	Power grinder and wire brush; sand-blaster	NA	NA	No	Yes	Yes	No
Lall et al. 1998	Full-depth keyway and top shear key	Two post-tensioning ties at third points in depth	More than 3	NG	Sandblast, cleaned, and pre-wetted	Full width bearing	NA	Yes	No	No	No
Greuel et al. 2000	Partial-depth keyway and mid-depth shear key	Non-post-tensioned rods	5	NG	NG	Neoprene bearing pad	Grout after installing rods	2.5 in. asphalt wearing surface	No	No	Yes
Miller et al. 1999	Partial-depth keyway and mid-depth shear key (Pocket near diaphragms)	Slightly post-tensioned rods	5	Non-shrink grout; epoxy	NG	NG	Post-tensioning before grouting	No	No	No	Yes
Issa et al. 2003	Full-depth keyway and mid-depth shear key	No	No	Set 45; set 45 HW; set grout; polymer concrete	Sandblast; air pressure and high pressure washing	NA	NA	NA	Yes	Yes	No
Badwan and Liang 2007a	Full depth and mid-depth shear key	Bonded post-tensioning tendons	No	NG	NG	NG	Post-tensioning before grouting	No	Yes	No	No
Badwan and Liang 2007b	Full-depth keyway and mid-depth shear key	Bonded post-tensioning tendons	No	NG	NG	NG	Post-tensioning before grouting	No	Yes	No	Yes
Dong et al. 2007	Full depth and mid-depth shear key; partial-depth keyway and mid- (bottom-) shear key	No	No	Yes	NG	NG	NA	No	Yes	No	No
Sharpe 2007	Partial-depth keyway and top shear key; Full-depth keyway and top shear key	Unbonded post-tensioning tendons	Spaced at 10 ft	Non-shrink grout	NG	Elastomeric bearing pads	NG	Yes	Yes	No	No
Attanayake and Aktan 2008	Full-depth keyway and top shear key (1.5-3 in.)	Bonded post-tensioning tendons	6	Type R-2, which is cement and fine aggregate mixture with 14 +/- 4% air	NG	NG	Post-tensioning after grouting	Yes	No	No	Yes

References	Keyway Geometries	Transverse Tie Details	Diaphragms	Grout	Keyway Preparation	Bearing Details	Construction Sequence	Concrete Deck	FE Analysis	Laboratory Testing	Field Testing
<b>Kim et al. 2008</b>	FEA: Full-depth keyway and no, top, mid-depth or bottom shear keys Test: Full depth and mid- depth shear keys (2-4.8 in.)	Bonded post-tensioning tendons	5	Cast-in-place concrete	NG	Elastometric rubber pad	NG	Yes	No	No	Yes
<b>Attanayake and Aktan 2009, Ulku et al. 2010</b>	Full-depth keyway and top shear key (1.5-3 in.)	Unbonded post-tensioning tendons	5-7	NG	NG	NG	Multi-staged construction: Post-tensioning after grouting and after deck placement	Yes	Yes	No	No
<b>Sang 2010</b>	Full-depth keyway and top shear key; Partial depth and top shear key	Post-tensioning tendons	NG	Fiber reinforced cementitious material; cementitious material: epoxy	NG	Placed under the keyway	Post-tensioning after grouting	Yes	Yes	Yes	No
<b>Fu et al. 2011</b>	Full-depth keyway and top shear key	Post-tensioning threaded rods	No	Non-shrink grout	NG	NG	Post-tensioning before grouting	Yes	Yes	No	Yes
<b>Hanna et al. 2011</b>	Full-depth keyway and no shear key; Partial depth and top shear key	Non-post- tensioning reinforcement; Non-post-tensioning threaded rods	No	Cast-in-place concrete; Non-shrink grout	Roughened	NG	NA	No	Yes	Yes	No
<b>Jenna et al. 2012</b>	Partial-depth keyway and top shear key	Non-post- tensioning threaded rods	No	Non-shrink grout	Roughened	Neoprene bearing pad	Post-tensioning after grouting	No	No	Yes	No
<b>Grace et al. 2012</b>	Full-depth keyway and top shear key	Unbonded post-tensioning CFRP	From FEA	Non-shrink grout	NG	Neoprene bearing pad	Post-tensioning after grouting	Yes	Yes	Yes	No

MAP = magnesium ammonium phosphate, NA = not applicable, CFRP = carbon fiber reinforced polymer; NG = not given

**Table 5. Summary of FE analysis**

References	Type of Analysis	Software	Box Beam	Keyway	Interface	Diaphragm	Deck	Tie	Bearing	Load
Huckelbridge 1995	NG	NG	NG	NG	NG	NG	NG	NG	NG	NG
El-Remaily, et al. 1996	Grillage analysis	NG	Beam elements	Common nodes	Common nodes	beam elements	None	NA	Simply supported	Dead and live loads (including barriers)
Huckelbridge and El-Esnawi 1997	3D	SAP	Solid elements	Solid elements	Common nodes	Solid elements	None	Directly apply forces	Simply supported	Concentrated load
	2D	SAP	Plane elements	Plane elements	Common nodes	None	None	None	Spring elements	Concentrated load
Issa et al. 2003	3D	ANSYS	Solid elements	Solid elements	Common nodes	None	None	None	NA	Concentrated load
Badwan and Liang 2007a	Grillage analysis	ANSYS	Beam elements	Common nodes	Common nodes	Beam elements	None	NA	Simply supported	HS-25 truck
Badwan and Liang 2007b	3D	ANSYS	Solid elements	Solid elements	Common nodes	None	None	Link element	Simply supported	Dump truck
Dong et al. 2007	3D	ABAQUS	Solid elements	Solid elements	Common nodes	None	None	None	NA	Concentrated load
Sharpe 2007	3D	ANSYS	Solid elements	Solid elements	Common nodes	Solid elements	Solid elements	None	Spring elements	HS-25 truck; shrinkage; thermal gradient
Kim et al. 2008	2D	DIANA	Plane elements	Plane elements	Common nodes	None	None	None	Simply supported	Concentrated load
	3D	DIANA	Solid elements	Solid elements	Common nodes	Solid elements	Solid elements	Bar elements	Simply supported	Concentrated load
Attanayake and Aktan 2009	Maro-mechanical model	Programming	Integrated Plate elements	Integrated Plate elements	NONE	None	Integrated Plate elements	None	Simply supported	HL-93
Ulku et al. 2010	3D	ABAQUS	Solid elements	Solid elements	NONE	Solid elements	Solid elements	Truss elements	Simply supported	HL-93
Sang 2010	Grillage analysis	NG	Beam elements	Common nodes	Common nodes	Beam elements	None	NA	Simply supported	HS-25 truck
	2D	ABAQUS	Plane elements	Plane elements	Common nodes	None	None	None	NA	Concentrated and distributed loads
Hanna et al. 2011	3D	SAP2000	Shell elements	Common nodes	Common nodes	None	None	Frame elements	Simply supported	HL-93
Fu et al. 2011	3D	ANSYS	Solid elements	Solid elements	Contact elements	None	None	Link elements	Simply supported	HL-93
Grace et al. 2012	3D	NG	Brick elements	Brick elements	Contact elements	Brick elements	Brick elements	Truss elements	Simply supported	HL-93 and temperature gradient

NG = not given, NA = not applicable

**Table 6. Summary of laboratory testing**

References	Testing Scale	Specimens	Length	Skew	Width	Depth	Number of Beams	Grout strength	Concrete Strength	Load	Temperature	Relative Displacement	Strain	Crack Detection
<b>Gulyas et al. 1995</b>	Small scale	Keyway specimens	3.25 in.	NA	6-6.5 in.	7-14 in.	NA	Non-shrink grout: 5.9 ksi; MAP mortars: 7.3 ksi	NG	Vertical shear; Direct tension; Longitudinal shear	No	NA	NA	Visually
<b>Huckelbridge and El-Esnawi 1997</b>	Small scale	Multi-beam slices	12 in.	0°	144	33 in.	3	Non-shrink grout: 5.5 ksi; MAP mortars: 5 ksi; epoxy: 13 ksi	6 ksi	Cyclic concentrated load	No	Direct Current Differential Transducer (DCDT)	Foil-backed strain gauges	Visually
<b>Issa et al. 2003</b>	Small scale	Keyway specimens	5-6 in.	0	17-21 in.	17-26 in.	NA	Set 45: 5.8 ksi; set 45 HW: 5.6 ksi; set grout: 7.7 ksi; polymer concrete: 10.8 ksi	6.5 ksi	Direct shear; Direct tension; Flexural bending	No	NG	NG	Visually
<b>Kim et al. 2008</b>	Full scale	Multi-box beam specimens	61 ft	0	95 in.	31.5 in.	3	4.9 ksi	8 ksi	Static concentrated load/ Cyclic concentrated load (Mid-span)	No	Linear variable differential transducers (LVDTs)	Strain gauges	Visually
<b>Sang 2010</b>	Small scale	Keyway specimens	5 in.	0	7 in.	17 in.	NA	Cementitious grout: 4.5 ksi; epoxy: 10 ksi	11.3	Direct shear	No	NG	NG	Visually
<b>Hanna et al. 2011</b>	Medium scale	Multi-box beam specimens	8 ft	0	8 ft	27 in.; 32 in.	2	6 ksi	8 ksi	Cyclic concentrated load	No	Yes	No	A water dam
<b>Jenna et al. 2012</b>	Medium scale	Multi-box beam specimens	8 ft	0	16 ft	27 in.	4	Non-shrink grout: 10 ksi	8 ksi	Cyclic concentrated load	No	Yes	No	A water dam; Visually
<b>Grace et al. 2012</b>	Full scale	Multi-box beam specimens	20 ft	0	75 in.	14 in.	4	Low-shrink grout: 8 ksi	Beam: 6 ksi; Deck: 5.7 ksi	Service concentrated load up to 80 kips	No (Recognize importance of temperature effects)	NG	No	Visually

NG = not given, NA = not applicable

**Table 7. Summary of field testing**

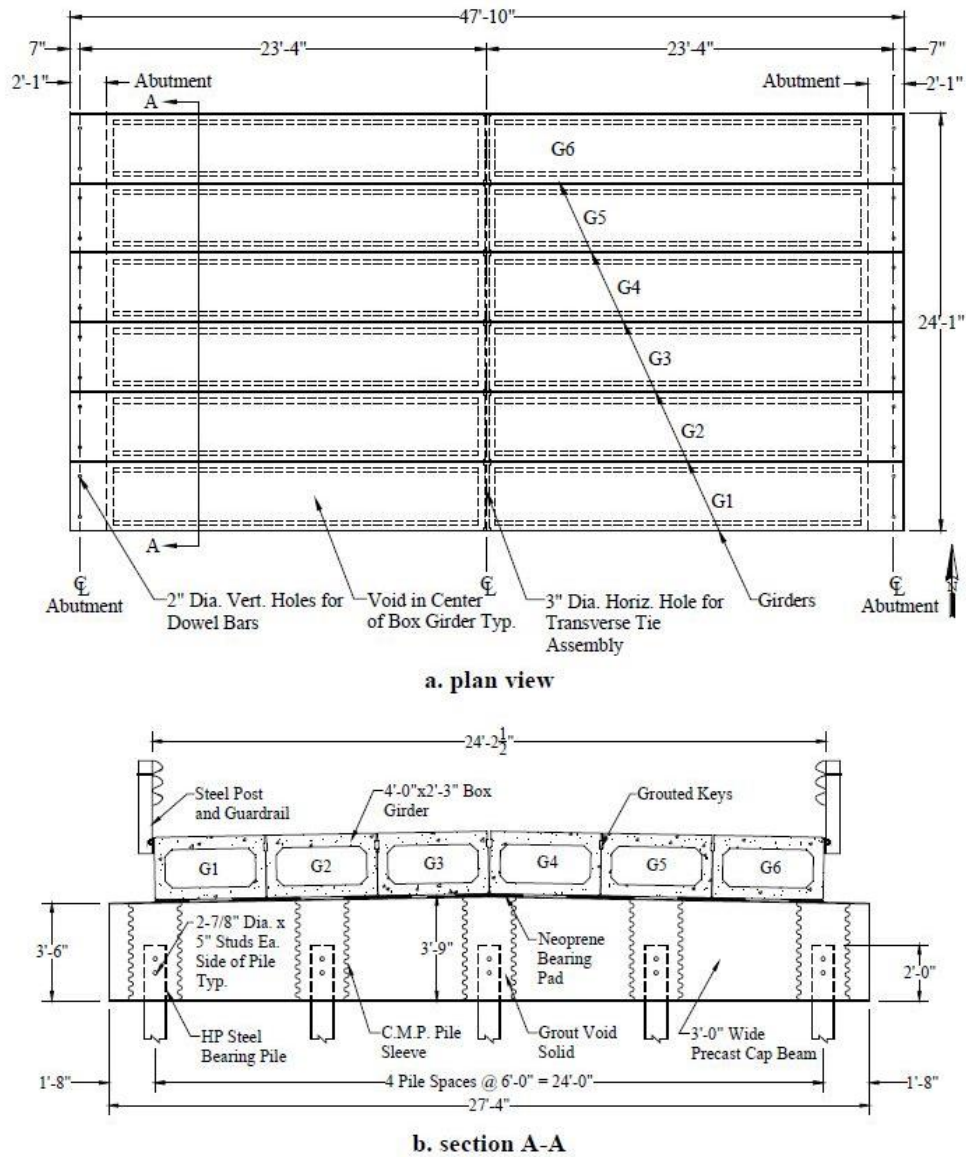
References	Bridge	Number of Spans	Span (ft)	Skew (degree)	Width (ft)	Number of beams	Beam width × depth (in.)	Grout Strength	Concrete Strength (ksi)	Temperature	Load	Relative Displacement	Strain	Crack Detection
Huckelbridge et al. 1995	No. 1	1	32.5	20	44	11	48 × 17	NA	NA	NG	50 kips dump truck (12 +38 kips)	Relative displacement transducers (Own made)	Vibrating wire gauge	Visually
	No. 2	4	40/54/54/40	17.4	68	17	48 × 27			NG				
Miller et al. 1999	4 (with same girders, different grouting)	1	75	0	16	4	48 × 33	5 ksi	Beam: 9.4	Yearly range: - 10-100 °F; summer: 50-90 °F	20kips on the loaded interior beam	Direct current differential transducer (DCDT)	Transverse omega clip gauges; vibrating wire gauge	Ultrasonic pulse velocity
Greuel et al. 2000	1	1	115.5	0	48	12	48 × 42	NG	Beam: 10	NG	Ohio DOT truck similar to HS-20 truck	Linear variable differential transformer (LVDT)	Vibrating wire gauge; foil strain gauges	NG
Badwan and Liang 2007b	1	2	29/29	30	44	6	87 × 15-18	NG	NG	NG	29 kips dump truck (9+20 kips)	No	Strain transducer	NG
Attanayake and Aktan 2008	1	2	79/79	0	93.5	22	48 × 33	NG	Deck: 6.4	Early summer	No	No	No	Visually
Kim et al. 2008	1	2	43/43	5	39	14	30 × 31.5	4.4 ksi	Beam: 7.3	NG	77.2 kips dump truck (16.7+60.5 kips)	Linear variable differential transducers (LVDTs)	Strain gauges	Visually
Grace et al. 2012	1	1	35	0	33	11	36 × 15	NG	Beam: 7.0; Deck: 4	NG	35 kips dump truck (10.8+24.2 kips)	No	Strain sensor	NG

NG = not given, NA = not applicable

## CHAPTER 3. FIELD BRIDGE INSPECTION

### 3.1 Inspection Results from Bridge-A: Madison County, Iowa

The first bridge inspected is located in the southern part of Madison County, Iowa. Figure 11 shows the plan and cross-section views of the bridge.



Phares 2009

**Figure 11. Madison County, Iowa bridge**

The bridge is a single span box girder bridge with a length of 47 ft and a width of 24 ft. The bridge consists of six adjacent box girders that were connected by partial depth narrow joints with a shear key. The joint was filled with Five Star Grout. The bridge was built in 2007 and

inspected in September 2014. No cracks were observed, and, overall, the bridge appeared to be in very good condition.

### 3.2 Inspection Results from Bridge-B: Buena Vista County, Iowa

The second bridge is located in Buena Vista County, close to Storm Lake, Iowa. Figure 12 shows the bridge plan and cross-section views.

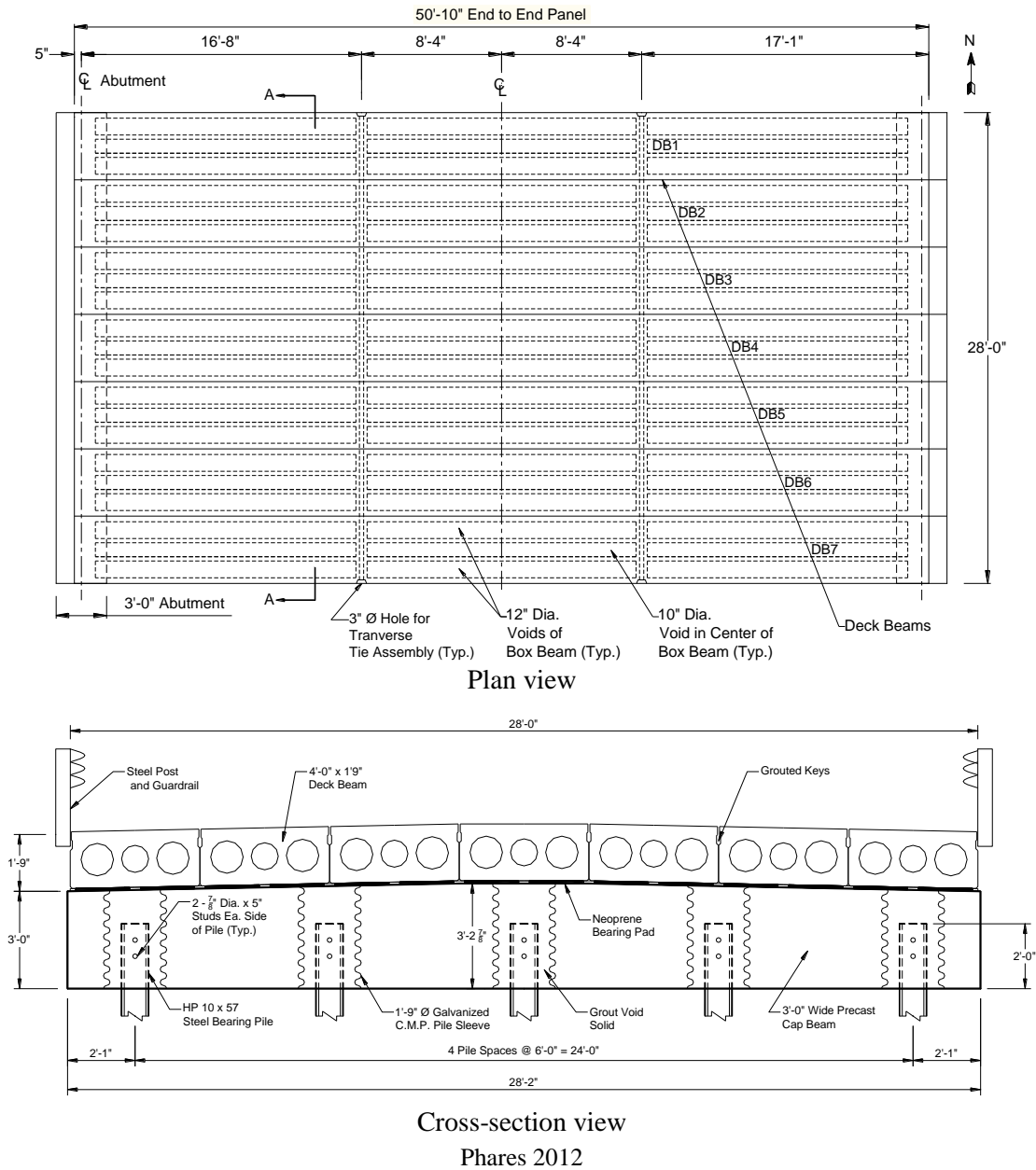


**Figure 12. Buena Vista County, Iowa bridge**

The bridge consists of seven precast, prestressed box beams that are connected by a partial-depth narrow joint with a shear key. The bridge is about 28 ft wide and 51 ft long and was constructed in 2009.

A bridge inspection was conducted on this bridge in April 2014. Significant water leakage issues were found between the box beams. Figure 13 shows the water staining at the bottom of the bridge girders near the abutment.



Phares 2012

**Figure 13. Water leakage stains under the Buena Vista County, Iowa bridge**

## CHAPTER 4. SPECIMEN DESIGN AND CONSTRUCTION

Based on the findings of the literature review, joint cracks are suspected to be caused by low bond strength between the joint material and box girder, large shrinkage of joint material, stress concentrations near the shear key, and temperature changes. Some potential solutions noted by previous research include the use of low-/zero-shrinkage material, increased bond strength and shear strength, and additional reinforcement in the joint.

Incorporating these potential and other concepts, an innovative joint (shown in Figure 14) was designed with the following features: wide joint (6-1/2 in.) without shear key, shrinkage-compensating concrete mixed with Type K cement, form retarder to create a rough surface on the sides of the box girder to increase the shear capacity, and reinforcing steel that crosses the interface between the joint and box girder.

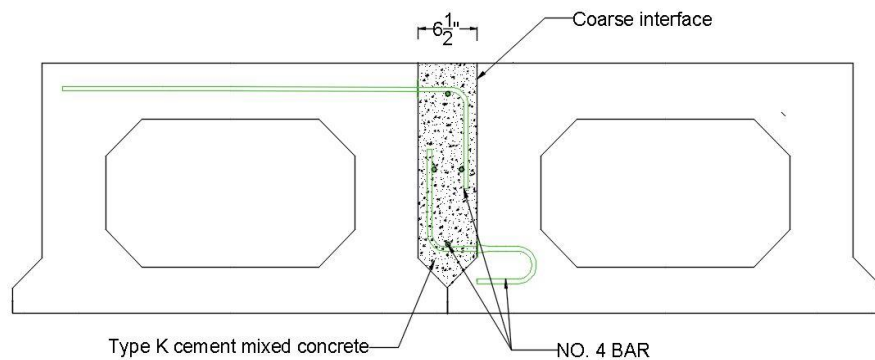


**Figure 14. Innovative joint design**

In this chapter, the innovative design features are detailed in Sections 4.1 through 4.4. A specimen consisting of two adjacent box girders with one joint in between was constructed in the Iowa State University Structural Engineering Research Laboratory. Sections 4.5 and 4.6 detail the construction of the box girders and the innovative joint.

### 4.1 Wide Joint

Traditional joints between adjacent box girders in the US are narrow joints (3/4 to 1-1/2 in.) and can either be partial- or full-depth. The joints were usually designed with one or more shear keys near the top, middle, or bottom of the joint. These shear keys are thought to provide better transfer of transverse moment and shear between the adjacent box girders.

However, past studies indicate that shear keys in the joint can introduce stresses high enough to induce cracking (Miller et al. 1999). El-Remaly (1996) indicates that the wide joints (about 6 in.) used in Japan are seldom associated with cracking.

Considering the literature findings, the new joint was designed to be 6-1/2 in. wide with no shear key. As shown in Figure 14, the bottom corner extended out from the girders to serve as the bottom of the joint formwork for the cast-in-place joint material.

#### 4.2 Type K Cement Jointed Concrete

Based on the results from an analytical study conducted by Sharp (2007) and field inspection by Attanayake and Aktan (2008), shrinkage of the cement-based grout, which is usually used to fill the traditional narrow joint, is regarded as a possible source of cracking. Because of this, the use of low- or zero-shrinkage material was preferred for the new design.

In this developmental work, the research designed the basic joint material to be standard Iowa DOT C4 concrete, because it is widely available across the state. However, to minimize/eliminate the shrinkage typically associated with normal concrete, 15% of the traditional portland cement was replaced by Type K shrinkage-compensating cement. Shrinkage testing conducted on the shrinkage-compensating concrete in the Iowa State University Structural Materials Testing Laboratory was conducted following ASTM C157, and the results (shown in Figure 15) indicated that the material will experience a self-volume expansion during the first 14 days and achieve the peak value (about 90 microstrain) at the 7th day.

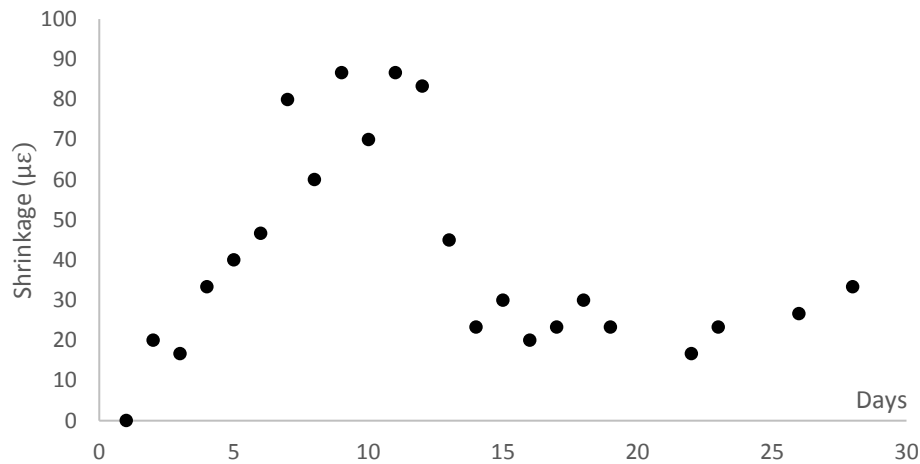


**Figure 15. Shrinkage of Type K cement**

After the 14th day, the residual volume expansion was about 20 microstrain. This residual expansion was regarded as acceptable by the research team. Note that the shrinkage/expansion magnitude can be controlled by adjusting the amount of the portland cement replaced by Type K cement.

### 4.3 Form Retarder

The joint between adjacent box girders was intended to transfer load between the girders. Without the use of a shear key, the shear capacity on the flat interface was a concern to the research team.

To enhance the shear transfer capability, the flat interface was roughened using form retarder and water blasting. The form retarder inhibits hydration of the cement near the surface between the aggregates. The unhydrated paste can then be easily removed by water blasting. After water blasting, the aggregate protruded about a quarter inch, creating a rough surface that would facilitate shear transfer.

### 4.4 Joint Reinforcement

To further enhance the load transfer capabilities of the innovative joint as well as to provide early-age resistance to shrinkage-induced cracking, reinforcing steel was detailed and included. The details of the steel reinforcement in the innovative joint are shown in Figure 16.

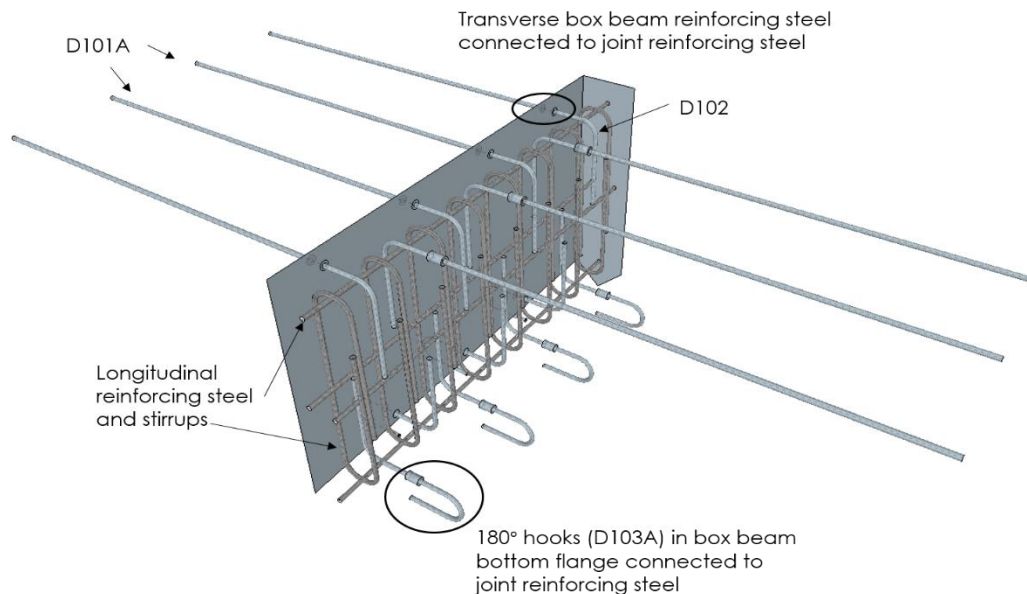


**Figure 16. 3D view of joint reinforcement design**

The interface between the joint material and the box girder was reinforced to prevent cracking and debonding. In addition to the reinforcement crossing the interface between the box beam and joint concretes, longitudinal reinforcing steel and stirrups were placed in the joint. This reinforcement was intended to further resist cracking while at the same time creating an internal reinforced beam within the joint. The size of longitudinal reinforcing steel and the spacing of the stirrups were detailed to be easily constructible within the other geometric constraints.

Figure 16 and Figure 17 show detailed information for the reinforcement within the joint.

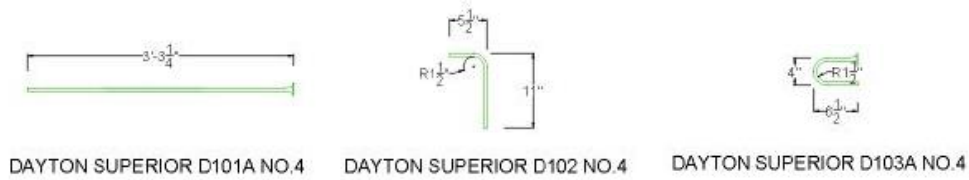


**Figure 17. Design details for the reinforcing steel across the interface**

A long straight bar (D101A) was placed in the top of the girder and a 180° hook bar (D103A) was placed at the bottom. Both straight bars and hook bars were connected to 90° hook bars (D102) in the joint using a commercially available coupler (shown in Figure 18).



**Figure 18. Coupler embedded in the box girder concrete (left) and hook bar installed (right)**

The coupler connection ensured that the strength of the connection is at least as high as that of the bar alone. No. 4 bars were used for all of the joint reinforcement.

#### **4.5 Box Girder Construction**

For the laboratory testing phase of this project, two 31 ft long box girders were constructed based on the design drawings shown in Figure 19 and Figure 20.

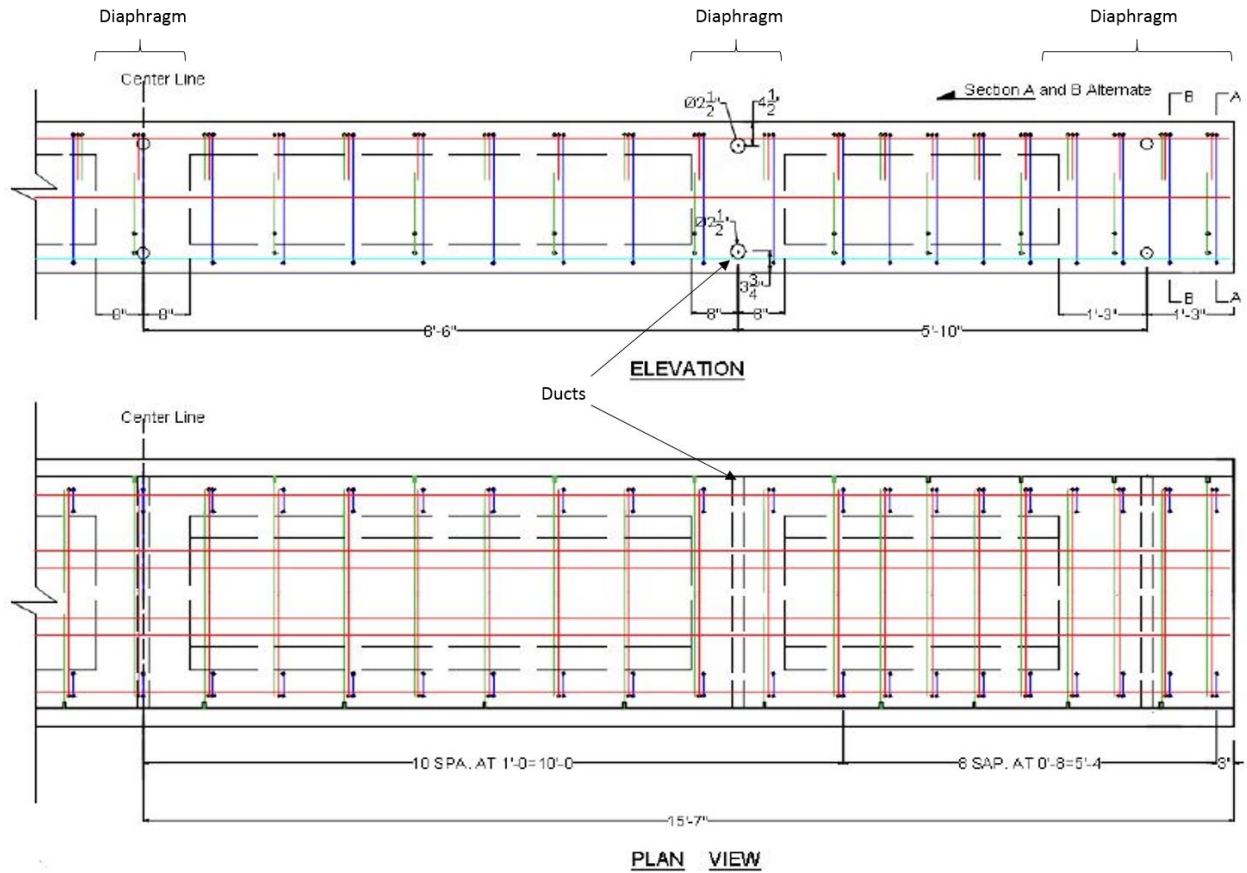


**Figure 19. Elevation and plan view of the box girder**

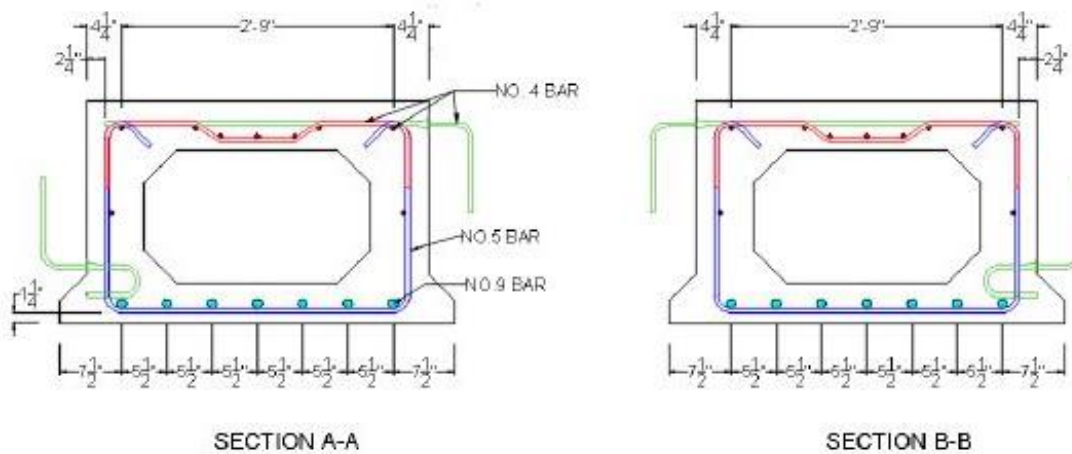


**Figure 20. Cross-section view of the box girder**

The box girders were constructed based on drawings provided by HDR, Inc. and only minor changes were made to facilitate the new features of the joint.

Five diaphragms were cast in each of the beams (at the two ends, middle span, and at the two quarter spans). In each diaphragm, two transverse plastic ducts were placed near the top and bottom and were sized to accommodate transverse post-tensioning rods. However, during the testing completed in this work, the specimen was never post-tensioned because good performance was observed without post-tensioning being applied. The spacing of reinforcing steel bar across the interface (D101A and D103A) was based on the spacing of the stirrups in the box girders, i.e., narrow spacing near the end regions and wide spacing in the middle region.

Figure 21 shows the box girder before and after placing the concrete.

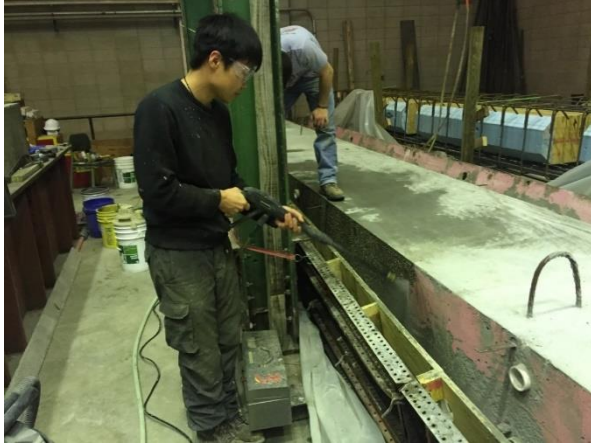


Box girder reinforcement

Box girder after pouring

**Figure 21. Box girder construction**

Before placement of the concrete, the wood formwork was “painted” with form retarder. Seven days after placing the box girder concrete, the wood formwork was removed and the side of the concrete girder was water blasted to create the roughened surface, as shown in Figure 22.



Water blasting



Coarse surface after water blasting

**Figure 22. Water blasting on the side of box girder painted with form retarder**

After water blasting, the 90° hook reinforcing steel bars (D102) were installed on the box girder (Figure 23).



**Figure 23. Side of the box girder with hook bars installed**

#### **4.6 Joint Construction**

Figure 24 and Figure 25 show the joint before placement of the joint material.



Two box beams placed side-by-side (left); Joint reinforcement with longitudinal bars and stirrups (right)

**Figure 24. Placement of joint reinforcement**



**Figure 25. Specimen before pouring of the joint material**

After the two beams were set side-by-side (Figure 24 left), the longitudinal reinforcing steel and stirrups were placed into the joint (Figure 24 right). The two ends were capped with wood formwork (Figure 25). Before pouring the joint material, the post tensioning ties were placed into the ducts to a snug-tight condition.

## CHAPTER 5. EARLY-AGE AND CYCLIC LOAD TESTING

The specimen was tested following the basic testing protocol conducted by Yuan and Graybeal (2016). A summary of Graybeal's test is documented in Section 2.4. In this chapter, the details of the short-term and long-term load testing of the specimen are presented, along with instrumentation details.

### 5.1 Early-Age Loading Test

The early-age testing portion of the project was designed to simulate the changing environmental conditions that would occur during field placement of the joint material. The loading types which, according to available literature, may influence the joint material behavior, include daily temperature variation, joint material expansion, concrete hardening, creep and heat of hydration.

The joint was placed in the Iowa State University Structural Engineering Research Laboratory on August 23, 2016 starting at approximately 1:30 p.m. Before placing the joint material, a temporary temperature isolation room made of blue foam panels was fabricated on top of the specimen as shown in Figure 26.

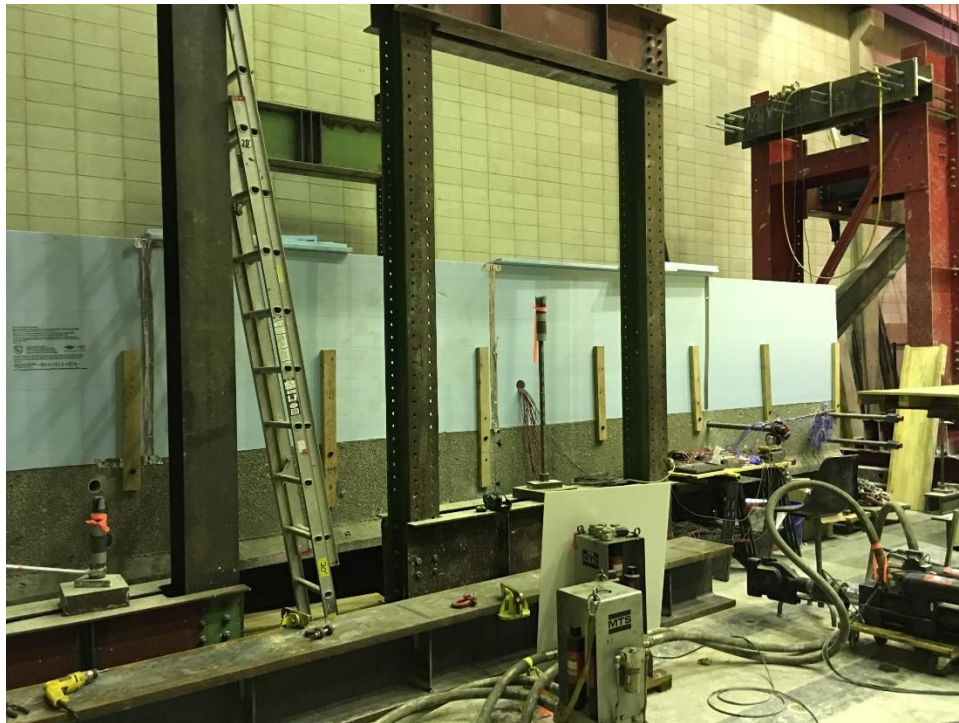


**Figure 26. Temporary temperature isolation room**

This temperature isolation room allowed for the application of heat that would simulate normal thermal radiation consisting of heating of the top surface. To create the heat source, 20 heat lamps and 2 electric heaters were placed in the temperature isolation room, as shown in Figure 27 and Figure 28.



**Figure 27. Heating devices in the temperature isolation room**

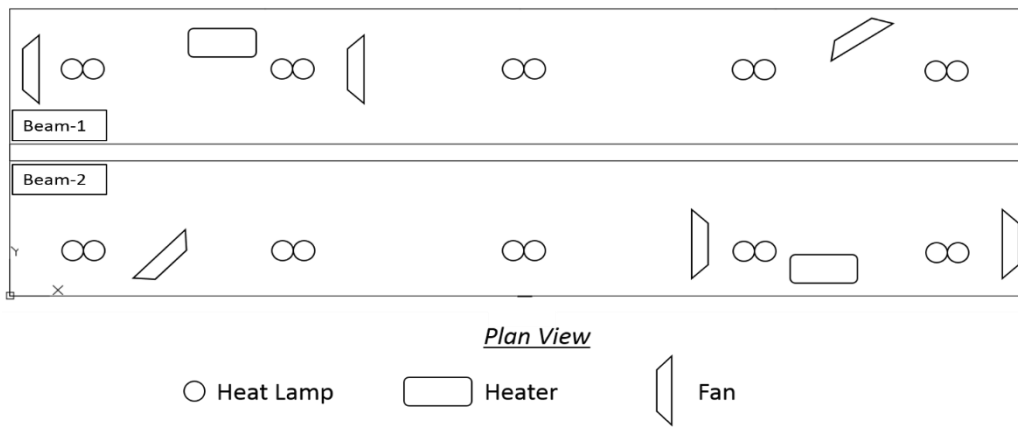


**Figure 28. Locations of heating devices and fans**

Six fans were used to circulate the air in the temperature isolation room to achieve a better temperature distribution as shown in Figure 28.

During a typical sunny, midwestern day, the extreme high and low temperatures usually occur at around 4:00 p.m. and 6:00 a.m., respectively. To simulate these temperature changes, the application of heat to the specimen followed this same schedule, (i.e., uniform temperature through the depth of the girder at 6:00 a.m. and the largest temperature gradient—about 40 °F—at 4:00 p.m.). To slowly warm/cool the top of the box beams in a controlled manner, the electric heaters and heat lamps at different locations were turned on and off in sequence to control the

temperature change with time. The average temperature distribution on the top and bottom surface before and for several days after placement of the joint material is shown in Figure 29.

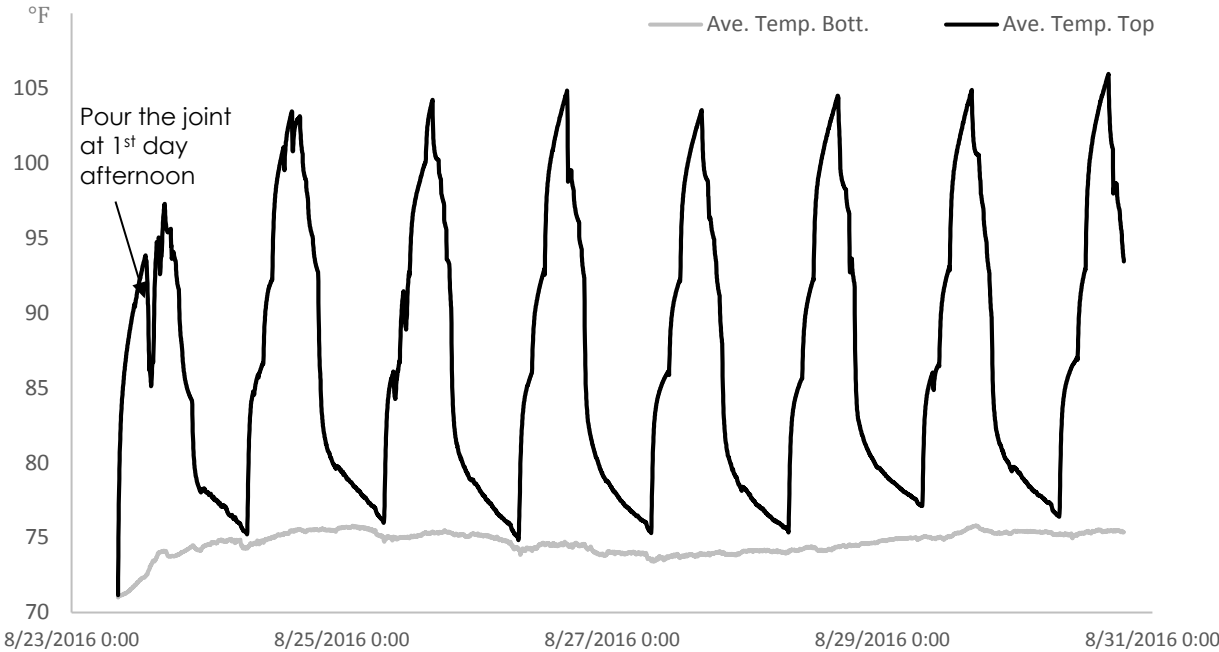


**Figure 29. Average temperature on the top and bottom surface of specimen**

The temperature at the bottom surface is very stable (about 75 °F) because the laboratory temperature is temperature controlled.

### 5.2 Joint Pouring

The joint material was placed in the afternoon when the temperature on the top of the specimen was relatively high. To achieve that, the heaters and lamps were turned on in the morning. The joint concrete material was placed using a large bucket, which required temporary removal of the top (shown in Figure 30) of the temperature control room.



**Figure 30. Pouring joint concrete**

This caused a slight temperature drop during the first day while the joint material was being placed. The placement of the joint material took about 1.5 hr to complete. After placement, the joint concrete was covered with burlap and plastic as shown in Figure 31.

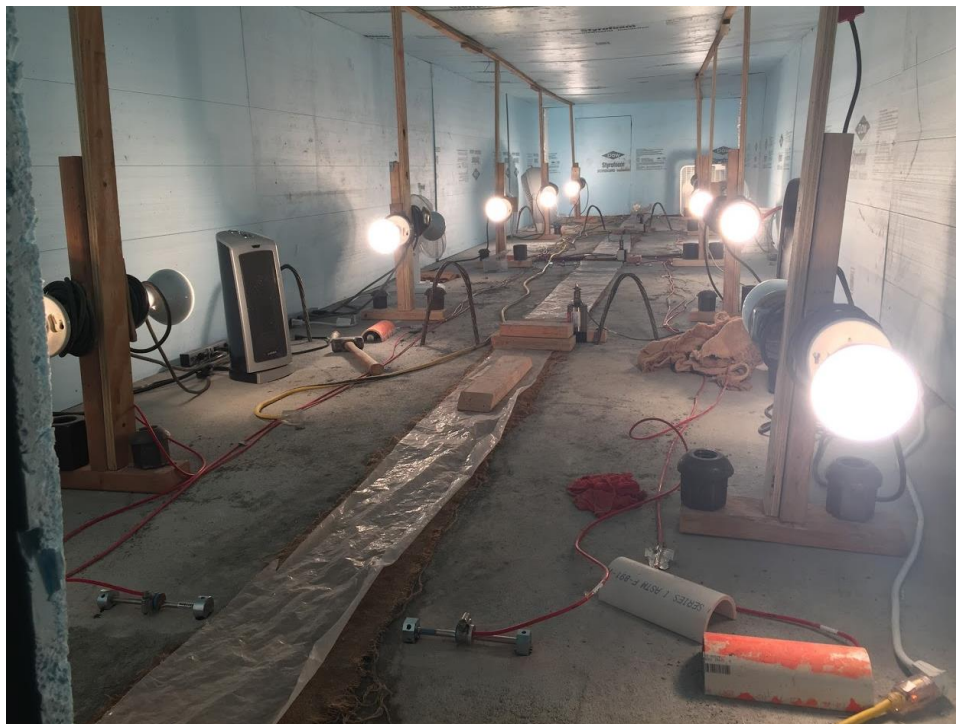


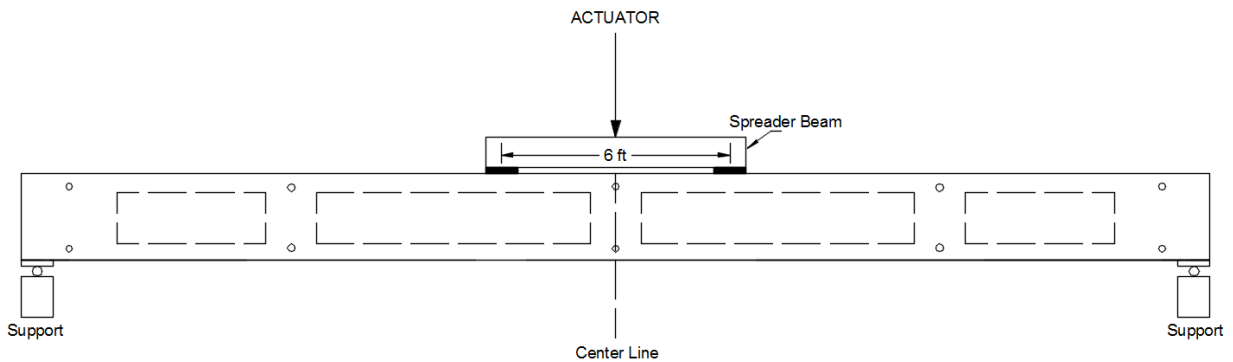
**Figure 31. Curing joint**

The burlap was kept wet by spreading water frequently during the first 7 days.

### 5.3 Cyclic Loading Test

Following full curing of the joint, a series of cyclic live loading tests were conducted on the specimen on November 1, 2016. Generally, the cyclic loading was applied at a frequency of 2 Hz and the beams were tested with two different boundary conditions: both beams simply supported and one beam restrained.

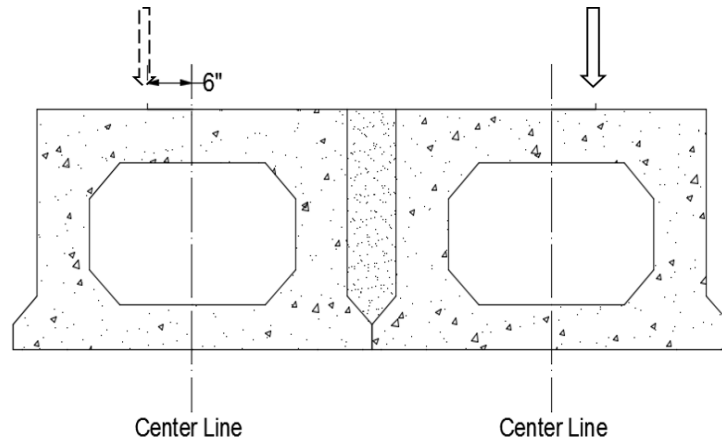
The specimen was first tested with simply supported conditions, as shown in Figure 32.



**Figure 32. Simply supported detail for cyclic live loading**

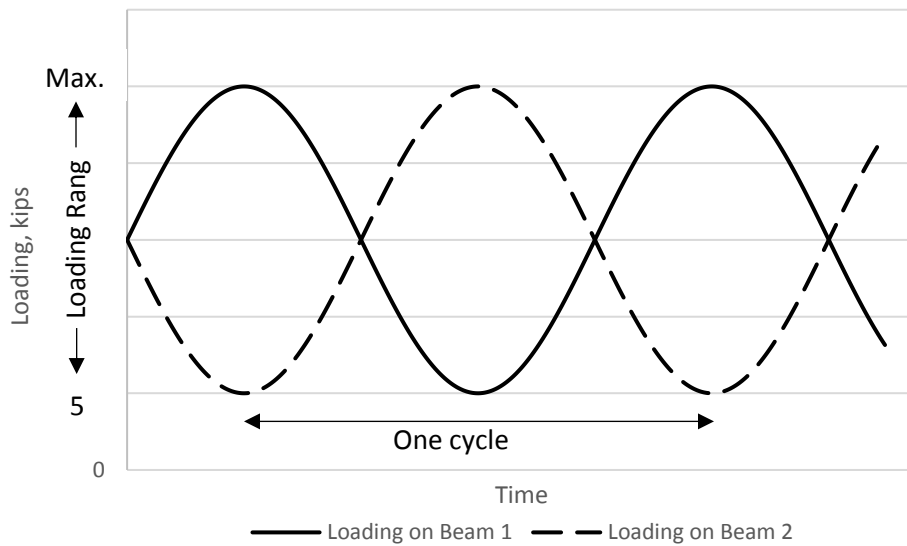
The load was applied by two actuators, one on each beam. The load was transferred to each box beam by a spreader beam and two 8×8 in. steel plates between the spreader beam and the specimen. The spacing between the two steel plates in the longitudinal direction was approximately 6 ft.

Figure 33 shows the transverse location where the load was applied. On each beam, the load was applied 6 in. off center.



**Figure 33. Cross-section view of load application**

Figure 34 shows a graphical representation of the cyclic loading applied to the specimen, subjected to the simply supported condition.



**Figure 34. Cyclic loading under the simply supported condition**

To keep the specimen stable, a minimum of 5 kips was held on both beams throughout the test. As can be seen, one beam was loaded to the maximum level at the same time the other was loaded to the minimum level.

After the simply supported condition was tested, the specimen was further tested with one beam restrained to generate higher stresses in the joint, as shown in Figure 35.

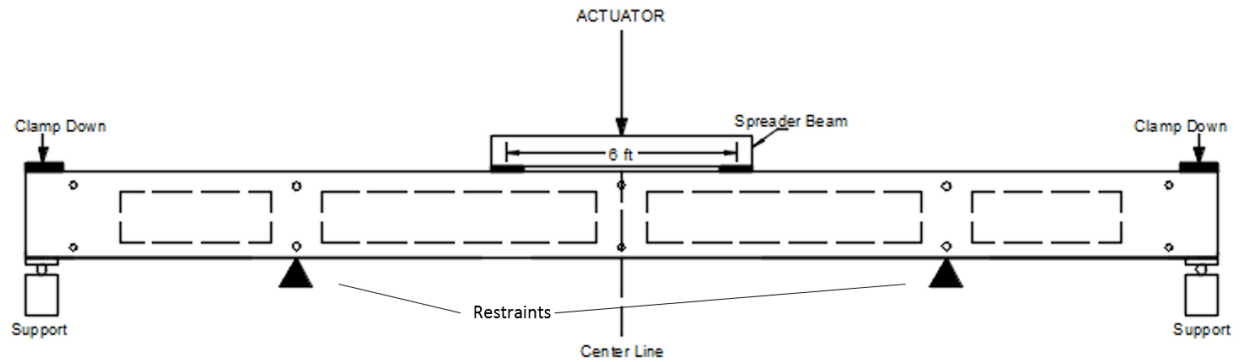


**Figure 35. Cyclic live loading detail for one beam restrained**

Figure 36 shows the restraints used to restrict deflection of the beam.



**Figure 36. Restraints under one beam**

During the test with one beam restrained, the loading on the restrained beam was held at 5 kips. Beam 2 was loaded as shown previously in Figure 34.

Table 8 shows a summary of the cyclic loading tests.

**Table 8. Summary of cyclic loading test**

<b>Support Condition</b>	<b>Max. Loading (kips)</b>	<b>Post-Tension</b>	<b>Number of Cycles</b>
Simply supported	18	Snug tight	1 million
Simply supported	36	Snug tight	1 million
Simply supported	42	Snug tight	1 million
Simply supported	42	None	400,000
One beam restrained	18	None	200,000
One beam restrained	36	None	400,000
One beam restrained	42	None	1 million

The specimen was first tested at a maximum of 18 kips, 36 kips, and 42 kips with the simply supported condition and with wrench-tightened transverse post-tensioning ties (very low level transverse force). The maximum load was 42 kips, which generated a moment on a 30 ft-long simply supported beam approximately equal to that induced by an HL-93 design truck based on the AASHTO LRFD Bridge Design Specification. For each loading, one million cycles were applied. After that, the post tension was completely removed and another 400,000 cycles of 42 kips was performed with the simply supported condition.

The specimen was tested with one beam restrained, subjected to 18 kips (200,000 cycles), 36 kips (400,000 cycles) and 42 kips (1 million cycles). During these tests, no post-tensioning force was applied on the specimen.

#### **5.4 Instrumentation**

During the test, strain, displacement, and temperature were collected using the following devices: vibrating wire strain gauges (VWSGs), displacement transducers, and thermocouples.

##### *Strain Data*

The strain data were collected using VWSGs attached on both top and bottom surfaces. Figure 37 shows the locations for VWSGs on the top surface, with labels shown.

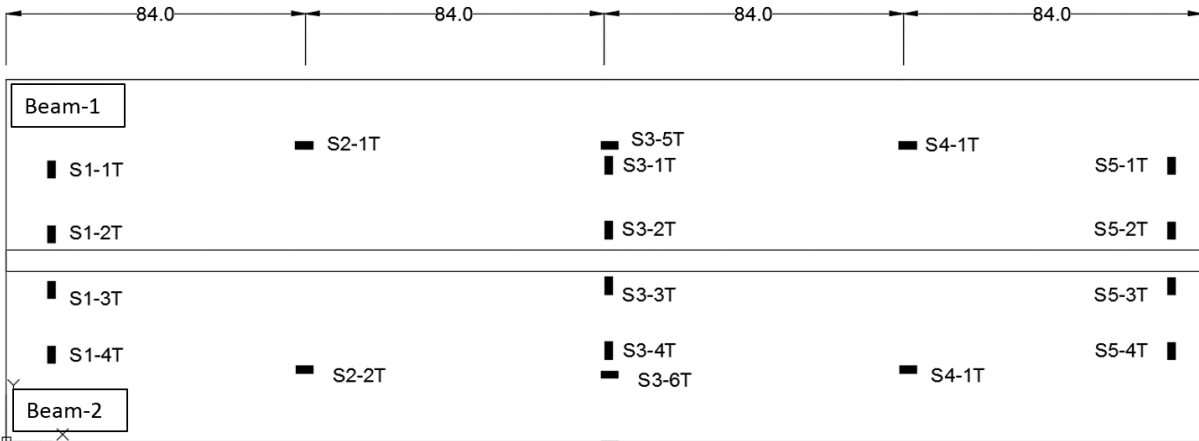


**Figure 37. Vibrating wire strain gauge (VWSG) instrumentation map on top surface (similar for bottom surface)**

In general, VWSGs were installed in three typical and symmetric cross-sections: Sections 1 and 5 are about 1 ft from each end; Sections 2 and 4 are at the quarter span; and Section 3 is at the middle span (in Figure 37). For each label, S represents the strain gauge, the first number is the section number, the second number is the gauge number in that section, and the last letter, T (or B), refers to top (or bottom) surface.

In Sections 1, 3, and 5, four VWSGs were utilized to measure the transverse strain. Gauges 1 and 4 were in the middle of the box girder, and Gauges 2 and 3 measured the strain 6 in. from the edge of the joint. In Sections 2, 3, and 4, two strain gauges were installed to measure the longitudinal strain 20 in. from the edge of the specimen. In total, 36 VWSGs were used (18 on the top surface and 18 on the bottom surface).

#### *Temperature Strain Data*

The temperature data were collected by the thermocouples and thermal gauges embedded in the VWSGs. The locations of the thermal gauges embedded in the VWSGs are shown previously in Figure 37. The temperatures collected from these VWSGs were used as the temperature at the top and bottom surfaces.

Nineteen thermal couples were used to measure the temperature both in the joint and at the exterior of the specimen. In the joint, Sections 3 and 5 were instrumented with six thermal couples, as shown in Figure 38.

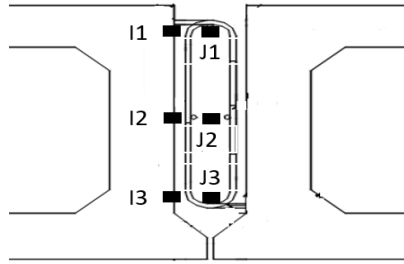


**Figure 38. Locations of thermal couples in Sections 3 and 5 in the joint**

Three thermal couples (I1, I2, and I3) were embedded at the interface between the joint and box girder at three levels: 2 in. from the top, in the middle, and 1 in. above the sloping surface. Another three (J1, J2, and J3) were placed in the middle of the joint.

Seven thermocouples were attached on the exterior of the specimen: four at the edge of specimen to measure the vertical temperature gradient at the middle span (shown in Figure 39), and three at one end and 4 in. from the top to measure the transverse temperature distribution (shown in Figure 40).

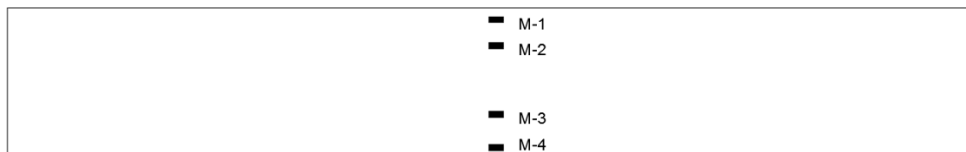


**Figure 39. Thermal couples on the exterior side of the specimen**

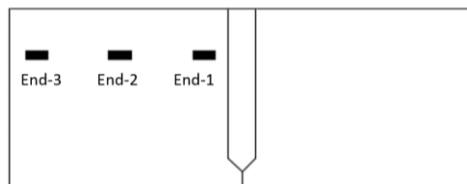


**Figure 40. Thermal couples on the exterior end of the specimen**

### *Displacement Data*

Displacement data were collected using displacement transducers. Figure 41 through Figure 44 show the locations of the transducers with labels. For the labels, the first letter, D, indicates displacement transducer, the first number is the section number, the second number is the gauge number in that section, and the last letter represents the top or bottom surfaces.

To measure transverse relative displacement near Sections 1 and 5 (shown in Figure 41), two transducers were installed on each end with the top locations 6 in. from the top surface and the bottom locations 1 in. above the sloping surface of the joint.

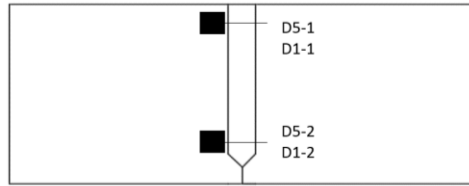


**Figure 41. Displacement transducers in Sections 1 and 5**

In Section 2 (shown in Figure 42), a transverse displacement transducer was attached on the top surface.

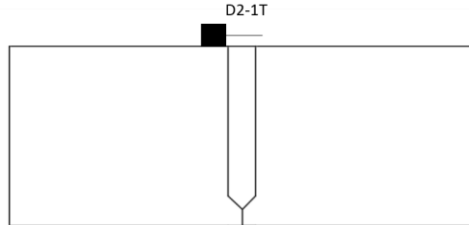


**Figure 42. Displacement transducers in Section 2**

At Section 3 (shown in Figure 43), two transverse displacement transducers were placed on the top and bottom surfaces and four transducers were used to measure the vertical displacement of the bottom surface.

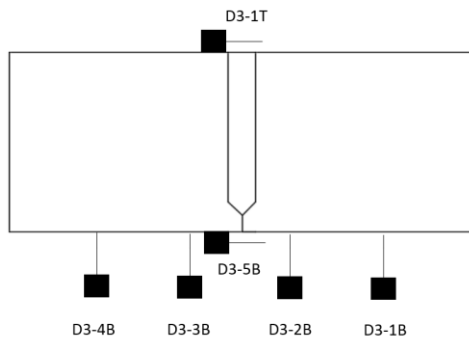


**Figure 43. Displacement transducers in Section 3**

In Section 4 (shown in Figure 44), one transverse displacement transducer was attached on both the top and bottom surfaces.

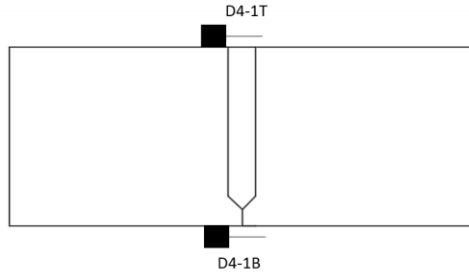


**Figure 44 Displacement Transducers in Section 4**

### 5.5 Material Test Results

Various material property tests were performed on the box girder concrete and the joint material to provide basic information on the constitutive properties of each. For the box girder concrete, the compressive strength was tested on the day the joint material was poured, in accordance with ASTM C39. The compressive strength was 8.2 ksi for Beam-2 and 5.9 ksi for Beam-1.

For the joint concrete, a time-dependent test was conducted for the compressive strength following ASTM C39 and, for the flexural tensile strength test, following ASTM C78. The time-dependent test was conducted at 6 hrs, 18 hrs, 24 hrs, 3rd day, 14th day, and 28th day. Figure 45 and Figure 46 show the results of the time-dependent compressive strength and flexural tensile strength tests, respectively.

It is worth mentioning that the Type K concrete evaluated here is likely more permeable than the UHPC that has been tested by FHWA. The higher impermeability of UHPC is likely indicative of a material with a longer service life.

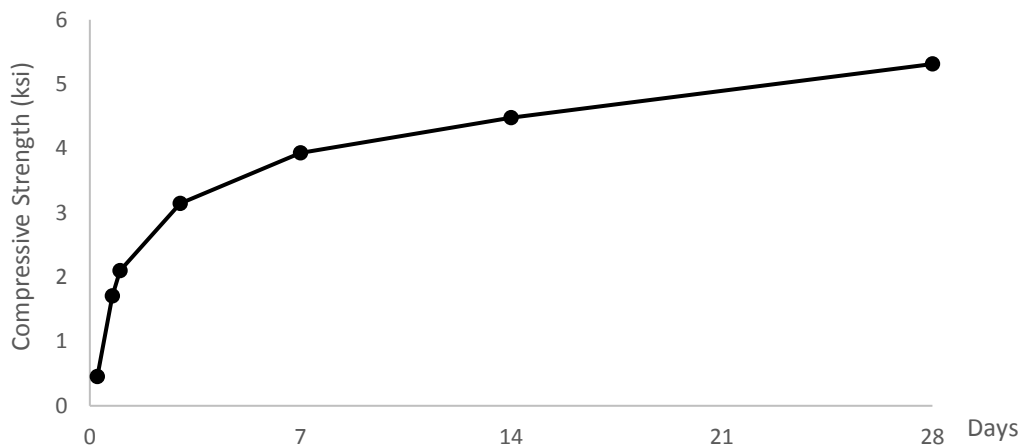


**Figure 45. Compressive strength of joint concrete**

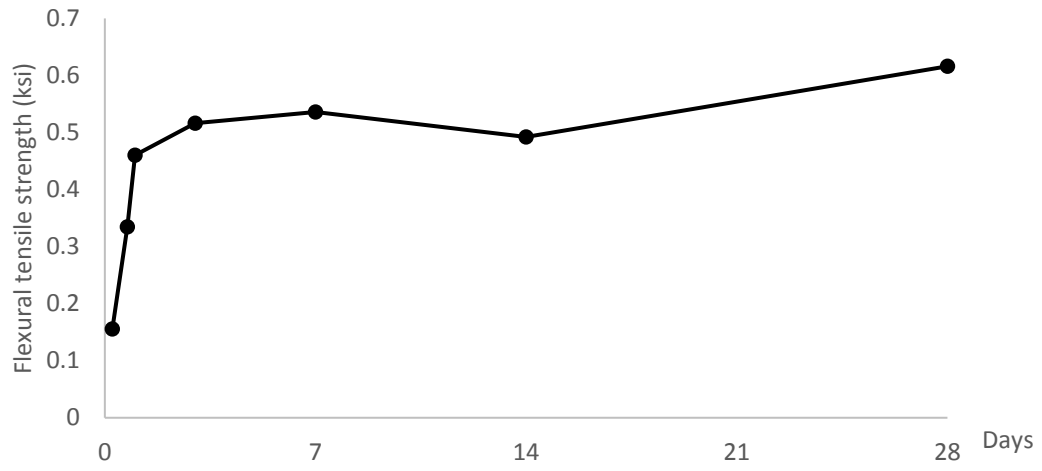


**Figure 46. Flexural tensile strength of joint concrete**

## CHAPTER 6. TEST RESULTS

### 6.1 Results of Early-Age Thermal Test

#### *Temperature*

Figure 47 through Figure 58 show the temperature data collected from the VWSGs attached on the top and bottom surfaces. The location of each VWSG can be found previously in Figure 37.

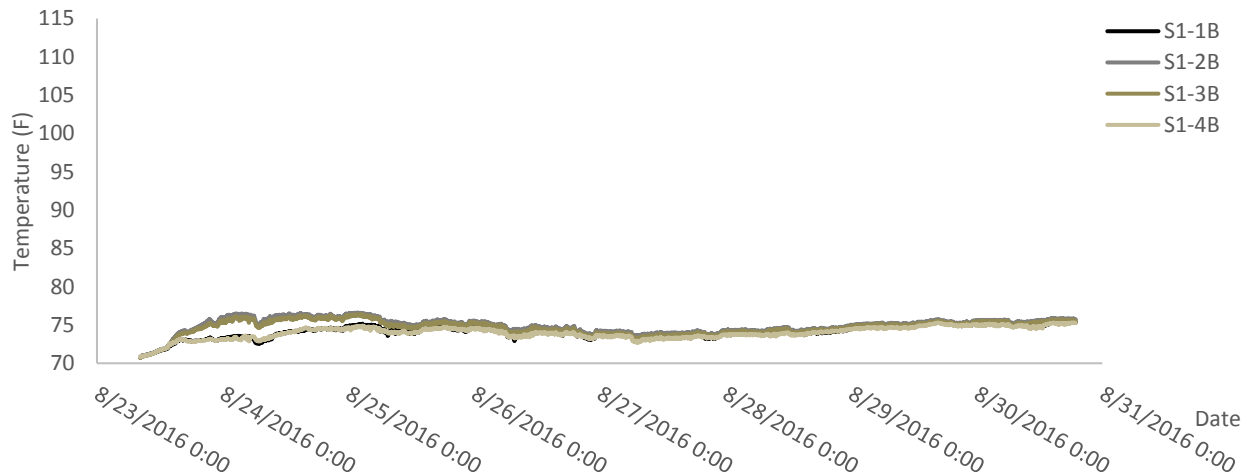


**Figure 47. Temperatures from Section 1 at the bottom surface**

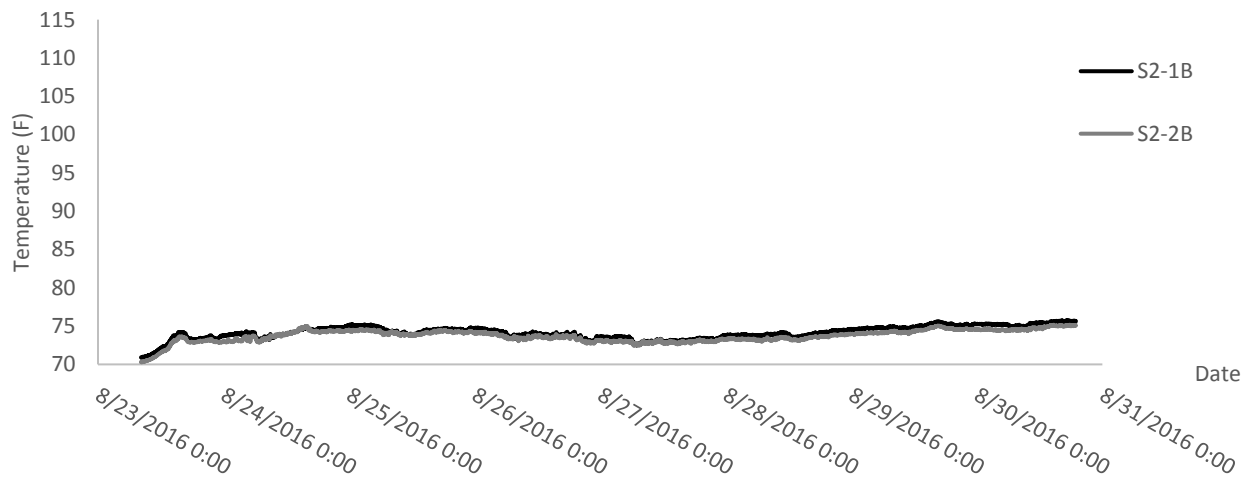


**Figure 48. Temperatures from Section 2 at the bottom surface**

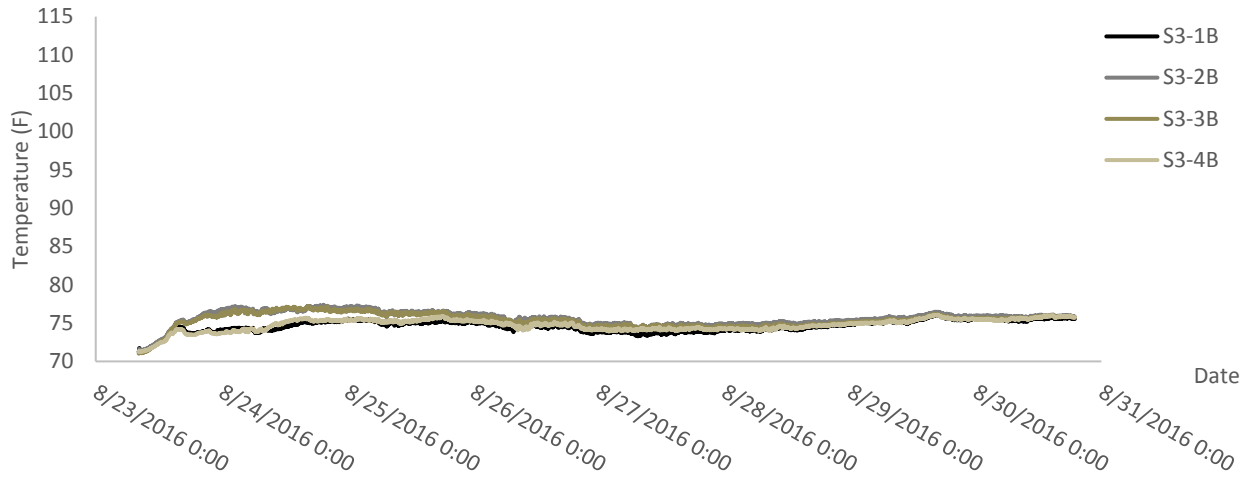


**Figure 49. Temperatures from Section 3 at the bottom surface-1**

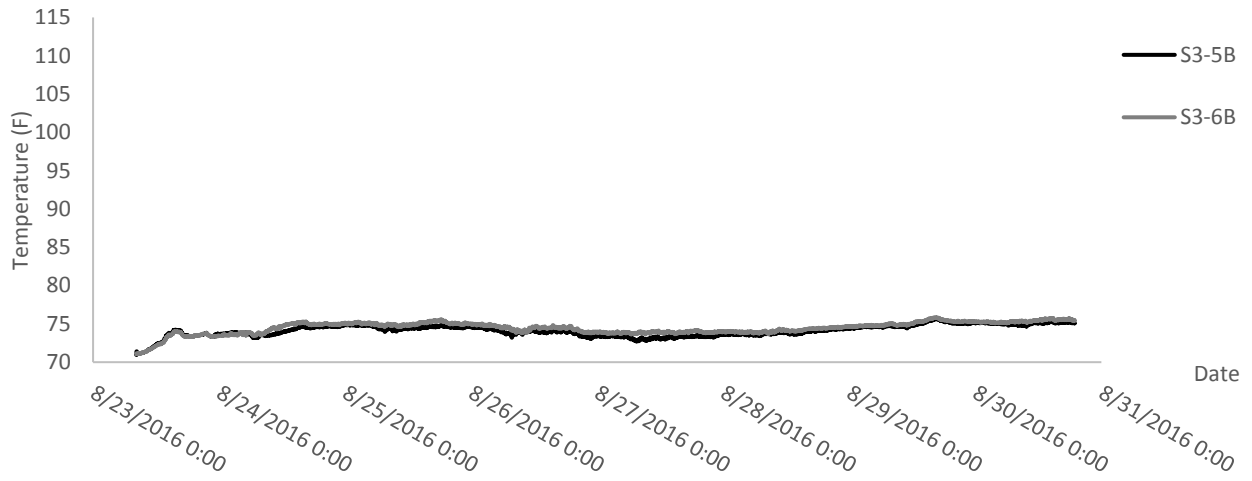


**Figure 50. Temperatures from Section 3 at the bottom surface-2**

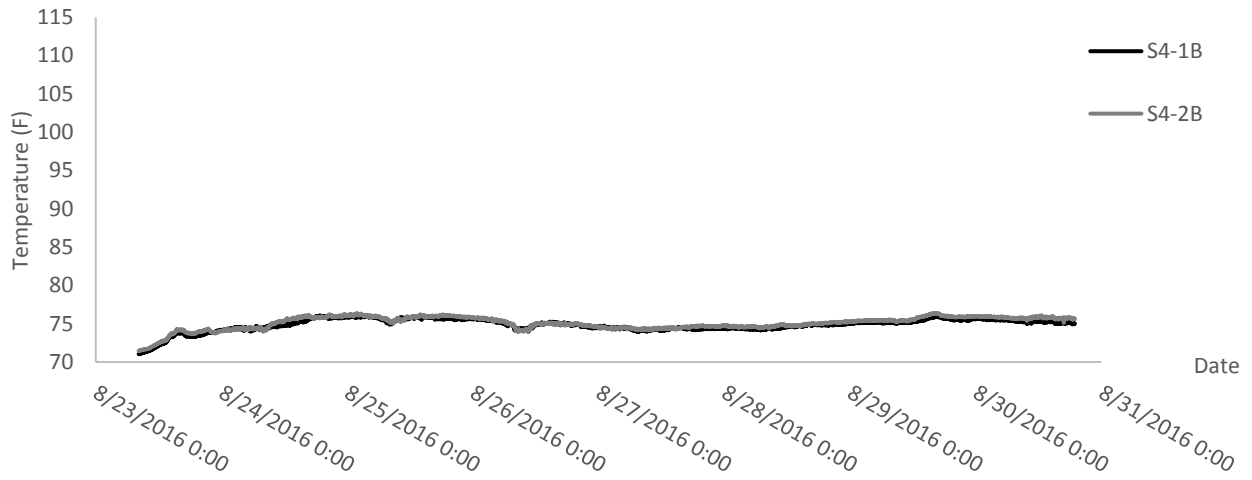


**Figure 51. Temperatures from Section 4 at the bottom surface**

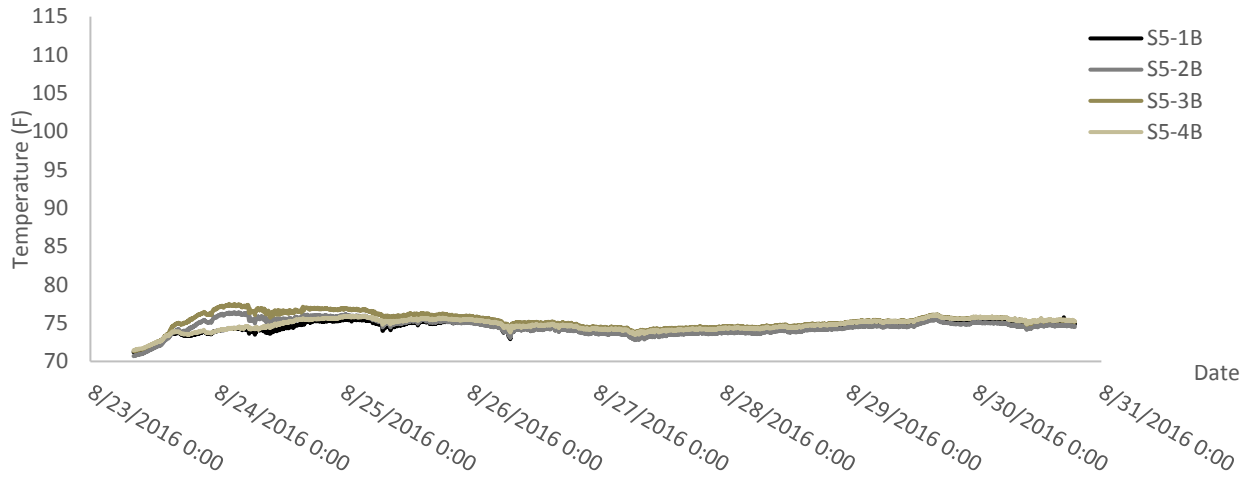


**Figure 52. Temperatures from Section 5 at the bottom surface**

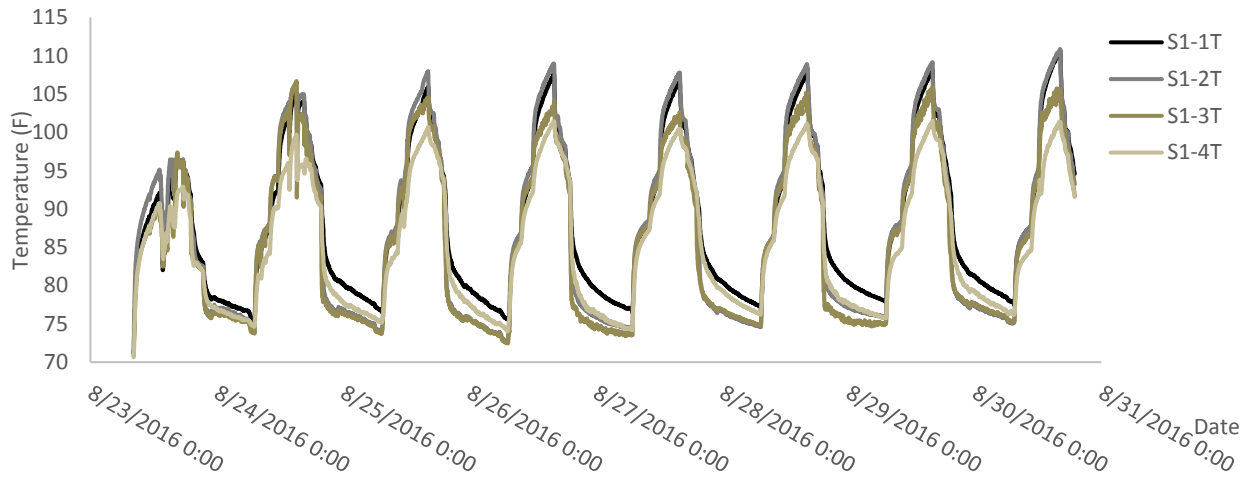


**Figure 53. Temperatures from Section 1 at the top surface**

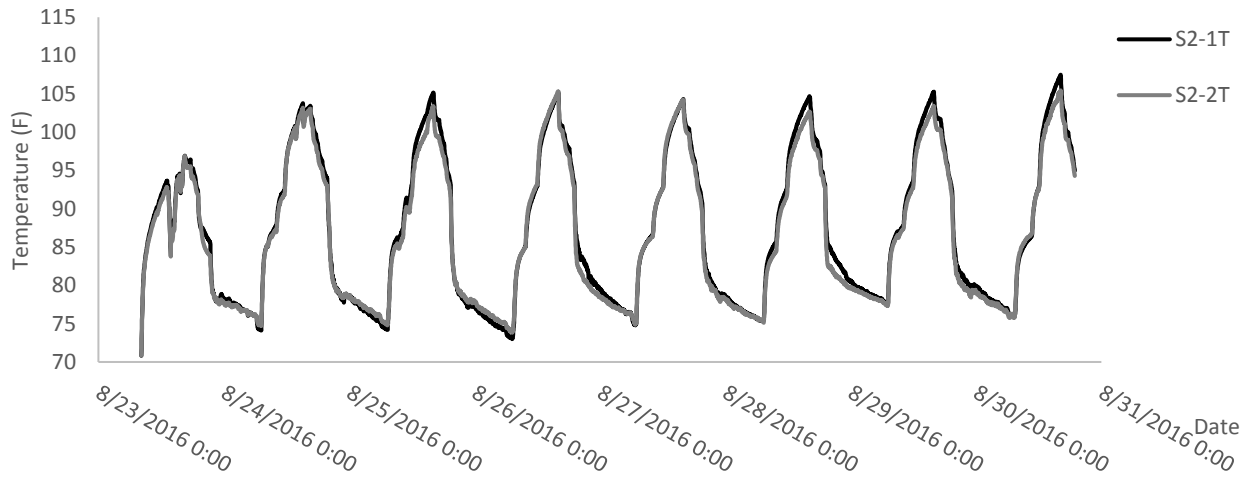


**Figure 54. Temperatures from Section 2 at the top surface**

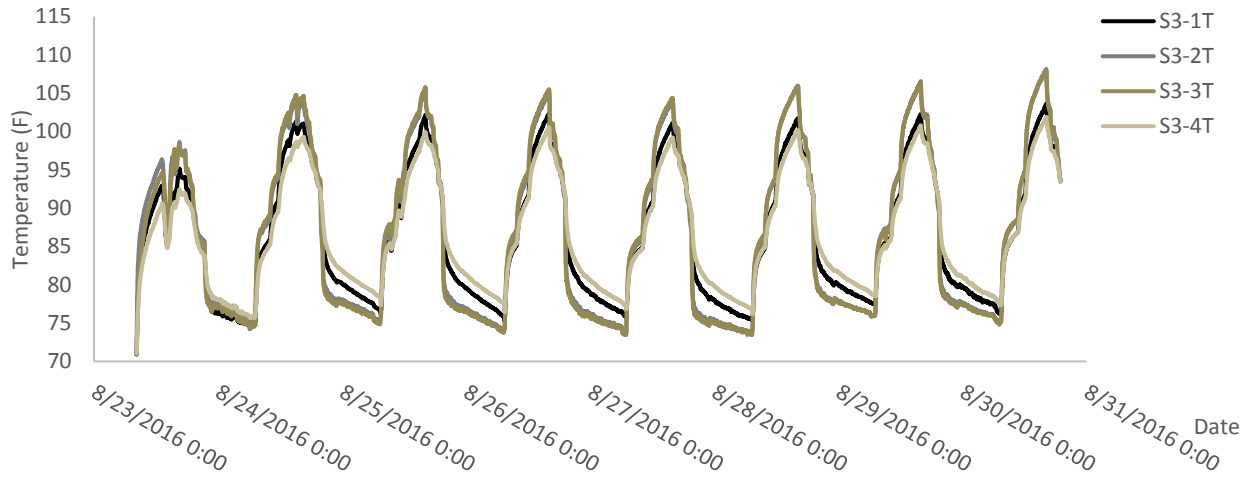


**Figure 55. Temperatures from Section 3 at the top surface-1**

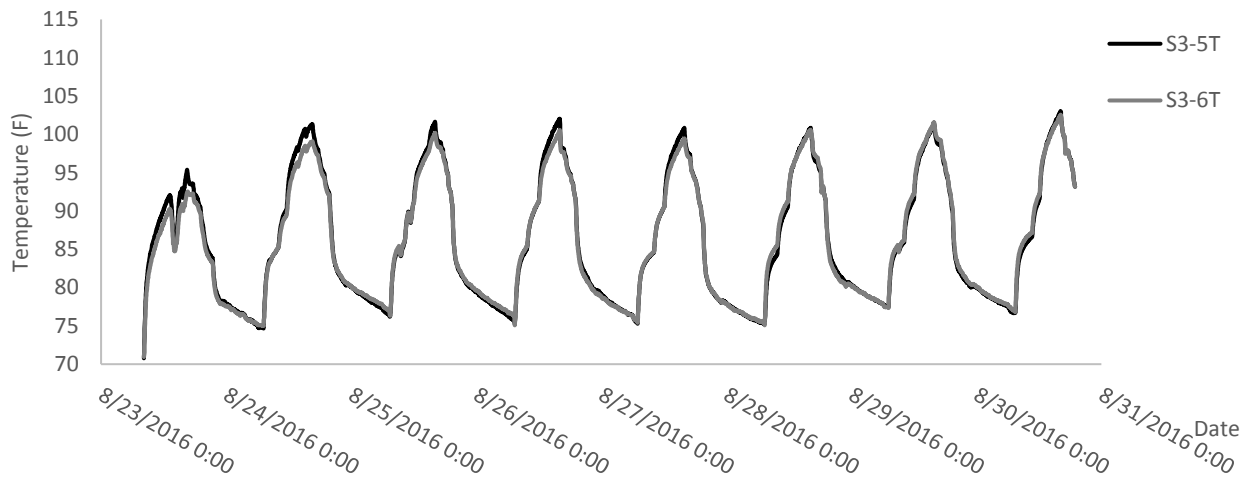


**Figure 56. Temperatures from Section 3 at the top surface-2**

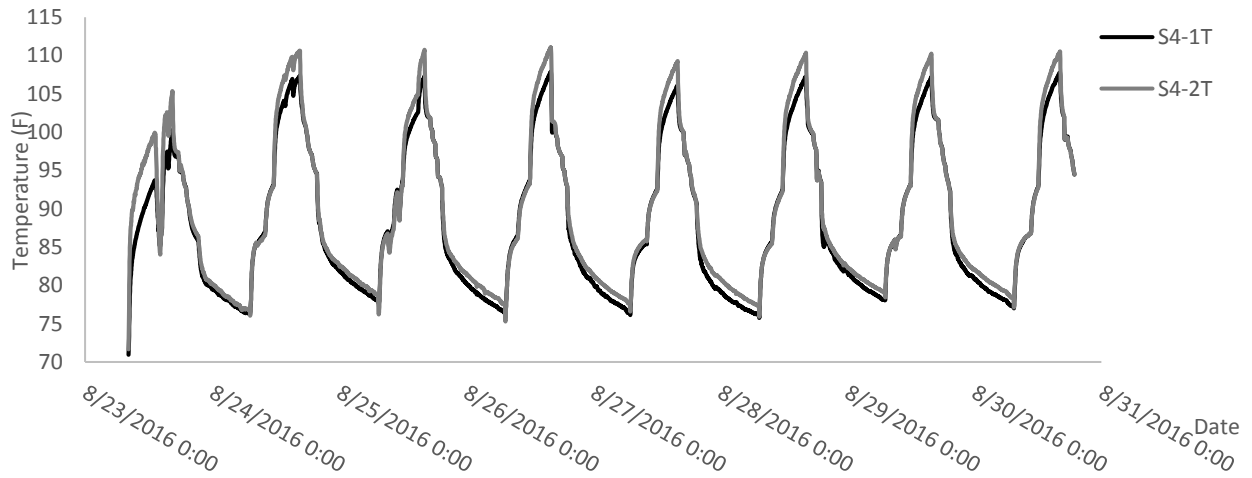


**Figure 57. Temperatures from Section 4 at the top surface**



**Figure 58. Temperatures from Section 5 at the top surface**

The temperature distribution was very uniform on both the top and bottom surfaces. On the bottom surface, the temperature difference was less than 5 °F. On the top surface, when the temperature reached its peak each day, the temperature difference was about 10 °F. Figure 59 compares the average temperature from the top and bottom surfaces to the maximum and minimum temperatures.

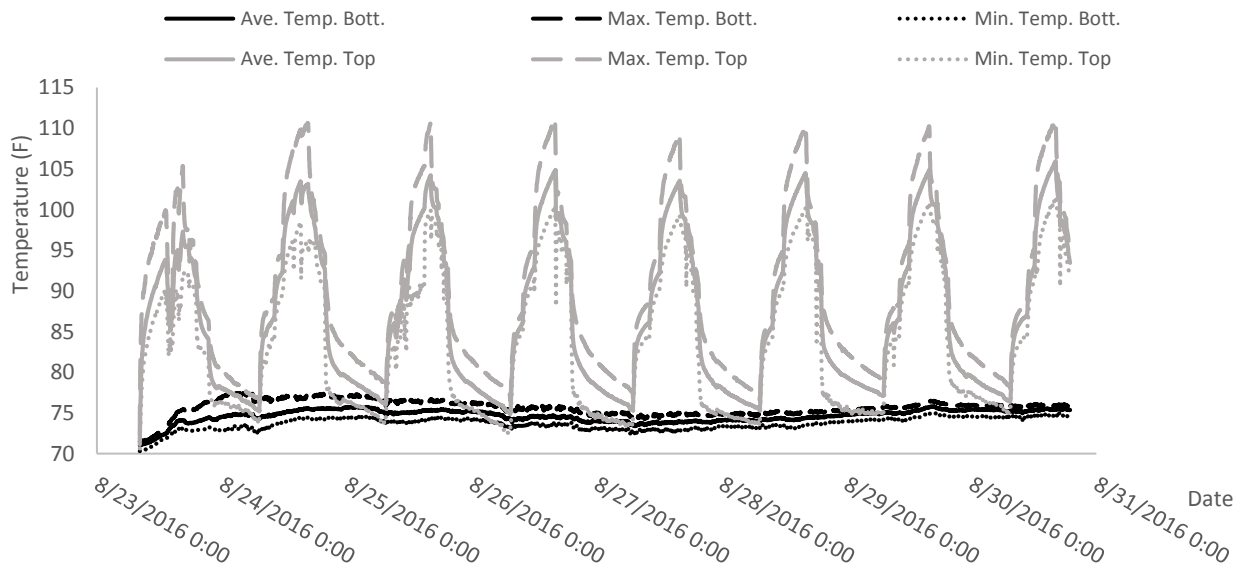


**Figure 59. Average temperatures on top and bottom surfaces**

Figure 60 and Figure 61 show the temperature distribution in the joint at Sections 3 and 5. The gauge locations were shown previously in Figure 38.

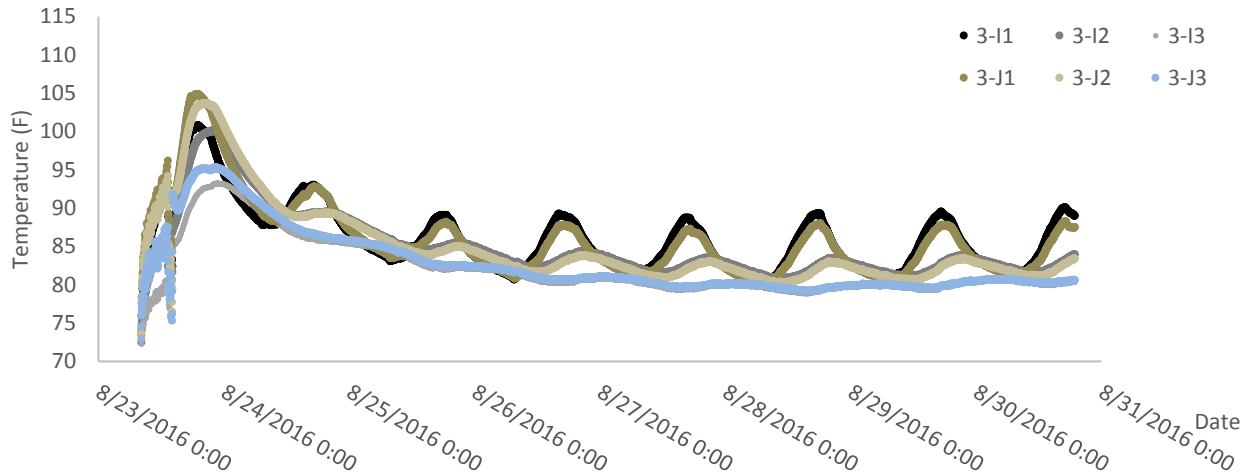


**Figure 60. Temperatures in the joint at Section 3**

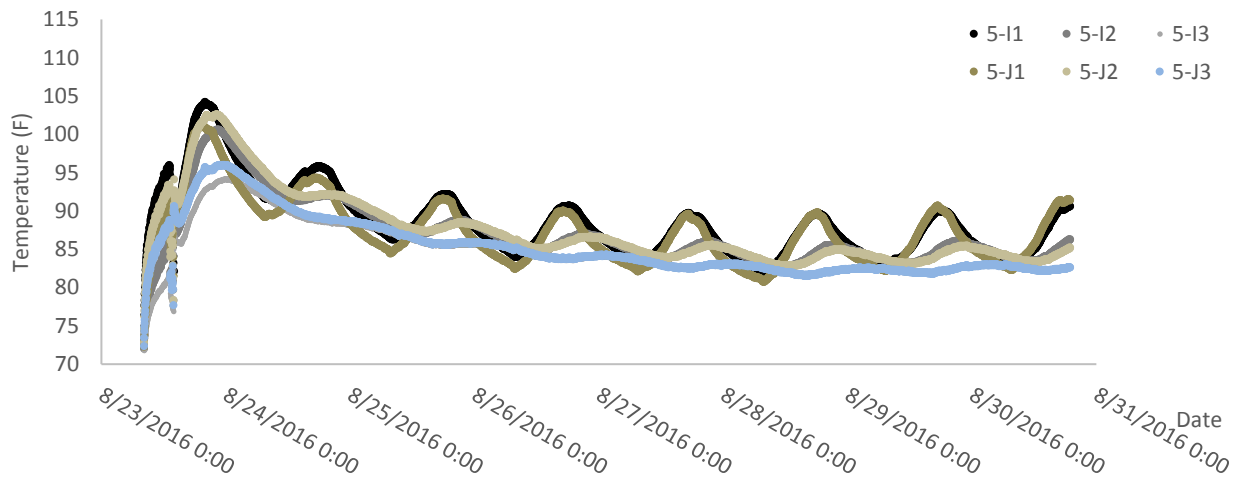


**Figure 61. Temperatures in the joint at Section 5**

The joint temperatures during the first 48 hours after placement of the joint material was significantly influenced by the environmental temperature and the heat of hydration. A vertical temperature gradient is evident in both joints. Comparing the temperatures from the gauges in the centers of the joints to those attached at the interfaces, there was no significant temperature difference.

Figure 62 and Figure 63 show the temperature distribution at the exterior of the specimen. The gauge locations were shown previously in Figure 39 and Figure 40.

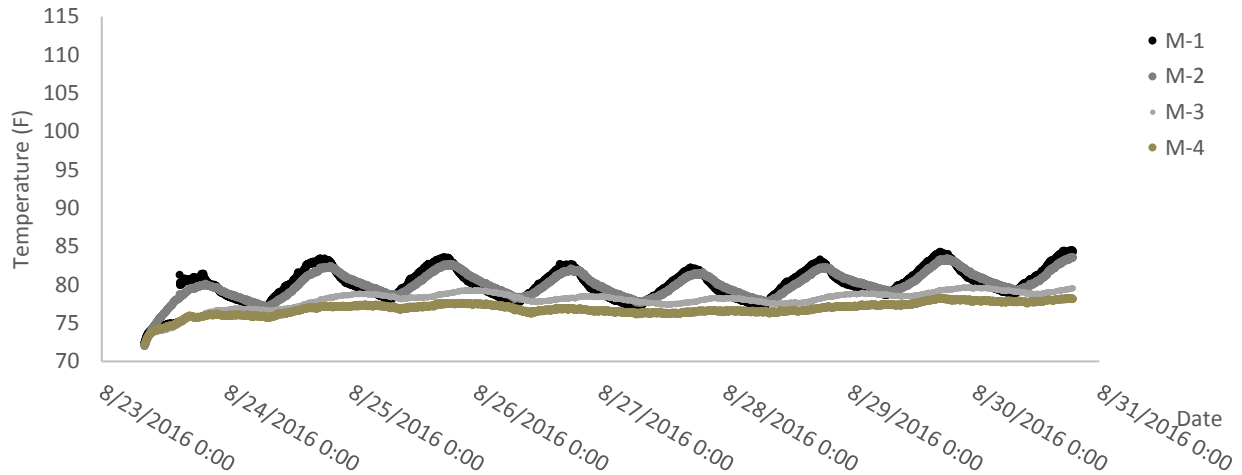


**Figure 62. Temperatures at the side of specimen**

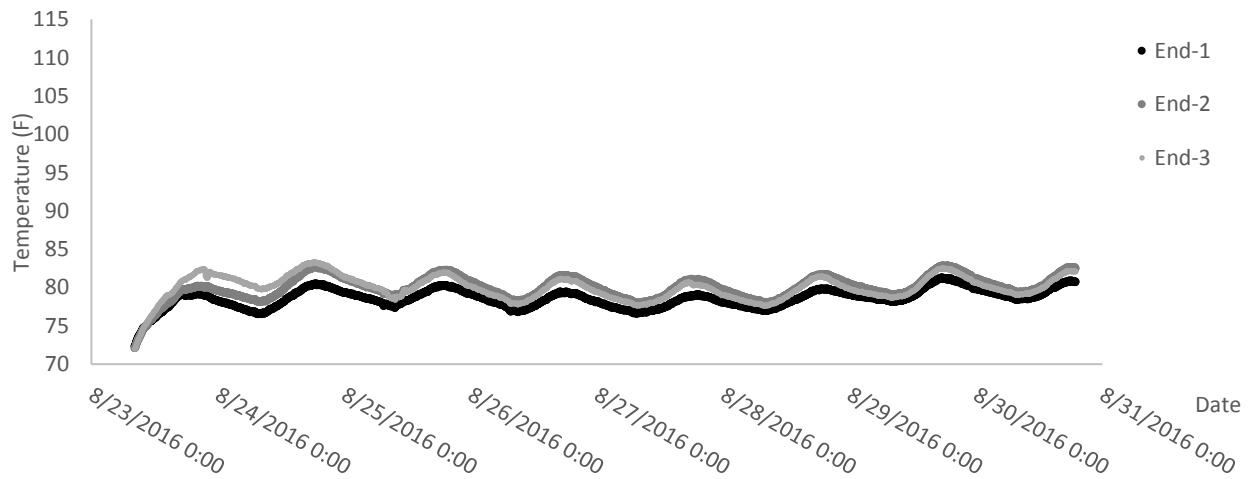


**Figure 63. Temperatures at the end of the specimen**

Figure 62 indicates a vertical temperature gradient at the side of the specimen. Compared to the gradient in Figure 59, the vertical gradient in Figure 62 is small, which results from the whole side face of the specimen being exposed to the air. Figure 63 indicates that the temperature at the end along the transverse direction was very uniform.

### *Strain*

Figure 64 through Figure 78 show the strain data collected from the VWSGs on the top and bottom surfaces.

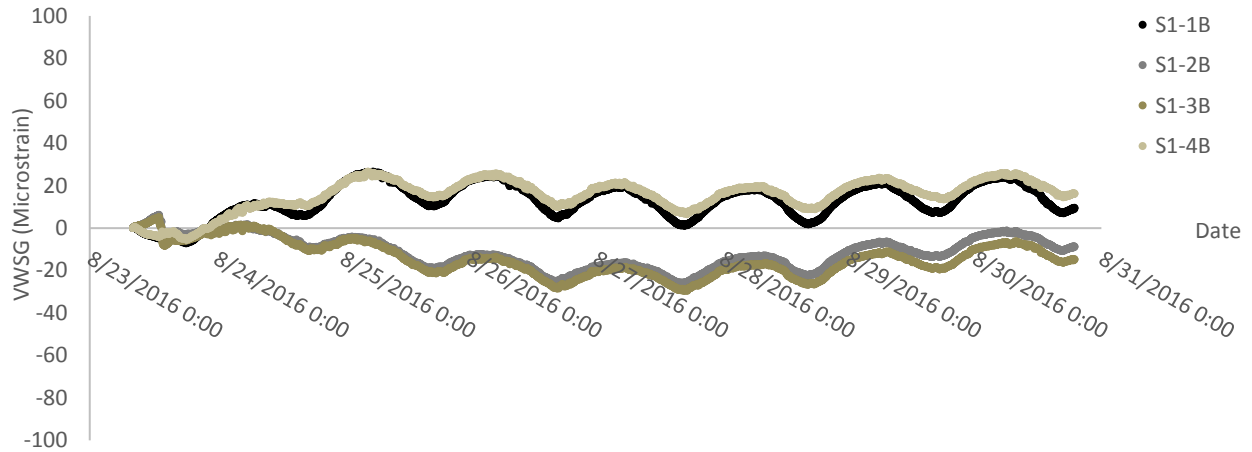


**Figure 64. Strains from Section 1 at the bottom surface**

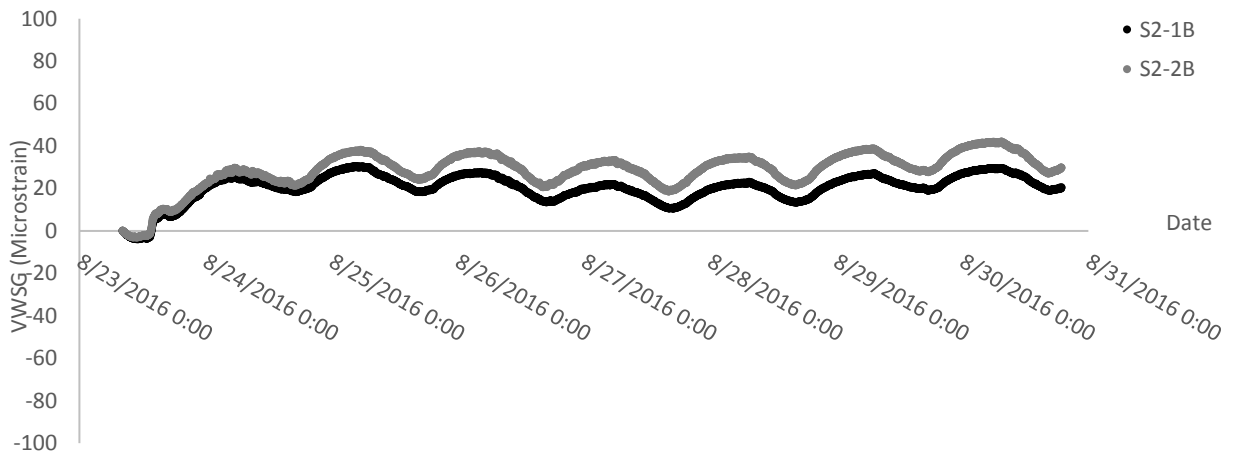


**Figure 65. Strains from Section 2 at the bottom surface**

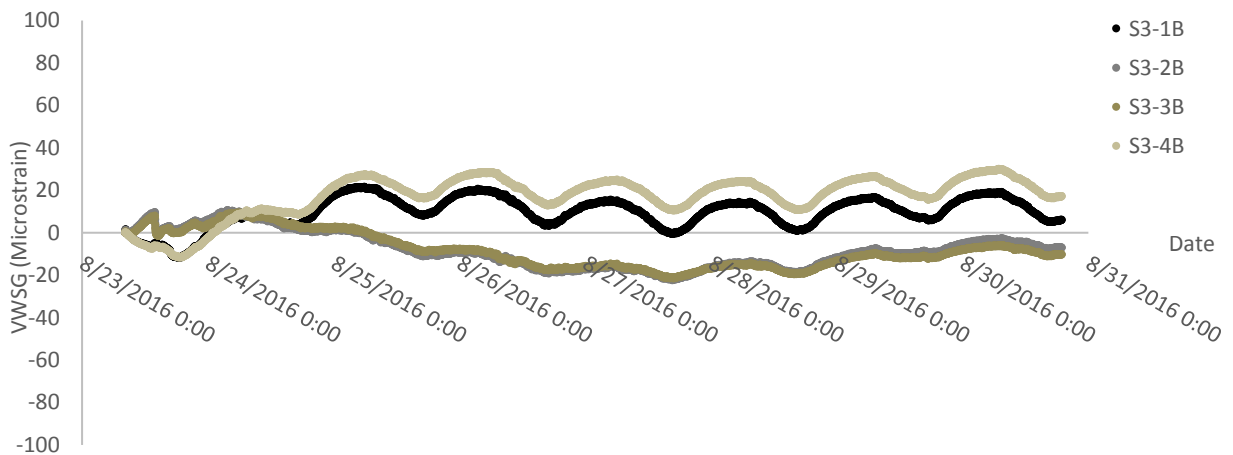


**Figure 66. Strains from Section 3 at the bottom surface-1**

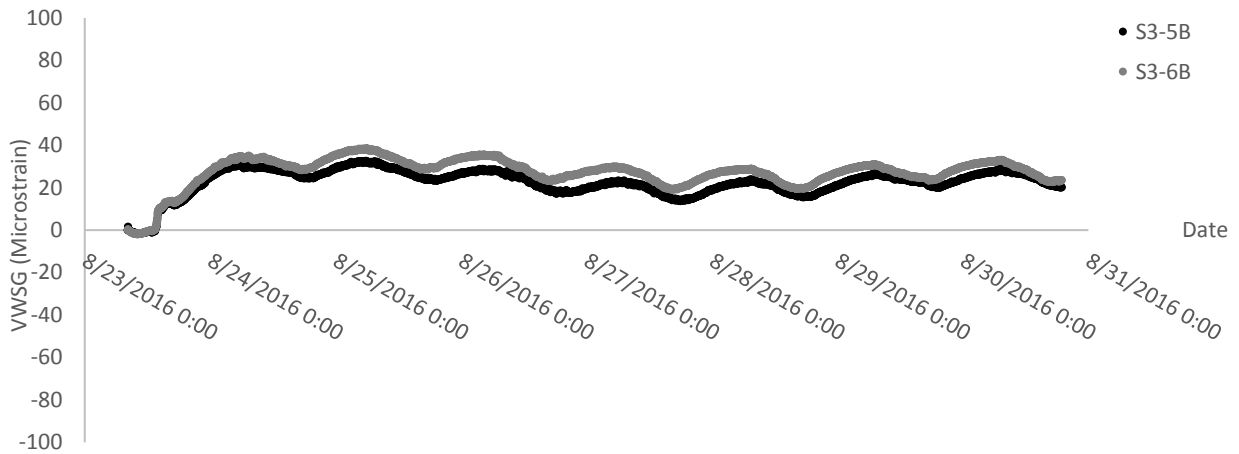


**Figure 67. Strains from Section 3 at the bottom surface-2**

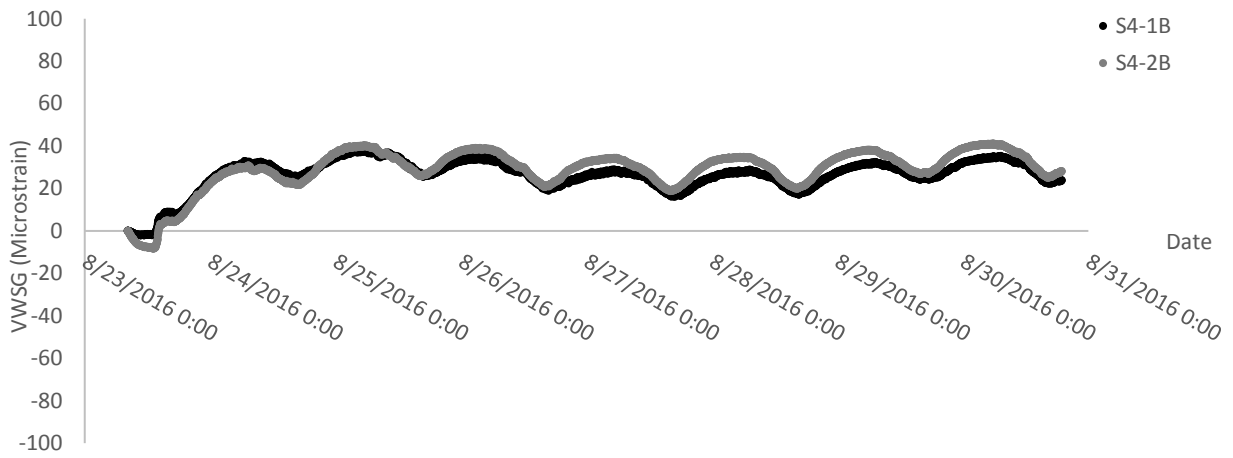


**Figure 68. Strains from Section 4 at the bottom surface**

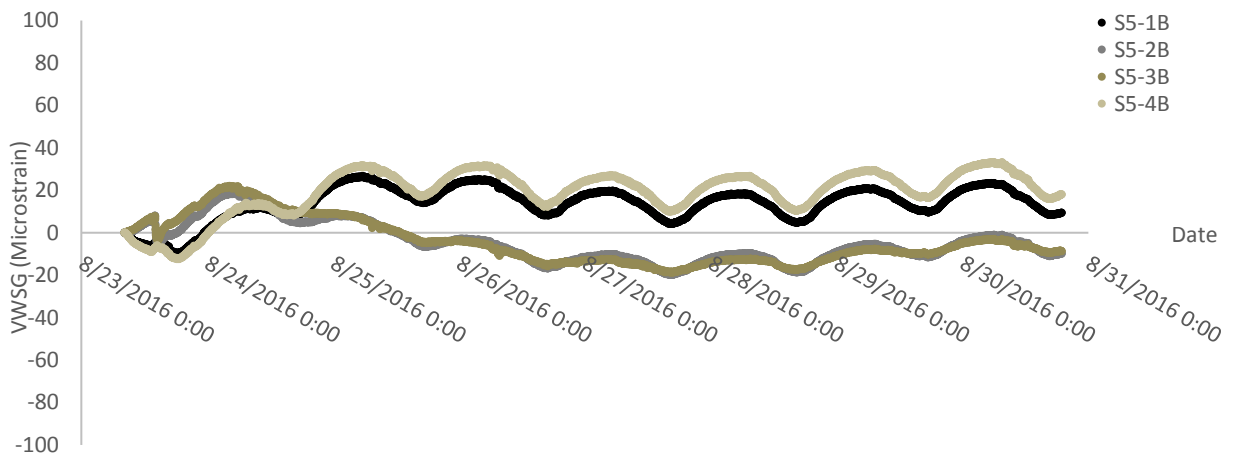


**Figure 69. Strains from Section 5 at the bottom surface**

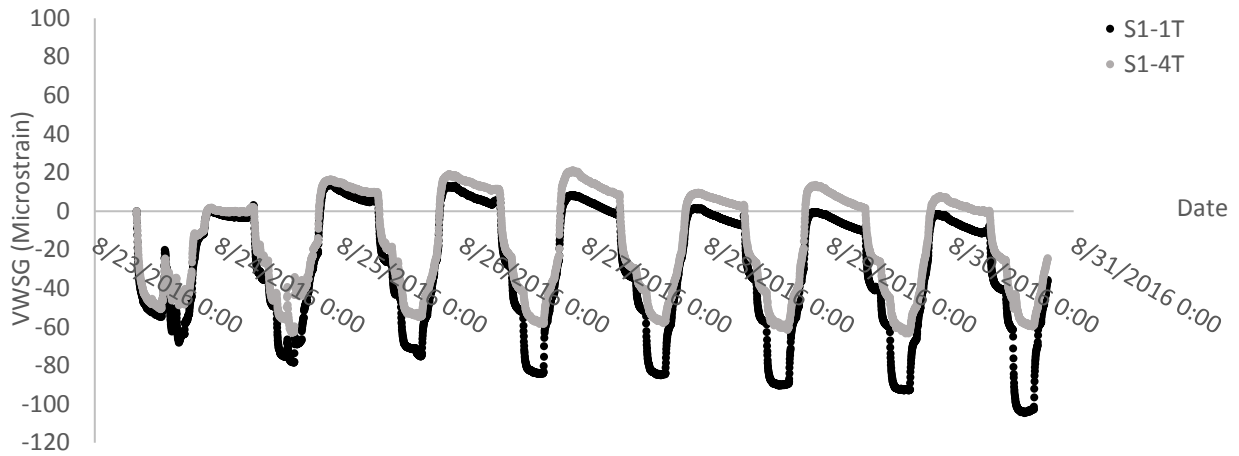


**Figure 70. Strains from Section 1 at the top surface-1**

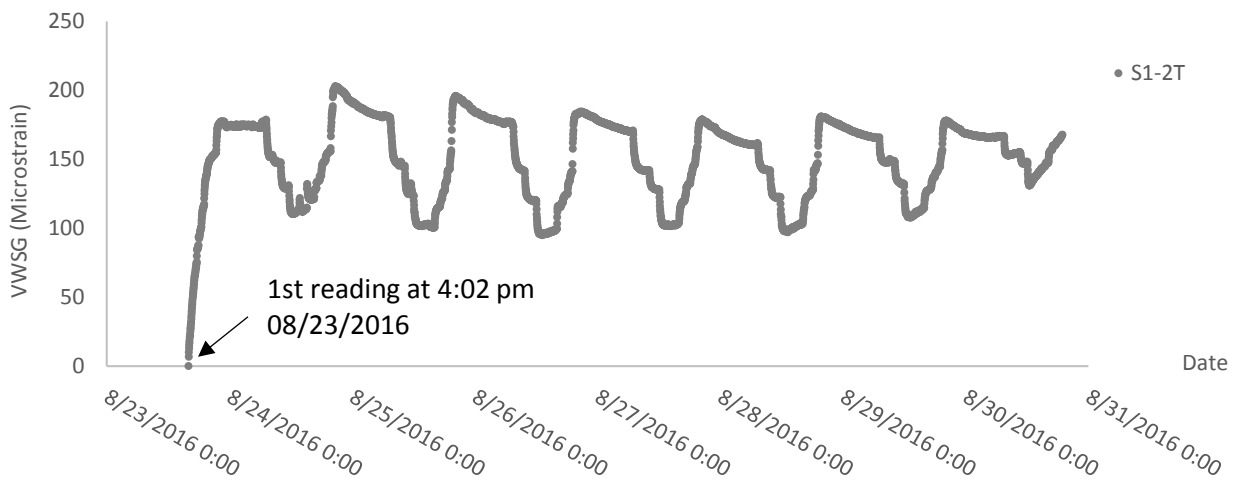


**Figure 71. Strains from Section 1 at the top surface-2**

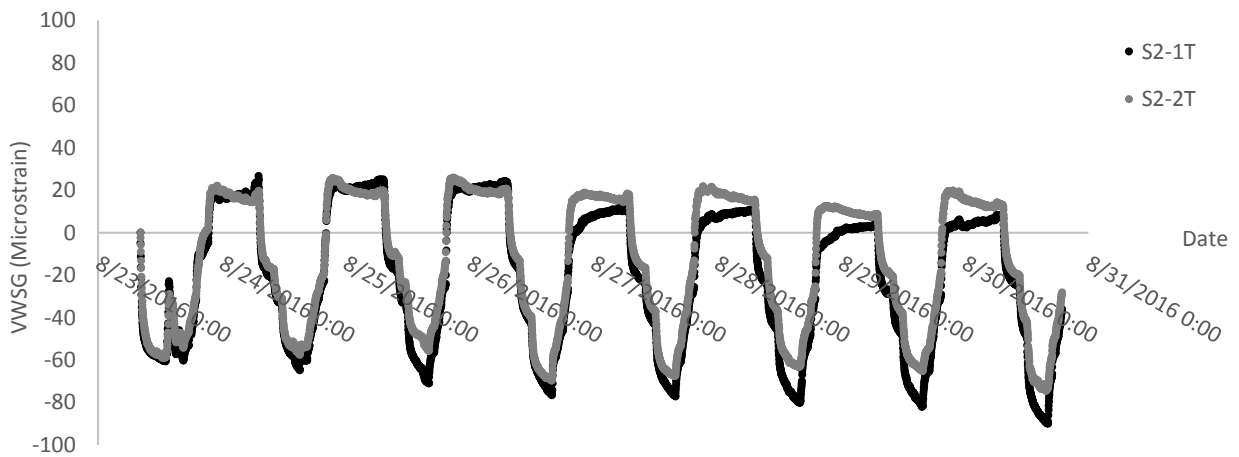


**Figure 72. Strains from Section 2 at the top surface**

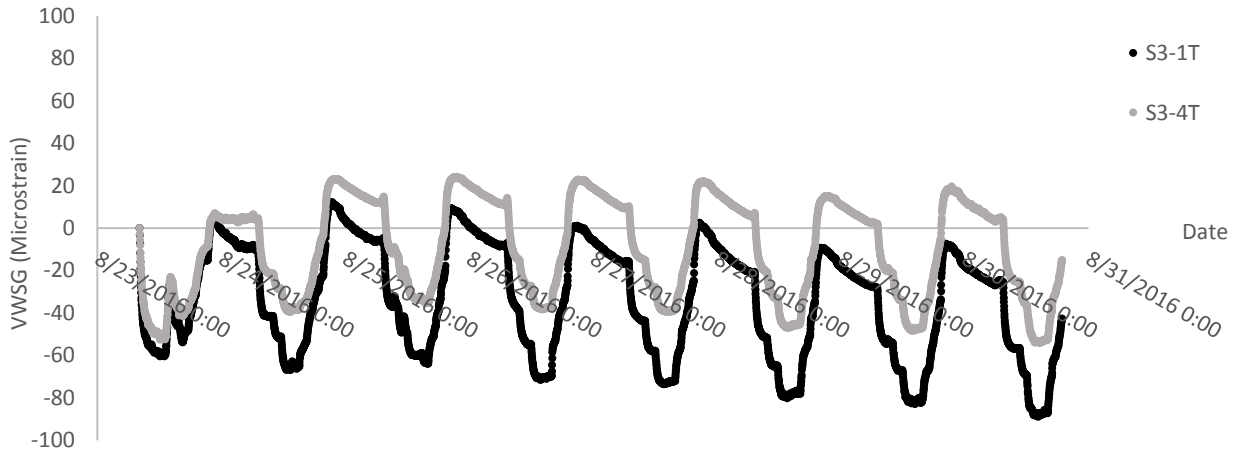


**Figure 73. Strains from Section 3 at the top surface-1**

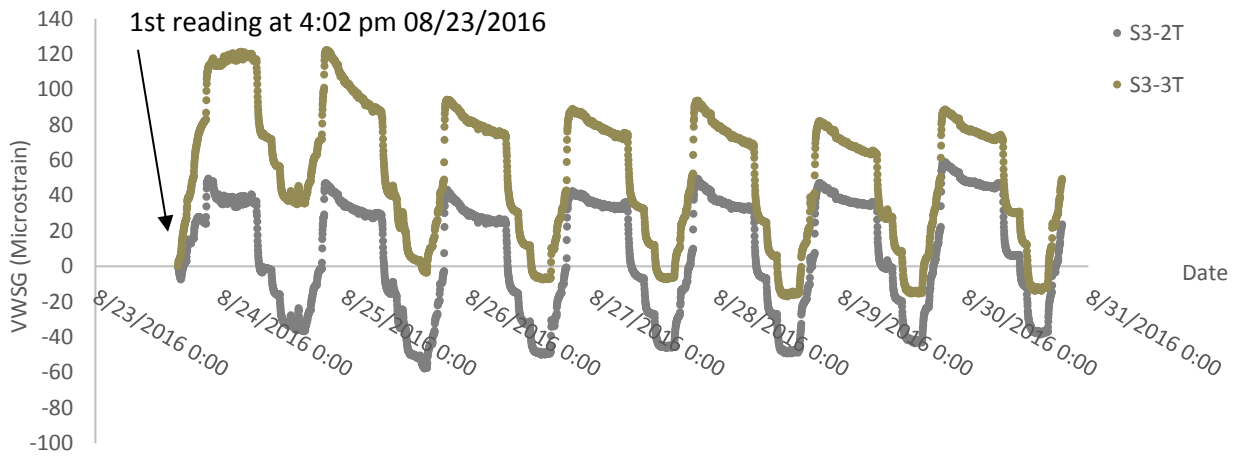


**Figure 74. Strains from Section 3 at the top surface-2**

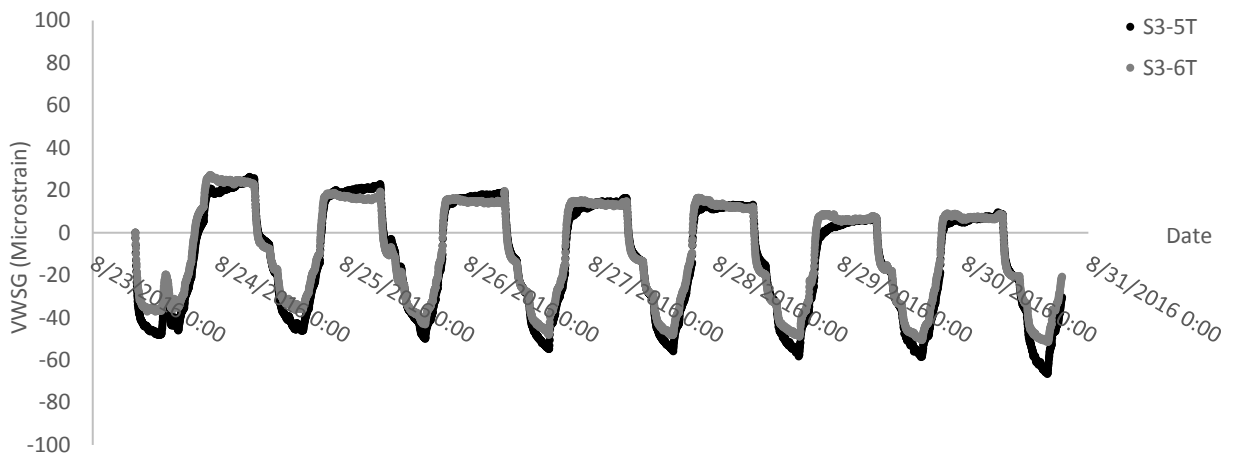


**Figure 75. Strains from Section 3 at the top surface-3**



**Figure 76. Strains from Section 4 at the top surface**



**Figure 77. Strains from Section 5 at the top surface-1**

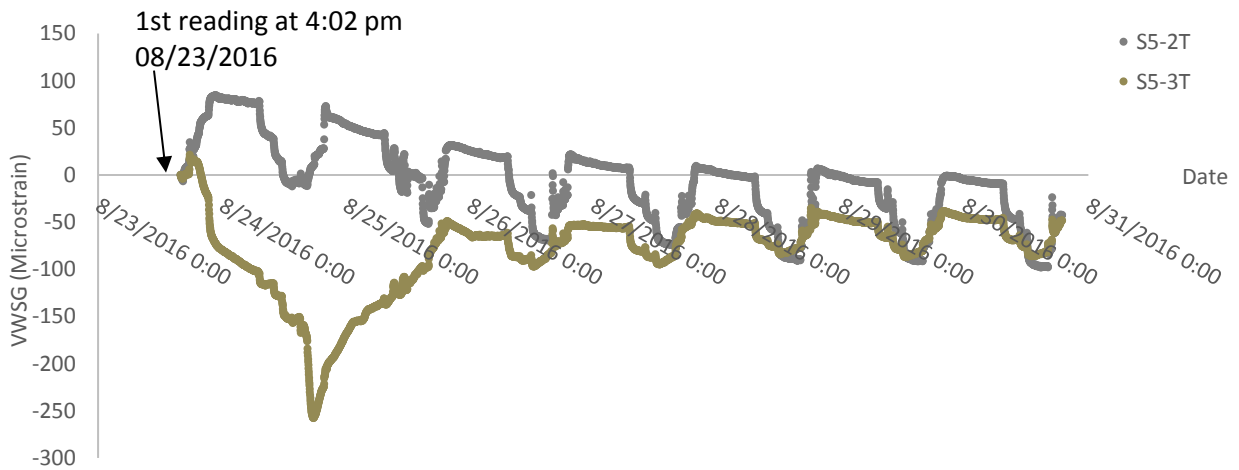


**Figure 78. Strains from Section 5 at the top surface-2**

Note that on the top surface, the gauges near the joint (S1-2T, S1-3T, S3-2T, S3-3T, S5-2T, and S5-3T) were installed after the joint material placement. Hence, the data in Figure 70, Figure 74, and Figure 78 started from 4:02 p.m. August 23, 2016. Note that S1-3T lost function at a very early age and its data are therefore not shown.

During post-processing, the strain data were adjusted for the temperature change, and the resulting strain values shown in Figure 64 through Figure 78 are the stress-induced strain. Since the data were collected before pouring of joint material, tension was generated due to the weight of the joint material, and, because of this, strain gauges on the bottom surface generally show positive readings. For gauges at the bottom surface and near the joint, the negative readings indicate that the weight of the joint generated compression at the bottom beam corner due to a cantilever effect. Gauges on the top surface attached before the pouring of concrete (Figure 70, Figure 72, Figure 73, Figure 75, Figure 76, and Figure 77) generally show negative readings during the day and positive (but close to zero) readings during the night. During the day, the high temperature on the top surface induced expansion and compressive stresses on the top surface.

### Displacement

During the thermal test, all of the displacement transducers (shown previously in Figure 41 through Figure 44) were activated to measure the specimen deformation. However, only four of the transducers at the middle span (which measure the vertical displacement) detected the deformation and show significant readings.

Figure 79 shows the vertical displacement at the middle span of the beam from four displacement transducers along the transverse direction (see previous Figure 43 for the transducer locations).



**Figure 79 Vertical displacement at the middle span at early-age**

Note that transducer D3-2B was a bad gauge and the data are not shown for it. The data from the other three transducers indicate that both beams had the same displacement and maintained good

integrity during the first seven days. The daily temperature rise during the day caused the middle of the beam to move upward, as shown by the displacements.

### Cracks

During the early-age test, no cracks were found in the joint or at the interface between the joint and the box girder. The lack of any cracking is a very positive indicator that the joint is unlikely to experience cracking later in life as well. This point is discussed further in subsequent sections.

## 6.2 Results of Cyclic Load Test

During the cyclic load test, a static test with three load applications was performed after each 200,000 cycles. Six static tests were performed for each one million cycles of loading. The strain and displacement data were collected during only the static load test. Not surprisingly, given the fact that the beams were designed without longitudinal post-tensioning, cracks initiated at the bottom of the box girder once the first cycle of loading was applied.

### Displacement

During the cyclic load test, only the four vertical displacement transducers had significant readings. Figure 80 through Figure 82 show the displacement data from the vertical transducers (D3-1B and D3-4B) at the middle span. Gauge D3-3B was a bad gauge and its data are not shown.

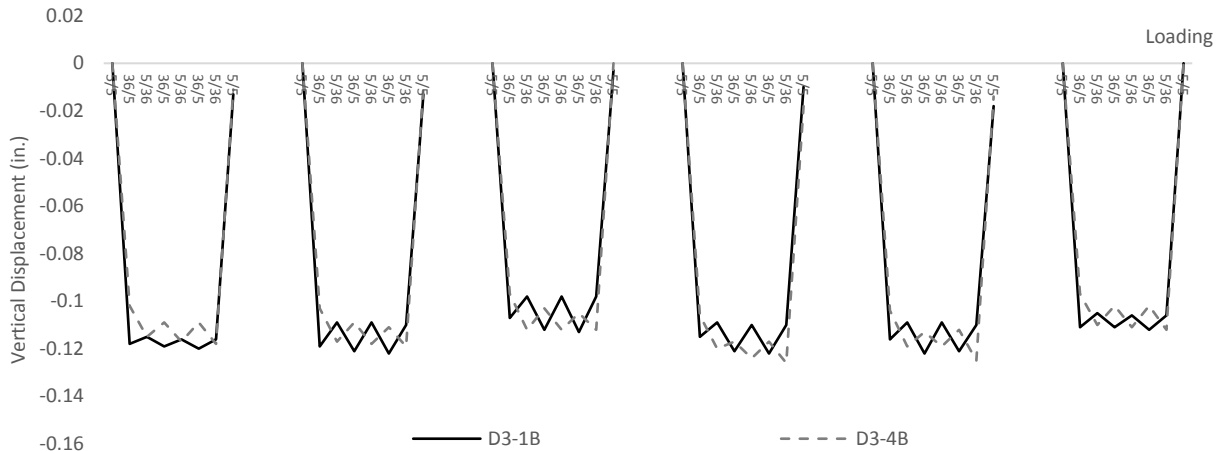
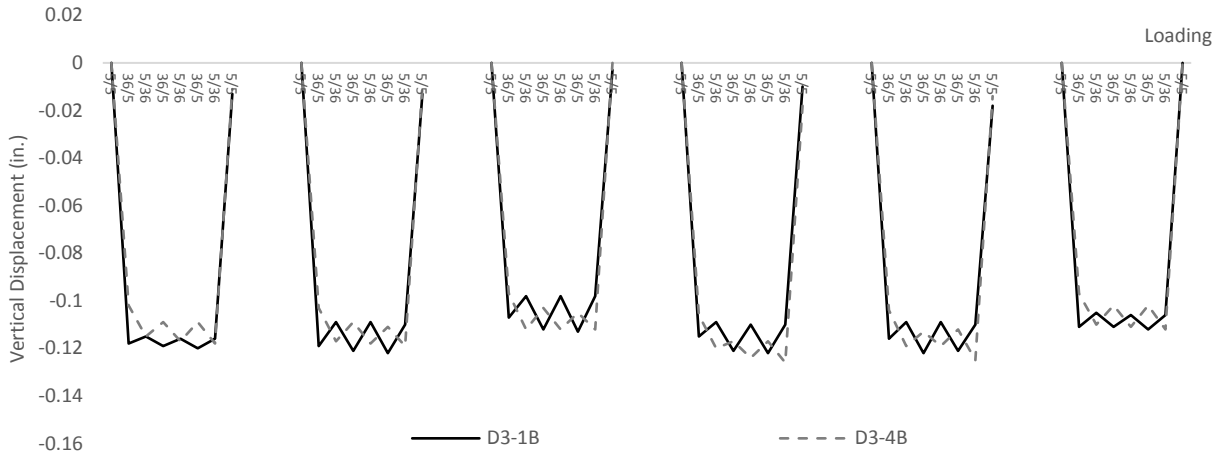
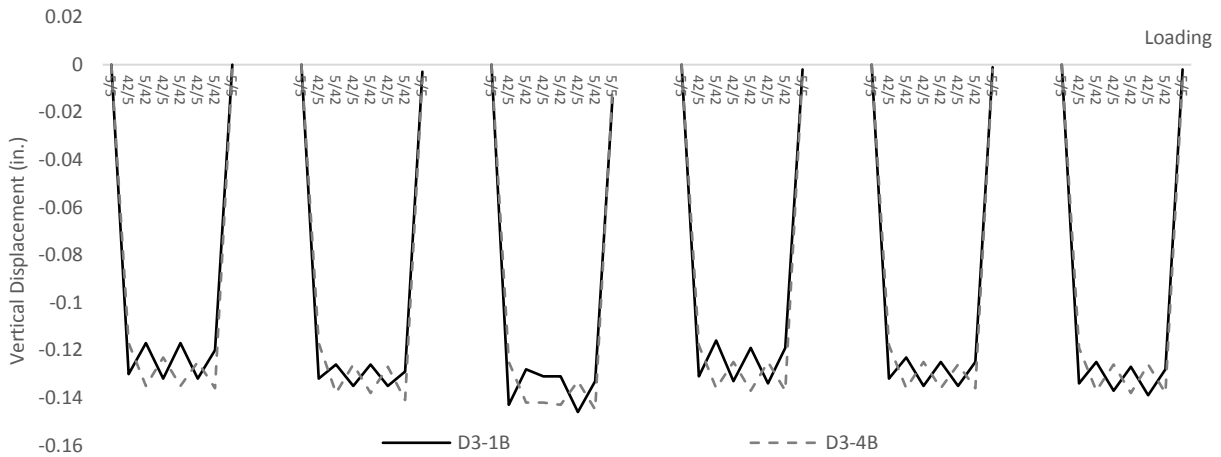


Figure 80. Displacement from 18 kips static tests



**Figure 81. Displacement from 36 kips static tests**



**Figure 82. Displacement from 42 kips static tests**

While the two beams were subjected to different loading (see previous Figure 33), the displacements collected from both beams were very close, which indicates that the joint was fully functional and transferring the load from one beam to the other, and that it maintained this integrity throughout testing. The displacement due to the same loading was similar before and after each one million cycles with no significant increase in displacement, which indicates that there was no evidence that the joint functionality changed with time.

The displacement data from transducers D3-1 and D3-4, which were at the center of each beam, were used to calculate the load distribution factors (LDFs). Since there was a large difference in the Young's modulus of the two box girders (see Section 5.5), the Young's modulus was taken into account in the LDFs. For example, the LDF of Beam-1 (see Section 5.5 for beam labels) can be calculated with the following equation:

$$LDF_1 = \frac{E_1 \Delta_1}{E_1 \Delta_1 + E_2 \Delta_2}$$

where,  $LDF_1$  is the load distribution factor for Beam-1,  $E_1$  is the Young's modulus of Beam 1,  $E_2$  is the Young's modulus of Beam 2,  $\Delta_1$  is the vertical displacement under Beam 1, and  $\Delta_2$  is the vertical displacement under Beam 2. Figure 83 shows the LDF changes during the first three million cycles.

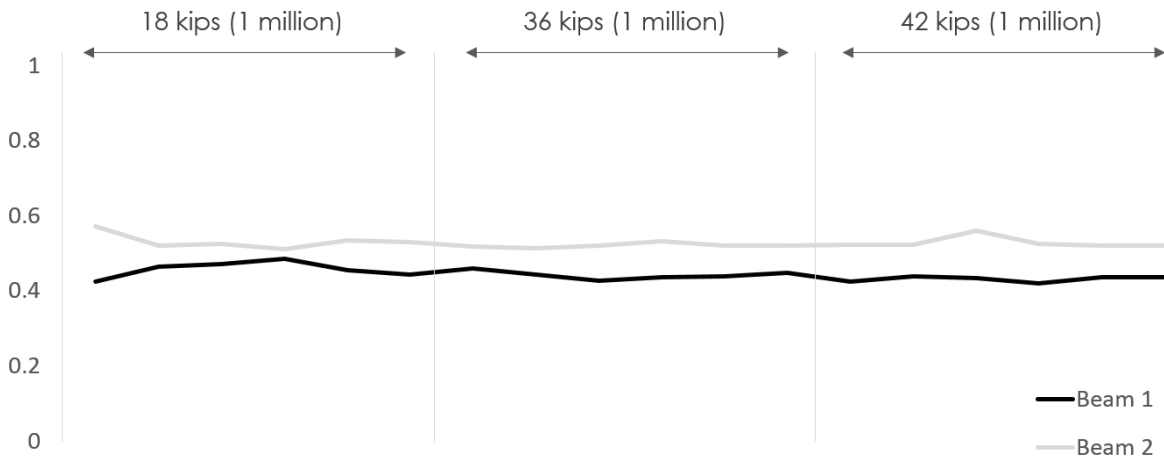


**Figure 83. Distribution factor change during the first three million cycles**

Figure 84 shows the displacement change at the middle span when one beam was restrained and the other beam was loaded for the 42 kips cyclic loading.

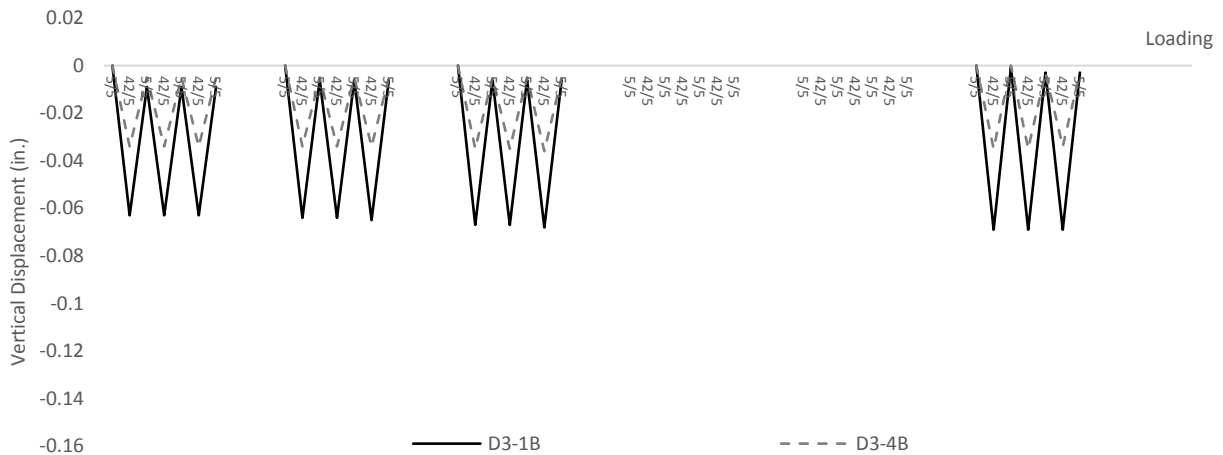


**Figure 84. Displacement from 42 kips static tests with one beam restrained**

The static data in the fourth and fifth static tests were not stored due to problems with the data logger. The data after one million load cycles (the sixth static test) were still available. There is no trend of increasing displacement after one million cycles.

### Strain

During each static test, all the VWSGs were activated to collect the strain data, but only data from S3-5B and S3-6B, which measured the longitudinal strain at the bottom of the specimen, and S3-1T, S3-2T, S3-3T, and S3-4T, which measured the transverse strain on the top surface, have significant readings and are presented herein.

Figure 85 through Figure 88 show the longitudinal strain at the bottom surface of the middle span for each static test (see previous Figure 37 for gauge locations). Both gauges crossed a crack (see the following Section for crack information), so the strain readings are artificially large.

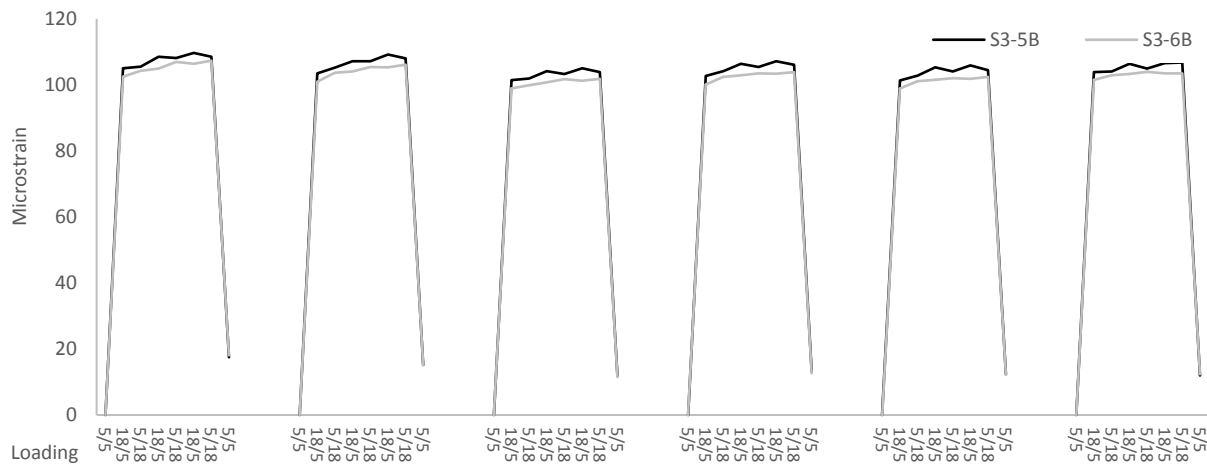


**Figure 85. Bottom longitudinal strains from 18 kips static tests**

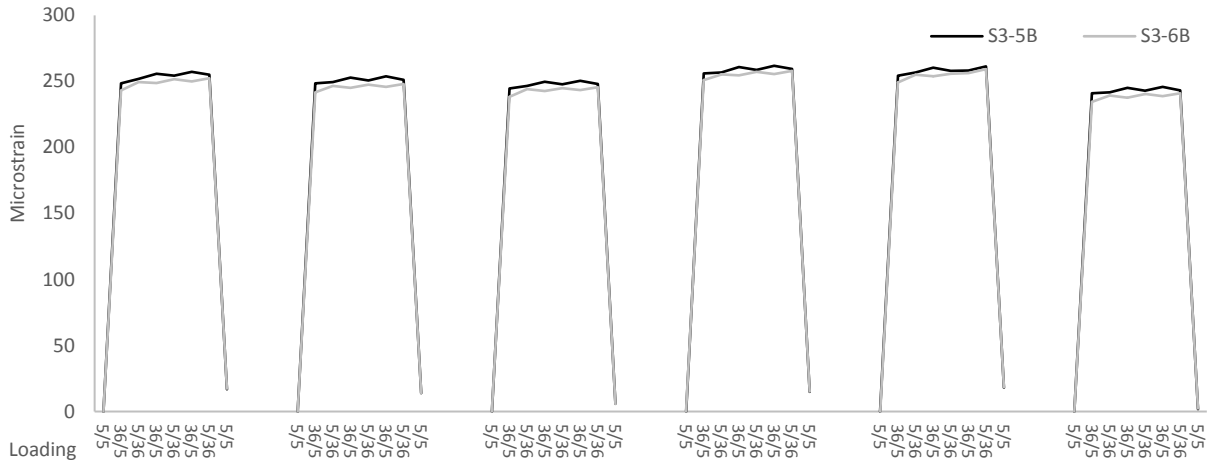


**Figure 86. Bottom longitudinal strains from 36 kips static tests**

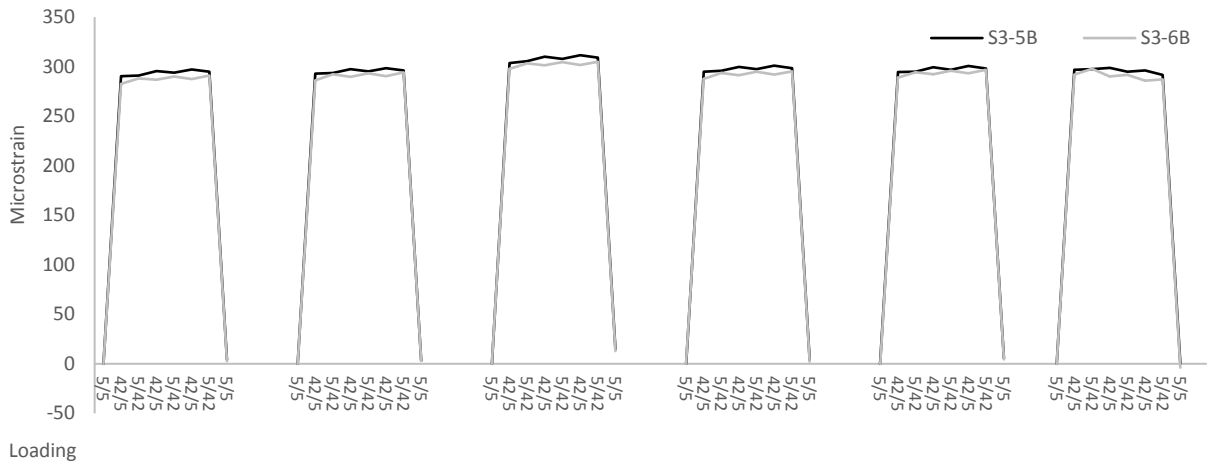


**Figure 87. Bottom longitudinal strains from 42 kips static tests**

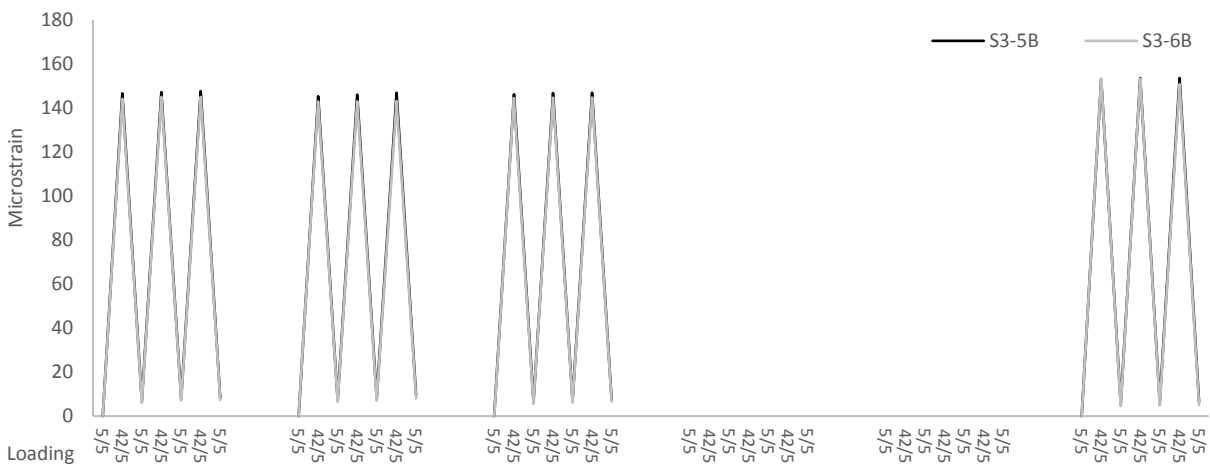


**Figure 88. Bottom longitudinal strains from 42 kips static tests (one beam restrained)**

Figure 89 through Figure 92 show the transverse strain at the top surface. The strain values from these four gauges were very small (maximum of ~25 microstrain) and well below the cracking strain.

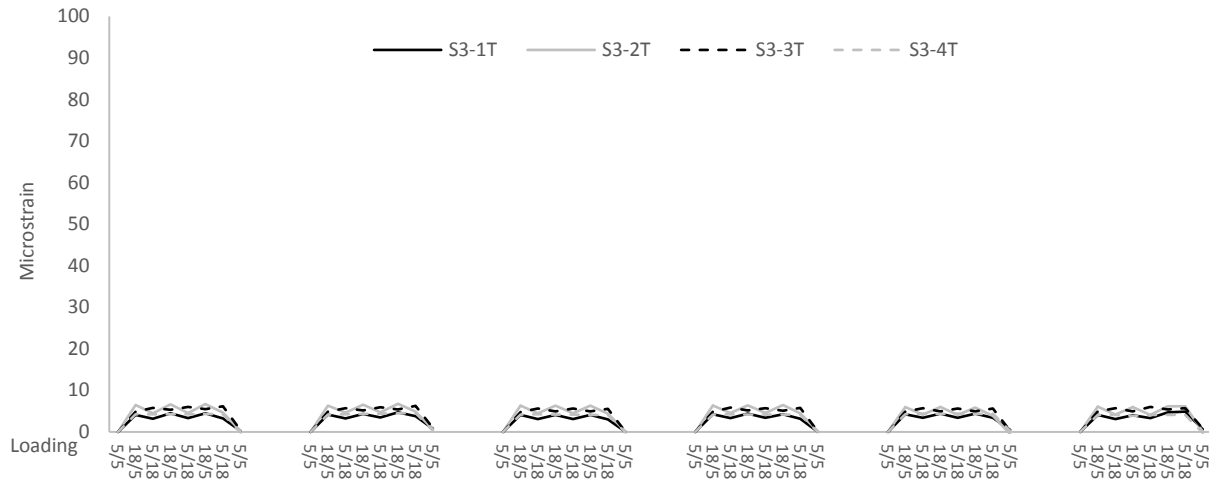


**Figure 89. Top transverse strains from 18 kips static tests**

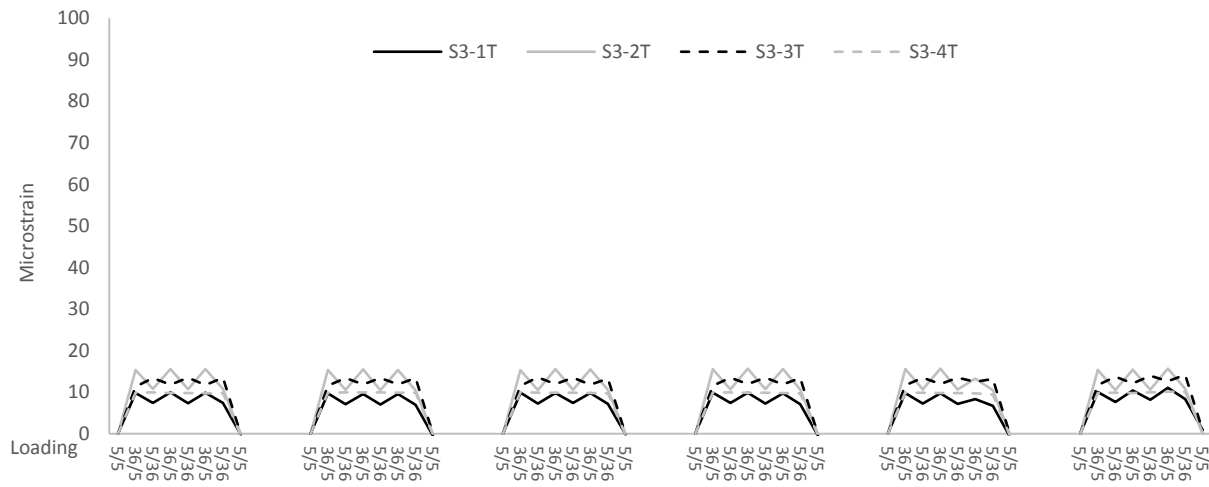


**Figure 90. Top transverse strains from 36 kips static tests**

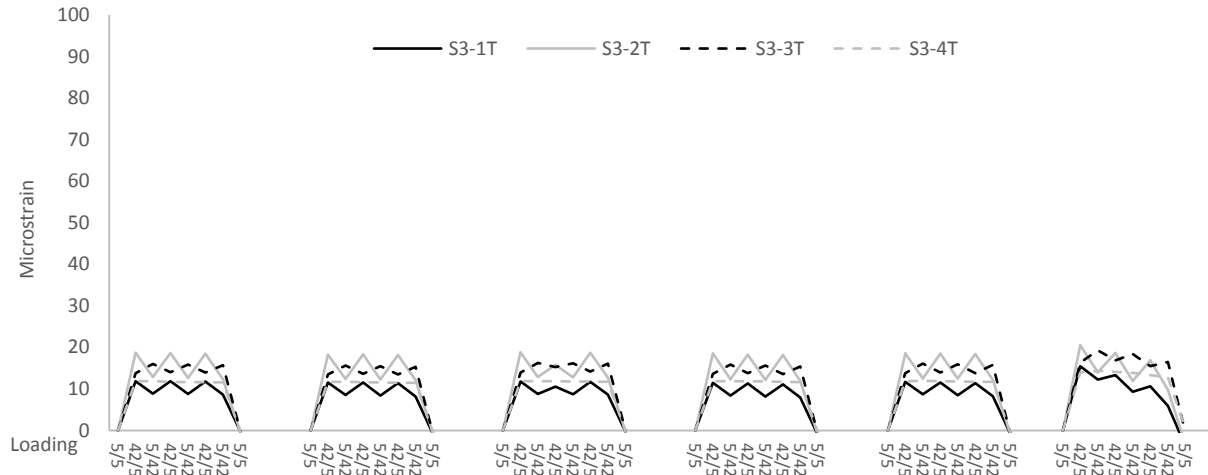


**Figure 91. Top transverse strains from 42 kips static tests**

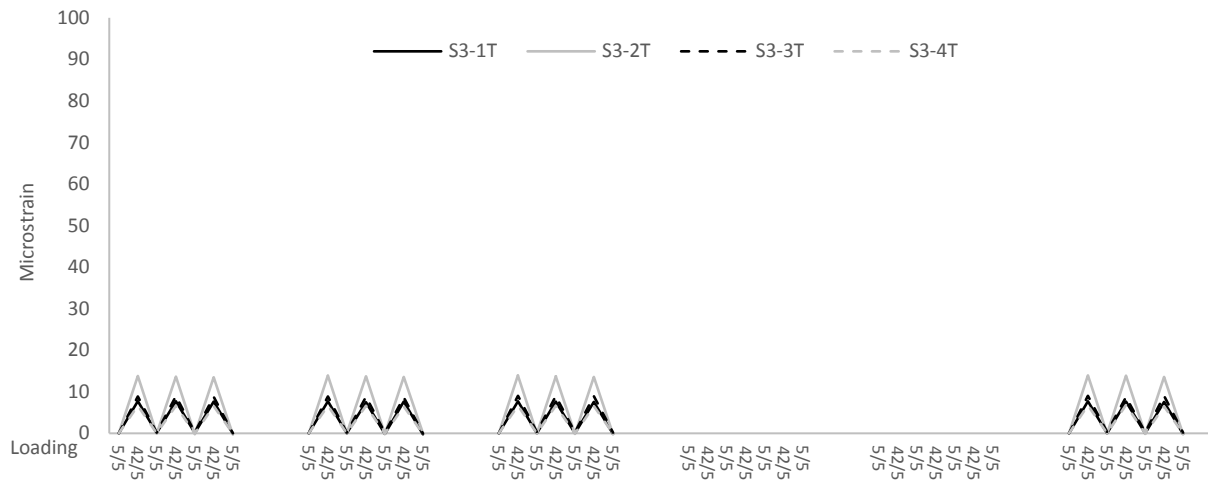


**Figure 92. Top transverse strains from 42 kips static tests (one beam restrained)**

### Cracks

Immediately after the application of the first cycle loading of 18 kips, transverse cracks occurred on the bottom of the box girder. Figure 93 shows the locations of all the transverse cracks.

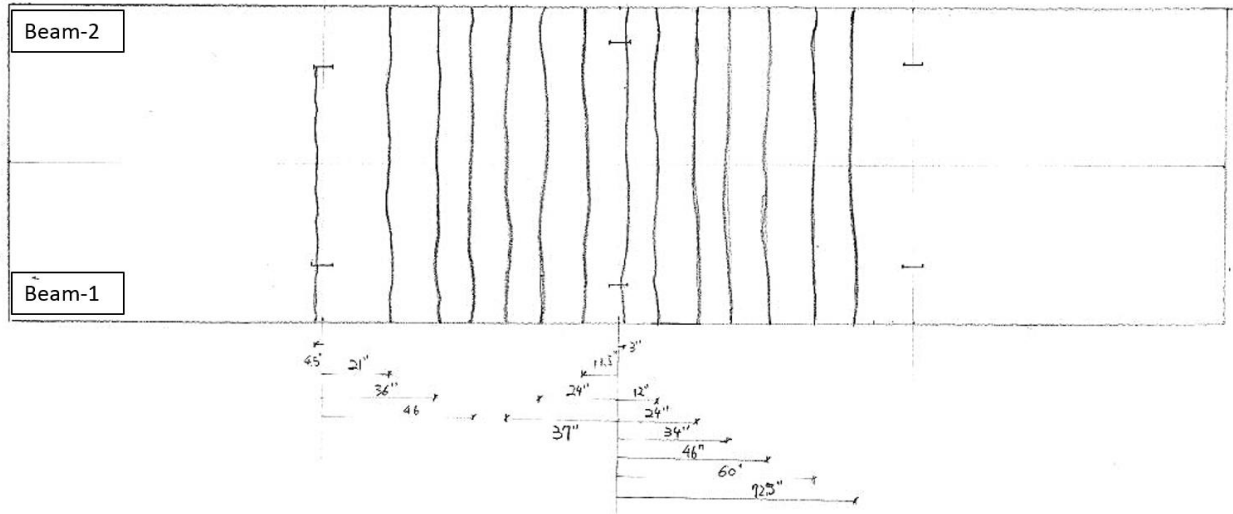


**Figure 93. Transverse cracks on bottom of box girder after first cycle loading of 18 kips**

The cracks were concentrated from one-quarter span to three-quarters span. Almost all of the cracks developed across the width of the specimen and were spaced almost evenly at about 1 ft. During the cyclic load test, no cracks occurred in the joint.

### 6.3 Results of Horizontal Load

After the cyclic loading test, the joint was intentionally cracked with an artificial horizontal load. Two steel frames were attached on top of the diaphragm at the quarter span. A horizontal load was applied using a hydraulic cylinder and transferred from the steel frame to the box girder. The test was repeated at both quarter-span diaphragm locations. Both tests ended with failure of the box girder concrete. The maximum horizontal loading was 25 kips at one diaphragm and 45 kips at the other diaphragm. For both tests, no cracks initiated in the joint or at the interface before the box girder concrete failed. Figure 94 shows the box girder after the test.



**Figure 94. Crushed box girder due to horizontal load**

The horizontal load test results were compared with the UHPC tests conducted by the FHWA in Table 9.

**Table 9. Joint performance comparison to FHWA's (Yuan and Graybeal 2016)**

Joint Material	Depth	Joint Width	Shear Key	Max. Horizontal Load	Crack Location
Conventional Grout	Partial	Narrow	Yes	40 kips	Interface between box girder and joint
UHPC + Rebar	Partial	Narrow	Yes	40 kips	Box Girder
	Full	Narrow	Yes	40 kips	Box Girder
Type K + Rebar	Full	Wide	No	45.5 kips	Box Girder

Type K + Rebar was the innovative joint that was developed and tested in the laboratory for this project

With the conventional grout, the cracks developed at the interface between the box girder and joint, when the horizontal load was 40 kips. The UHPC joint resisted 40 kips horizontal load without cracks. The new innovative joint using the conventional concrete with Type K cement and reinforcement achieved the same basic load level as the UHPC joint detail.

## CHAPTER 7. SUMMARY AND CONCLUSIONS

### 7.1 Summary

Adjacent precast box beams are connected by cast-in-place joints, which have historically suffered from cracking issues. For this project, a comprehensive literature review was conducted on cracking in the joint between adjacent box girders. Joint cracking was suspected to be induced by low bond strength between the joint material and box girder, large shrinkage of the joint material, stress concentration near the shear key, and temperature changes. Some potential solutions given by previous research included the use of low- or zero-shrinkage material, increased bond strength and shear strength, and additional reinforcement in the joint.

The researchers inspected two box beam bridges in Iowa for cracks in the joints. No cracks were found in the joint of the bridge in Madison County. Moisture staining was found at the bottom surface of the bridge in Buena Vista County, which indicated that the bridge had cracks and experiences water leakage.

The research team constructed and tested a 30 ft long specimen consisting of two box girder beams and one joint in the laboratory. An innovative joint was designed with unique details:

- Wide joint dimensions (about 6.5 in.)
- Application of shrinkage-compensating cement for the joint concrete
- High surface roughness between the joint material and the box girders
- Use of commercially available reinforcing steel couplers to connect the joint material and box beam materials to provide both transverse strength and stiffness

The researchers performed a laboratory test on the innovative joint, replicating the testing completed by the FHWA including temperature loading and cyclic vertical loading. The temperature loading was applied during the early age of the joint concrete in conjunction with concrete expansion, heat of hydration, and concrete hardening.

During the early-age testing of the innovative joint that was developed in this work, the daily temperature loading simulated a 40 °F vertical temperature gradient through the depth of the specimen. The test continued for seven days and no cracks were found.

The cyclic load was applied when the joint concrete was two months old with both beams simply supported and a subsequent round of testing with one beam restrained. The maximum applied load was 42 kips, which is equivalent to a design truckload based on AASHTO specifications. In total, more than 5,000,000 cycles of live loading were applied during the cyclic load testing. The live load did not induce cracks in the joint.

The specimen was intentionally cracked by applying a horizontal force across the joint similar to what the FHWA did. No cracks initiated on the joint before the box girders crushed due to loading of 45.5 kips.

The evaluation completed here did not consider the permeability of the joint material. The UHPC connection developed and tested by the FHWA utilizes UHPC, which is known to be very impermeable. Such impermeability may enhance the long-term service life of that connection.

## **7.2 Conclusions and Recommendations**

Based on the results of the literature review and laboratory tests, the wide joint between the roughened interface surface, filled with shrinkage-compensating concrete and reinforced by reinforcement steel, can create a crack-free joint without the utilization of a shear key nor transverse post-tensioning.

This joint is as functional as the traditional cement grout-filled narrow joint with respect to the transfer of the moment and shear between the girders, while also performing better than the traditional joint in resisting joint cracks in both early-age loading and the long-term service life of the bridge.

At the same time, the test results for the new innovative joint detail appear to compare very well with the UHPC-based joint detail developed and tested by the FHWA. To further investigate the performance of this joint detail, the researchers recommend that a field trial be completed. During this field trial, the bridge should be monitored and evaluated during early-age concrete curing as well as for a period of at least two years following construction.



## REFERENCES

- AASHTO. 2002. *Standard Specifications for Highway Bridges*, 17th ed., American Association of State Highway and Transportation Officials, Washington, DC.
- AASHTO. 2007. *AASHTO LRFD Bridge Design Specifications*, 4th ed. (plus 2008 Interim Revisions), American Association of State Highway and Transportation Officials, Washington, DC.
- Anderson R. E. 2007. New PPG Deck Beam Designs and Details on State System. Memorandum 07.2, Illinois Department of Transportation, Springfield, August 29, 2007.
- Attanayake, U. and H. Aktan. 2008. Issues with Reflective Deck Cracks in Side-by-Side Box Beam Bridges. 2008 Concrete Bridge Conference, May 3–5, St. Louis, MO.
- Attanayake, U. and H. M. Aktan. 2009. Side-by-Side Box-Beam Bridge Superstructure: Rational Transverse Post-Tension Design. Transportation Research Board Annual Meeting, January 11–15, Washington, DC.
- Badwan, I. Z. and R. Y. Liang 2007a. Transverse Post-Tensioning Design of Precast Concrete Multi-Beam Deck. *PCI Journal*, Vol. 52, No. 4, pp. 84–92.
- Badwan, I. Z. and R. Y. Liang. 2007b. Performance Evaluation of Precast Post-Tensioned Concrete Multi-Beam Deck. *Journal of Performance of Constructed Facilities*, Vol. 21, No. 5, pp. 368–374.
- Dong, H., Y. Li, and T. M. Ahlborn. 2007. Performance of Joint Connections between Decked Prestressed Concrete Bridge Girders. 2007 National Bridge Conference, October 19–22, Phoenix, Arizona.
- El-Remaily, A., M. K. Tadros, T. Yamane, G. and Krause. 1996. Transverse Design of Adjacent Precast Prestressed Concrete Box Girder Bridges. *PCI Journal*, Vol. 41, pp. 96–113.
- Fu, C. C., Z. Pan, and M. S. Ahmed. 2011. Transverse Post-Tensioning Design of Adjacent Precast Solid Multibeam Bridges. *Journal of Performance of Constructed Facilities*, Vol. 25, No. 3, pp. 223–230.
- Grace, N. F., E. A. Jensen, and M. R. Bebawy. 2012. Transverse Post-Tensioning Arrangement for Side-by-Side Box-Beam Bridges. *PCI Journal*, Vol. 57, No. 2, pp. 48–63.
- Greuel, A., T. M. Baseheart, B. T. Rogers, R. A. Miller, and B. M. Shahrooz. 2000. Evaluation of a High Performance Concrete Box Girder Bridge. *PCI Journal*, Vol. 45, No. 6, pp. 60–71.
- Gulyas, R. J., G. J. Wirthlin, and J. T. Champa. 1995. Evaluation of Keyway Grout Test Methods for Precast Concrete Bridges. *PCI Journal*, Vol. 40, No. 1, pp. 44–57.
- Hanna, K. E., G. Morcouc, and M. K. Tadros. 2007. Transverse Design and Detailing of Adjacent Box Beam Bridges. 2007 National Bridge Conference, October 19–22, Phoenix, AZ.
- Hanna, K. E., G. Morcouc, and M. K. Tadros. 2009. Transverse Post-Tensioning Design and Detailing of Precast, Prestressed Concrete Adjacent-Box-Girder Bridges. *PCI Journal*, Vol. 54, No. 4, pp. 160–174.
- Hanna, K., G. Morcouc, and M. K. Tadros. 2011. Adjacent Box Girders without Internal Diaphragms or Post-Tensioned Joints. *PCI Journal*, Vol. 56, No. 4, pp. 51–64.
- Hansen, J., K. Hanna, K., and M. K. Tadros. 2012. Simplified Transverse Post-Tensioning Construction and Maintenance of Adjacent Box Girders. *PCI Journal*, Vol. 57, No. 2, pp. 64–79.

- Harries, K. A., C. Earls, R. Gostautas, C. and Stull. 2006. *Full-Scale Testing Program on De-Commissioned Girders from the Lake View Drive Bridge*. University of Pittsburg, PA.
- Huckelbridge, A. A., Jr., H. El-Esnawi, and F. Moses. 1995. Shear Key Performance in Multi-Beam Box Girder Bridges. *Journal of Performance of Constructed Facilities*, Vol. 9, No. 4, pp. 271–285.
- Huckelbridge, A. A., Jr. and H. H. El-Esnawi. 1997. *Evaluation of Improved Shear Key Designs for Multi-Beam Box Girder Bridges*. Department of Civil Engineering, Case School of Engineering, Case Western Reserve University, Cleveland, OH.
- Illinois DOT. 2008. Concrete Deck Beams. *Guide Bridge Special Provisions (GBSP)*. Illinois Department of Transportation, Springfield, IL, No. 62. [www.idot.illinois.gov/doing-business/procurements/engineering-architectural-professional-services/Consultants-Resources/guide-bridge-special-provisions](http://www.idot.illinois.gov/doing-business/procurements/engineering-architectural-professional-services/Consultants-Resources/guide-bridge-special-provisions).
- Issa, M. A., C. L. R. do Valle, H. A. Abdalla, S. Islam, and M. A. Issa. 2003. Performance of Transverse Joint Grout Materials in Full-Depth Precast Concrete Bridge Deck Systems. *PCI Journal*, Vol. 48, No. 4, pp. 92–103.
- Kim, J. H. J., J. W. Nam, H. J. Kim, J. H. Kim, and J. B. Keun. 2008. Overview and Applications of Precast, Prestressed Concrete Adjacent Box-Beam Bridges in South Korea. *PCI Journal*, Vol. 53, No. 4, pp. 83–107.
- Lall, J., E. F. DiCocco, and S. Alampalli. 1997. *Full-Depth Shear-Key Performance in Adjacent Prestressed-Beam Bridges*. Special Report No. 124, Transportation Research and Development Bureau, New York State Department of Transportation, Albany, NY.
- Lall, J., S. Alampalli, and E. F. DiCocco. 1998. Performance of Full-Depth Shear Keys in Adjacent Prestressed Box Beam Bridges. *PCI Journal*, Vol. 43, No. 2, pp. 72–79.
- Macioce, T. P., H. C. Rogers, R. Anderson, R., and D. C. Puzey. 2007. Prestressed Concrete Box Beam Bridges—Two DOTs’ Experience. 2007 National Bridge Conference, October 19–22, Phoenix, Arizona.
- Miller, R. A., G. M. Hlavacs, T. Long, and A. Greuel. 1999. Full-Scale Testing of Shear Keys for Adjacent Box Girder Bridges. *PCI Journal*, Vol. 44, No. 6, pp. 80–90.
- Nottingham, D. 1995. Discussion of “Evaluation of Keyway Grout Test Methods for Precast Concrete Bridges.” *PCI Journal*, Vol. 40, No. 4, pp. 98–103.
- PCI. 1997/2004. *PCI Bridge Design Manual*. Updated July 2004, Precast/Prestressed Concrete Institute, Chicago, IL.
- PCI. 2003. *PCI Bridge Design Manual*. Second Edition, Precast/Prestressed Concrete Institute, Chicago, IL.
- Russell, H. G. 2009. *NCHRP Synthesis 393: Adjacent Precast Concrete Box Beam Bridges: Connection Details*. National Cooperative Highway Research Program, Washington, DC.
- Sang, Z. 2010. *A Numerical Analysis of the Shear Key Cracking Problem in Adjacent Box Beam Bridges*. PhD dissertation, Pennsylvania State University, University Park, PA.
- Sharpe, G. P. 2007. *Reflective Cracking of Shear Keys in Multi-Beam Bridges*. PhD dissertation, Texas A&M University, College Station, TX.
- Ulku, E., U. Attanayake, H. M. and Aktan. 2010. Rationally Designed Staged Post-Tensioning to Abate Reflective Cracking on Side-by-Side Box-Beam Bridge Decks. *Transportation Research Record: Journal of the Transportation Research Board*, Vol. 2172, No. 1, pp. 87–95.
- Yamane, T., M. K. Tadros, and P. Arumugasaamy. 1994. Short to Medium Span Precast Prestressed Concrete Bridges in Japan. *PCI Journal*, Vol. 39, No. 2, pp. 74–100.

- Yuan, J. and B. Graybeal. 2016. Full-Scale Testing of Shear Key Details for Precast Concrete Box-Beam Bridges. *Journal of Bridge Engineering*, Vol. 21, No. 9.
- Yuan, J., B. Graybeal, and Z. Haber. 2014. Field-Cast Connections for Prefabricated Bridge Elements. *Proceedings of the 2014 National Accelerated Bridge Construction Conference*, December 3–5, Miami, FL, pp. 771–780.